REGULATION AND FUNCTION OF MACROPHAGES DURING ACUTE LIVER INJURY AND ACUTE LIVER FAILURE

Ву

Katherine Jane Roth

A DISSERTATION

Submitted to
Michigan State University
in partial fulfillment of the requirements
for the degree of

Cell and Molecular Biology – Environmental Toxicology – Doctor of Philosophy

2019

ABSTRACT

REGULATION AND FUNCTION OF MACROPHAGES DURING ACUTE LIVER INJURY AND ACUTE LIVER FAILURE

By

Katherine Jane Roth

Acetaminophen (APAP) is one of the most commonly used over-the-counter analgesic and antipyretic agents. When taken at high doses, APAP produces liver injury that can rapidly progress to acute liver failure (ALF). Pharmacological therapies for APAP overdose are limited to N-acetyl-cysteine (NAC), which is only highly efficacious when administered early after APAP overdose. Unfortunately, many patients do not seek medical attention until liver injury is extensive and NAC is no longer effective. Therefore, a more detailed understanding of the mechanisms controlling liver repair after injury could provide insight into better therapies and new ways to stimulate repair in ALF patients

Hepatic macrophages, including Kupffer cells and monocyte-derived macrophages, are critical for liver repair following APAP overdose. These macrophages produce pro-mitogenic cytokines and growth factors and phagocytose dead cell debris, a process that is critical for resolution of inflammation. However, the factors that regulate these dynamic functions of macrophages after APAP overdose are not fully understood. The fibrinolytic enzyme, plasmin, is known to regulate various macrophage functions. Therefore, we hypothesized that plasmin is critical for macrophage functions after APAP overdose. To test this hypothesis, we inhibited plasmin with tranexamic acid in a mouse model of APAP overdose, which delayed upregulation of proinflammatory cytokines after APAP overdose. In culture, plasmin directly, and in synergy with high-mobility group B1 (HMGB1), stimulated macrophages to produce cytokines by a mechanism that required NF-kB. Furthermore, inhibition of plasmin *in vivo* prevented trafficking of monocyte-derived macrophages into necrotic lesions after APAP overdose. This prevented phagocytic removal of dead cells, prevented maturation of monocyte-derived macrophages into

F4/80-expressing macrophages, and prevented termination of proinflammatory cytokine production. These data demonstrate that plasmin is an important regulator of macrophage function after APAP overdose.

Clinical studies demonstrate that ALF patients with the worst prognosis have the highest systemic levels of both pro- and anti-inflammatory cytokines. Although the cause remains unknown, it has been proposed that cytokine dysregulation in ALF results from impaired macrophage function. We hypothesized that macrophage function would be dysregulated in a mouse model of ALF and that the dysregulation would impact liver repair. To test this hypothesis, we treated mice with either 300 mg/kg APAP, a dose that produces moderate, fully repaired liver, or with 600 mg/kg acetaminophen, a dose that recapitulates many of the features of ALF in patients. In mice treated with 600 mg/kg APAP, proinflammatory monocyte-derived macrophages accumulated in the liver but failed to traffic into the necrotic lesions and failed to remove dead cell debris. Further, the proinflammatory macrophages did not switch phenotype to pro-repair macrophages, leading to the sustained production of several proinflammatory cytokines. Similar to ALF patients, systemic IL-10 concentrations were also higher in mice treated with 600 mg/kg APAP. Administration of an IL-10 neutralizing antibody fully restored macrophage trafficking into the necrotic lesions. Neutralization of IL-10 did not, however, stimulate macrophage-dependent clearance of dead cells from the liver or promote survival.

Collectively, these studies demonstrate that plasmin is an important regulator of macrophage function after APAP overdose. Furthermore, macrophages become dysregulated in ALF, leading to impaired intrahepatic macrophage trafficking, impaired phagocytic clearance of dead cells, and failed macrophage phenotype switching, resulting in the sustained production of proinflammatory cytokines. Overall, these studies demonstrate the mechanisms and functions of macrophages during acute liver injury, as well as how these functions are dysregulated in ALF.

Copyright by KATHERINE JANE ROTH 2019

TABLE OF CONTENTS

LIST OF FIGURES		viii
KEY TO ABBREVIA	TIONS	x
	and Physiology of the Liver	
	er Failure	
1.2.1	Causes of Acute Liver Failure	
1.2.2	Symptoms of Acute Liver Failure	
	Acute Liver Failure Treatment Options in the Clinic	
1.3 Acetamin	ophen-induced Acute Liver Failure	
1.3.1	Mechanism of APAP-induced Liver Injury	6
1.3.2	Treatment of APAP Overdose	6
1.3.3	Macrophage Function in APAP-induced Liver Injury	7
	1.3.3.1 Hepatic Macrophages	7
	1.3.3.2 Developmental Origins of Hepatic Macrophages	8
	1.3.3.3 Macrophage Phenotypes	8
	1.3.3.4 Functions of Kupffer Cells in APAP-induced Liver Injury	10
	1.3.3.5 Function of Monocyte-derived Macrophages in APAP-ir	ıduced
	Liver Injury	12
1.3.4	Impaired Macrophage Function in APAP-induced ALF Patients	14
1.3.5	Impaired Macrophage Function in an Animal Model of APAP-in	duced ALF
		16
1.4 Plasmin F	Regulation of Macrophage Activation	17
1.5 Purpose		20
Chanter 2		22
	f Plasmin in Regulation of Macrophage Function after Acetamino	
	on	
	and Methods	
	Animal Treatments	
2.3.2	Sample Collection	25
2.3.3	Isolation and Culture of Cells	26
2.3.4	LAL Assay	28
	Immunohistochemistry	
	Western Blot	
	Flow Cytometry	
	Real-Time PCR	
	Luminex Immunoassay	
	Statistical Analysis	
	Diagram inhihitian augustasa andu artalina industion after ADA	
2.4.1	Plasmin inhibition suppresses early cytokine induction after APA	

	2.4.2 Plasmin stimulates proinflammatory cytokine production by Kupffer cells			
	oone marrow-derived macrophages			
	Activation of signal transduction pathways in plasmin-treated macropha			
2.4.4	HMGB1 enhances activation of macrophages by plasmin	37		
	Plasmin inhibition prevents removal of necrotic cells from the liver after			
	P overdose			
	Plasmin inhibition prevents trafficking of macrophages into necrotic les			
	APAP overdose			
	Effect of plasmin inhibition on neutrophil accumulation after APAP over			
2.4.8	Impact of plasmin inhibition on expression of cytokines late after APAP	40		
	dose			
	Necrotic hepatocytes decrease cytokine expression in proinflammatory			
mond	ocytes	51		
	on			
2.6 Acknowle	edgements	60		
Chapter 3		61		
	ge Function in Mice with Acetaminophen-induced Acute Liver Failure			
	tion			
	s and Methods			
	Animal Treatments			
	Sample Collection			
	Immunofluorescence			
	Luminex Immunoassay			
	Flow Cytometry Real-Time PCR			
	Statistical Analysis			
	Statistical Arialysis			
	Impaired clearance of necrotic cells from the livers of mice with APAP-			
	ced ALF			
	Reduced accumulation of neutrophils and failed trafficking of macropha			
	necrotic lesions in mice with ALF			
	Sustained cytokine production in mice with APAP-induced ALF			
	IL-10 prevents trafficking of macrophages into necrotic lesions in mice			
	P-induced ALF			
3.4.5	Impact of IL-10 on clearance of necrotic cells from the livers of APAP-			
	ed mice	75		
3.5 Discussi	on	79		
	se of Hepatic Monocyte-derived Macrophages and Kupffer Cells to Bact			
	tion			
	s and Methods			
	Animal Treatments Bone Marrow Transplant			
4.5 /	DONE MALOW HAUSDIAN	ന		

4.3.3 Isolation of Kupffer cells and monocy	
mice4.3.4 Isolation of Kupffer cells and monocy	
marrow transplanted mice	
4.3.5 Flow Cytometry	
4.3.6 LPS Treatment	
4.3.7 Immunohistochemistry	
4.3.8 Real-Time PCR	
4.3.9 Statistical Analysis	
4.4 Results 4.4.1 Purification of Kupffer cells and MDN	
• • • • • • • • • • • • • • • • • • •	
4.4.2 Differential upregulation of cytokines	
4.4.3 Generation of chimeric mice	90
4.4.4 Isolation of Kupffer cells and MDMs	irom chimeric mice and treatment with
LPS	
4.5 Discussion	90
Chantar F	100
Chapter 5 Crosstalk Among Kupffer Cells and Hepatic Stellate Cells	
· · · · · · · · · · · · · · · · · · ·	•
during Liver Injury	
5.1 Abstract	
5.2 Introduction	
5.3 Materials and Methods	
5.3.1 Animal Treatments	
5.3.2 Isolation of Cells	
5.3.3 Culture and Treatment of Cells	
5.3.4 Immunohistochemistry	
5.3.5 Western Blot	
5.3.6 Real-Time PCR	
5.3.7 Statistical Analysis	
5.4 Results	
5.4.1 Necrotic hepatocytes activate HIF1α	
5.4.2 MyD88 and IKK2 are critical for active	
hepatocytes	
5.4.3 Necrotic hepatocytes do not directly	induce cytokine expression in Kupffer
cells	
5.4.4 Conditioned medium from HSCs treat	
cytokine expression in Kupffer cells	111
5.4.5 Potential role of arachidonic acid me	tabolites in activation of Kupffer cells
by HSCs	117
5.5 Discussion	120
Chapter 6	
Discussion	
6.1 Summary and Significance	125
6.2 Future Directions	130
RIRI IOCRAPHY	133

LIST OF FIGURES

Figure 1.1 APAP-induced Liver Injury11	
Figure 1.2 APAP-induced ALF	
Figure 1.3 Plasmin Activity and Regulation of Macrophages	
Figure 2.1 Plasmin Inhibition Suppresses Early Cytokine Induction after APAP Overdose 31	
Figure 2.2 Plasmin Stimulates Proinflammatory Cytokine Production by Macrophages 33	
Figure 2.3 Plasmin-activated Signaling Pathways in Macrophages	
Figure 2.4 HMGB1 Enhances Activation of Macrophages by Plasmin38	
Figure 2.5 Plasmin Inhibition Prevents Removal of Necrotic Cells	
Figure 2.6 Effect of Plasmin Inhibition on Proliferation after APAP Overdose42	
Figure 2.7 Effect of Plasmin Inhibition on Complement after APAP Overdose43	
Figure 2.8 Plasmin Inhibition Prevents Trafficking and Maturation of Macrophages 44	
Figure 2.9 Effect of Plasmin Inhibition on Macrophage Phenotype47	
Figure 2.10 Effect of Plasmin Inhibition on Neutrophils	
Figure 2.11 Impact of Plasmin Inhibition on Cytokine Expression Late after APAP Overdose. 52	
Figure 2.12 Necrotic Hepatocytes Decrease Cytokine Expression in Proinflammatory Monocytes53	;
Figure 3.1 Impaired Clearance of Necrotic Cells after APAP-induced ALF	
Figure 3.2 Macrophages Fail to Traffic into Necrotic Lesions after APAP-induced ALF69	
Figure 3.3 Macrophages Fail to Traffic into Necrotic Lesions and Mature71	
Figure 3.4 Effect on Macrophage Phenotype after APAP-induced ALF72	
Figure 3.5 Sustained Cytokine Production after APAP-induced ALF74	
Figure 3.6 High IL-10 Levels after APAP-induced ALF	
Figure 3.7 High IL-10 Levels Prevents Trafficking of Macrophages into Necrotic Lesions 77	
Figure 3.8 Impact of High IL-10 Levels on Clearance of Necrotic Cells	

Figure 4.1 Resident Kupffer Cell and MDM Populations in the Liver	91
Figure 4.2 Isolation of Kupffer Cells and MDMs from the Liver	92
Figure 4.3 Basal Expression Levels of Kupffer Cells and MDMs	93
Figure 4.4 Differential Upregulation of Cytokines in Kupffer Cells and MDMs by LPS	94
Figure 4.5 Generation of Chimeric Mice after Whole Body Irradiation and Bone Marrow Transplantation	95
Figure 4.6 Generation of Bone Marrow Transplant Mice after Partial Body Irradiation	97
Figure 4.7 Isolation of Kupffer Cells and MDMs from Bone Marrow Transplant Mice	98
Figure 4.8 Differential Upregulation of Cytokines in Kupffer Cells and MDMs from Bone Mar Transplant Mice	
Figure 5.1 Necrotic Hepatocytes Activate HIF-1α in HSCs	110
Figure 5.2 Signaling Pathways Involved in Activation of HIF-1α in HSCs	112
Figure 5.3 Inhibition of Signaling Pathways Involved in Activation of HIF-1α in HSCs	114
Figure 5.4 Differential Upregulation of Cytokines by Peritoneal Macrophages and Kupffer C	
Figure 5.5 Conditioned Medium from HSCs Treated with Necrotic Hepatocytes Induces Cytokine Expression in Kupffer Cells	118
Figure 5.6 Effect of Inhibition of Eicosanoid Production in HSCs on Induction of Cytokine Expression in Kupffer Cells	119
Figure 5.7: Induction of Arachidonic Acid Metabolizing Enzymes in HSCs by Necrotic Hepatocytes	121
Figure 6.1 Macrophage Functions and Associated Mediators Following APAP-induced Live Injury	

KEY TO ABBREVIATIONS

ALF Acute liver failure

APAP Acetaminophen

HIF1 α Hypoxia-inducible factor-1 α

HSC Hepatic stellate cells

SIRS Systemic inflammatory response syndrome

CARS Compensatory anti-inflammatory response syndrome

VEGF Vascular endothelial growth factor

GLUT1 Glucose transporter 1

NAC N-acetyl cysteine

Cxcl Chemokine (C-X-C motif) ligand

IL Interleukin

JNK c-Jun N-terminal kinase

MAPK Mitogen-activated protein kinase

ERK Extracellular signal-regulated kinase

MDM Monocyte-derived macrophage

PAI-1 Plasminogen activator inhibitor 1

ALT Alanine aminotransferase

TA Tranexamic acid

Ccl Chemokine (C-C motif) ligand

CCl₄ Carbon tetrachloride

TNF- α Tumor necrosis factor alpha

ROS Reactive oxygen species

MMP Matrix metalloproteinase

DAMP Damage-associated molecular pattern

HMGB1 High mobility group protein B1

uPA Urokinase-type plasminogen activator

tPA Tissue-type plasminogen activator

NF-κB Nuclear factor kappa B

M-CSF Macrophage colony-stimulating factor

GM-CSF Granulocyte-macrophage colony-stimulating factor

BMDM Bone marrow-derived macrophage

NAPQI N-acetyl-*p*-benzoquinone imine

COX Cyclooxygenase

ALOX Arachidonate lipoxygenase

PTGES Prostaglandin E synthase

Chapter 1

Introduction

1.1 Anatomy and Physiology of the Liver

The liver is the largest internal organ in the body, situated in the upper right quadrant of the abdominal cavity. The liver is made up of several different cell types, the major types including hepatocytes, hepatic stellate cells, Kupffer cells, biliary epithelial cells and sinusoidal endothelial cells. Hepatocytes are the parenchymal cells of the liver, making up the majority of the liver's volume. These cells perform most of the functions ascribed to the liver, including the metabolism of macronutrients absorbed by the intestines, the metabolism of xenobiotics, the excretion of bile, and the synthesis of proteins, such as those important for blood clotting. The liver is comprised of four distinct lobes, termed the left, right, caudate, and quadrate lobes (Abdel-Misih and Bloomston, 2010). The structural and functional subunits of the liver are known as liver lobules, which are hexagonal structures composed of portal triads (portal vein, hepatic artery, and bile duct), plates of hepatocytes along a capillary network (hepatic sinusoids), and a central vein. The liver lobules receive a dual supply of blood, from the hepatic artery, which brings oxygenated blood from the heart, and the portal vein, which brings blood from the digestive tract and spleen. This mixture of blood enters through the portal triad and travels through the hepatic sinusoids. In contrast to many other organs, the parenchymal cells of the liver (i.e., hepatocytes) are in direct contact with the blood due to the presence of fenestrations within the sinusoidal endothelial cells. After the blood flows through the sinusoids, it exits the liver through the central vein (Abdel-Misih and Bloomston, 2010). The liver has been subdivided into different zones based upon distance from the arterial blood supply. The region farthest from the hepatic artery (Zone 3) is the least oxygenated and is important for processes such as glycolysis and xenobiotic metabolism. Hepatocytes in this region express the highest levels of cytochrome P450s, and therefore, drug metabolism is largely localized to this region of the liver (Trefts, 2017).

1.2 Acute Liver Failure

1.2.1 Causes of Acute Liver Failure. Acute liver failure (ALF) is a severe, and often fatal, clinical syndrome in which there is a sudden loss of hepatic function in the absence of preexisting liver disease (Lee, 2008). Although rare, ALF is often unpredictable and severe in its course, has limited treatment options, and has a high mortality rate. In the United States, adults with ALF spontaneously recover in 45% of cases with supportive care alone; 25% of cases survive after a liver transplant; and 30% of ALF patients die either before or after a liver transplant is performed according to the U.S. ALF Study Group (Lee, 2008). Other studies, however, have reported survival rates as low as 15% in those who do not receive a liver transplant (de Ataide, 2018). ALF can arise from multiple etiologies, including viruses, acute ischemic hepatitis, and drug or toxin-induced liver injury. Worldwide, viral hepatitis is the most frequent cause of ALF, with hepatitis A and E being the most common (Lee, 2012). However, other viruses, including herpes simplex virus and Epstein-Barr virus, are also known to cause ALF (Ichai, 2008). Acute ischemic hepatitis occurs most frequently in intensive care patients and is accompanied by a transient rise in aminotransferase levels caused by hypoxic necrosis (Henrion, 2012). Acute ischemic hepatitis mainly occurs in patients suffering from severe sepsis, respiratory failure, or cardiac failure, which account for over 90% of cases (Henrion, 2012) (Bernal, 2013). In the United States and western Europe, drug-induced liver injury is the predominant cause of ALF, with acetaminophen (APAP) overdose being the most common cause of ALF (Lee, 2012) (Bernal, 2013). However, in 15% of adult cases of ALF, a specific cause cannot be identified (Lee, 2008). The progression and outcome of ALF can vary depending on the cause. The pathogenesis of ALF often follows general patterns, defined as hyperacute, acute, and subacute (O'Grady, 1993). APAP-induced and ischemic ALF are characterized by hyperacute liver failure, exhibiting a rapid burst of active injury, finite necrosis, and often associated with more favorable outcomes (Lee, 2008). On the other hand, most other forms of ALF, including viral hepatitis and cases of unknown etiology, are characterized by

acute and subacute liver failure. In these cases, the injury progresses over weeks and is long-lasting (O'Grady, 1993). These patients generally have a poorer prognosis and worse survival (Lee, 2008) (Blackmore and Bernal, 2015).

1.2.2 Symptoms of Acute Liver Failure. ALF was originally defined in 1970 as a severe, potentially reversible liver injury of any kind presenting with hepatic encephalopathy and coagulation defects in the absence of pre-existing liver disease (Trey, 1970). The duration and progression of symptoms can vary depending upon the etiology of ALF. However, there are general clinical signs and symptoms that often occur in ALF regardless of the cause, including hepatic encephalopathy, coagulopathy, massive hepatic necrosis, systemic inflammatory response syndrome (SIRS), and in severe cases multi-organ failure (Lee, 2008) (Bernal and Wendon, 2013). Patients with hepatic encephalopathy present with symptoms of confusion or disorientation (Munoz, 2014). As hepatic encephalopathy progresses, it can lead to intracranial hypertension and cerebral edema, which are associated with poor rates of survival (Bernal, 2013). Encephalopathy develops more rapidly in hyperacute ALF, where high grades of encephalopathy indicate a poor prognosis. However, in subacute ALF, even low grades of encephalopathy are associated with a poor outcome (Bernal, 2013). ALF patients also often present with coagulopathy of varying severity (Munoz, 2009). Coagulopathy is widely assessed by measuring the time it takes for blood to clot via the prothrombin time test. This result can be standardized when compared to the International Normalized Ratio (INR), and an INR greater than 1.5 is often observed in ALF (Munoz, 1991). However, significant bleeding in patients with ALF is rare, most likely due to a decreased hepatic synthesis of both procoagulant factors as well as anticoagulant factors (Macdougall, 1977) (Munoz, 2009). Patients with ALF can also develop systemic inflammatory response syndrome (SIRS). This condition is characterized by wide-spread inflammation occurring throughout the body, which is thought to be initiated by cytokines from the liver that spill over into the systemic circulation. Patients with SIRS exhibit elevated body temperature, heart rate, respiratory rate, and white blood cell counts (Bone,

1992). SIRS is associated with elevated levels of both pro- and anti-inflammatory cytokines, indicating dysregulation of the immune system (Antoniades, 2008). This condition leads to systemic vasodilation, increased risk of infection, and, in ALF patients, worsening of encephalopathy (Martin, 1994) (Marchant, 1995) (Rolando, 2000). As ALF progresses, other critical body systems begin to fail, including the cardiovascular system, the pulmonary system and the kidneys. This ultimately culminates in death (Munoz, 2014).

The liver is unique in its capacity to repair and recover after extensive surgical resection or after extensive injury produced by hepatotoxicants (Michalopoulos, 2007) (Mehendale, 2005). In cases of ALF, however, the regenerative capacity of the liver is often impaired. For instance, in patients with APAP-induced liver injury, a favorable outcome is determined in large part by the liver's capacity to regenerate (Schmidt, 2005). Patients with high blood levels of α -Fetoprotein, a marker of liver regeneration, recover without extensive intervention, whereas patients with low blood levels of α -Fetoprotein, indicating impaired liver regeneration, typically require a liver transplant or die. Other studies using a murine model of APAP toxicity have shown that stimulation of liver regeneration with growth factors, such as vascular endothelial growth factor (VEGF), can enhance hepatocyte regeneration and potentially prevent progression of injury (Donahower, 2010). This could be used as a new therapy for patients with markers indicating defective liver repair.

1.2.3 Acute Liver Failure Treatment Options in the Clinic. Treatment options for ALF are largely limited to supportive care and liver transplantation. Unfortunately, the rapid progression of ALF and the limited supply of transplantable livers severely restricts its use in ALF patients. In fact, less than 10% of all transplantable livers are transplanted into ALF patients (Germani, 2012). Given the limited availability of transplantable livers, prognostic evaluation is used to prioritize patients for liver transplantation. The criteria used for evaluation include the presence of encephalopathy and coagulopathy, the severity of the liver injury, as well as additional risk factors such as age (Simpson, 2009) (Lee, 2013). Supportive treatments

for ALF are aimed at managing stable metabolic and hemodynamic levels in order to promote hepatic regeneration and prevent complications (Bernal and Wendon, 2013) (Lee, 2013). The only therapeutic agent that is available to treat ALF is N-acetylcysteine (NAC) (Ichai, 2008) (Saito, 2010). Although NAC has been evaluated in ALF of diverse etiologies, it is most efficacious in the treatment of APAP-induced ALF.

1.3 Acetaminophen-induced Acute Liver Failure

- 1.3.1 Mechanism of APAP-induced Liver Injury. APAP is one of the most commonly used analgesic and antipyretic agents in the United States. Although APAP is considered safe at low, therapeutic doses (i.e., 4 g/day), APAP overdose, either accidental or intentional, results in approximately 56,000 emergency room visits, 26,000 hospitalizations and 458 deaths each year (Lee, 2004) (Lee, 2017). Furthermore, according to data from the U.S. Acute Liver Failure Study Group, APAP poisoning is responsible for approximately 50% of all cases of ALF in the United States (Lee, 2004). At low doses, APAP is rapidly metabolized in the liver and excreted into the urine by the kidneys. Under these conditions, APAP primarily undergoes glucuronidation via UDP-glucuronosyltransferases or sulfation via sulfotransferases to pharmacologically inactive conjugates. A small quantity of APAP can be oxidized to the hepatotoxic intermediate, N-acetyl-p-benzoquinone imine (NAPQI). However, at therapeutic doses, NAPQI is detoxified by glutathione. At toxic doses of APAP, though, glucuronidation and sulfation pathways become saturated, which shifts metabolism towards oxidation to NAPQI. High concentrations of NAPQI ultimately deplete glutathione, leading to the accumulation of NAPQI. At this point, NAPQI forms protein adducts and stimulates oxidative stress, mitochondrial permeability transition, and a loss of ATP, which culminates in the death of hepatocytes by necrosis (Hinson, 2010).
- 1.3.2 Treatment of APAP Overdose. Pharmacological treatment of APAP-induced acute liver injury is limited to N-acetylcysteine (NAC), which is a precursor of glutathione. It has been proposed that NAC increases the concentration of glutathione that is available for

conjugation to NAPQI, which prevents the further progression of injury (Lauterburg, 1983). In addition, it has been proposed that NAC may limit liver injury by scavenging of reactive oxygen species and promoting mitochondrial energy metabolism (Saito, 2010). However, because NAC works primarily by preventing APAP-induced liver damage, it is most efficacious when administered within the first 24 hours after APAP ingestion (Rumack, 1981) (Smilkstein, 1988). Clinically, when NAC is administered within 10 hours of APAP overdose, hepatotoxicity develops in only 6.1% of patients, while NAC administered 10-24 hours after APAP overdose results in 26.4% of patients developing liver injury (Smilkstein, 1988). Unfortunately, many overdose patients do not seek medical attention until this early, critical time has passed and liver injury becomes extensive. In these patients, treatment is largely limited to supportive care and liver transplantation. Nearly one-third of cases of APAP-induced ALF require a liver transplant, although many of these patients die before a suitable liver is identified (Lee, 2017). Even in those patients that do receive a transplant, one-year survival is 85% (Lee, 2008).

1.3.3 Macrophage Function in APAP-induced Liver Injury

normally present on the luminal side of the hepatic sinusoid. These cells detect, phagocytose, and degrade foreign materials, pathogens, and cellular debris that enter the liver largely through the portal circulation. A second, distinct population of hepatic macrophages was recently identified that resides just under the Glisson's capsule (Yona, 2013) (Sierro, 2017). Studies indicate that these macrophages protect the liver from pathogens that invade from the peritoneal cavity (Sierro, 2017). These two hepatic macrophage populations can be distinguished based upon their level of expression of CD11b, CX3CR1, and F4/80. Kupffer cells are F4/80^{hi}, CX3CR1-, and CD11b^{low} whereas macrophages adjacent to the Glisson's capsule are F4/80^{low}, CX3CR1hi, and CD11b^{hi} (Schulz, 2012) (Yona, 2013) (Sierro, 2017). Collectively, these two macrophage subtypes play an important role in regulating immune responses in the liver through antigen presentation and by releasing cytokines and chemokines that recruit and

activate other immune cell types. In addition, these cells contribute to liver regeneration by releasing growth factors and pro-mitogenic cytokines that stimulate hepatocyte and sinusoidal endothelial cell proliferation (Ju and Tacke, 2016). Overall hepatic macrophages can display distinct phenotypes and perform different functions depending on their origin and their polarization in a specific local environment (Varol, 2015).

1.3.3.2 Developmental Origins of Hepatic Macrophages. It was recently revealed that macrophages arise from two distinct developmental lineages (Varol, 2015). Kupffer cells arise from progenitor stem cells generated in the fetal yolk-sac early during development (Epelman, 2014). These cells migrate to the liver where they reside in the sinusoids and carry out the many functions discussed above. During homeostasis or after toxininduced liver injury, these cells are replenished through the local proliferation of mature Kupffer cells (Yona, 2013). Under conditions where a substantial loss of Kupffer cells occurs, such as after exposure to lethal irradiation, these cells can be replenished from bone marrow progenitors (Scott, 2016). Over time, the gene expression signature in these cells begins to mirror that of Kupffer cells. In contrast to Kupffer cells, hepatic macrophages that reside adjacent to the Glisson's capsule arise from bone marrow-derived, circulating monocytes generated from hematopoietic stem cells (Schulz, 2012) (Sierro, 2017). Similar to other macrophage populations, Kupffer cells and monocyte-derived hepatic macrophages demonstrate great phenotypic plasticity. Depending upon signals that they receive from the local environment, hepatic macrophages can produce proinflammatory cytokines and toxic mediators aimed at eliminating pathogens, or they can release cytokines and growth factors that stimulate liver repair and the resolution of inflammation (Antoniades, 2012).

1.3.3.3 Macrophage Phenotypes. Macrophages are commonly subdivided into two broad classifications based upon their phenotype. These two macrophage subpopulations are referred to as classically-activated macrophages (M1) and alternatively-activated macrophages (M2) (Goerdt, 1999). Whether macrophages adopt an M1 or M2 phenotype

depends largely on their adaptive response to different stimuli (Mills, 2000). For example, macrophages develop an M1 phenotype after exposure to bacterial lipopolysaccharide (LPS) or Th1 cytokines, such as interferon gamma (IFNy) and tumor necrosis factor alpha (TNFα), released during a bacterial infection. M1 macrophages produce microbicidal mediators, such as reactive oxygen species and proteases, and they release proinflammatory cytokines that recruit other immune cell types, such as neutrophils (Benoit, 2008). While M1 macrophages are important for protection from pathogens, dysregulation of these cells leads to the excessive production of pro-inflammatory cytokines and cytotoxic mediators that can damage host tissue. It is believed that this contributes to chronic inflammation that is critical for the pathogenesis of several diseases ranging from Parkinson's disease to cancer (Wynn and Vanella, 2016). In addition to an M1 phenotype, macrophages can develop an M2 phenotype in response to various Th2 cytokines, including interleukin (IL)-4, IL-10, and IL-13, as well as other stimuli, such as prostaglandins and apoptotic cells (Gordon, 2003). M2 macrophages produce mediators, such as transforming growth factor-β1 (TGF-β1) and IL-10 that attenuate inflammation through downregulation of proinflammatory cytokines and chemokines as well as downregulation of various MHC class II and co-stimulatory molecules in macrophages (Moore, 2001) (Couper, 2008). M2 macrophages also produce growth factors, such as platelet-derived growth factor (PDGF), TGF-β1, and VEGF that stimulate tissue repair by promoting cellular proliferation and blood vessel development (Wynn and Vanella, 2016). While macrophage phenotypes have largely been defined as proinflammatory M1 or anti-inflammatory M2, recent studies have indicated that this classification system is extremely simplified. In fact, macrophages are highly plastic and comprise a dynamic continuum of functional states depending upon the cues received from the local environment. In fact, studies have demonstrated that a macrophage may take part in both the inflammatory phase as well as the resolution and reparative phases after tissue injury (Porcheray, 2005) (Martinez, 2014). For

instance, this occurs in the liver after APAP overdose, where monocyte-derived macrophages, which rapidly accumulate in the liver, exhibit either an M1-like proinflammatory phenotype or an M2-like pro-restorative phenotype depending upon the particular phase of liver repair (Zigmond, 2014).

1.3.3.4 Functions of Kupffer Cells in APAP-induced Liver Injury.

Macrophages perform several important functions in the liver after APAP overdose, including production of immunomodulatory cytokines, phagocytosis of dead cell debris, and production of pro-mitogenic growth factors (Fig. 1.1) (Ju and Tacke, 2016). While it is clear that macrophages perform these critical functions, the importance of Kupffer cells to these processes has been a matter of debate. Early studies indicated a pathogenic role for Kupffer cells after APAP overdose. In these studies, treatment of mice with the macrophage inhibitor, gadolinium chloride, protected against APAP hepatotoxicity (Laskin, 1995). Subsequent studies indicated that inhibition of Kupffer cells with gadolinium chloride prevented production of reactive oxygen species and peroxynitrite after APAP overdose, leading to reduced liver toxicity (Michael, 1999). Accordingly, it was concluded that Kupffer cells were critical for liver toxicity after APAP overdose (Michael, 1999). More recent studies, however, which used clodronate-containing liposomes to fully deplete Kupffer cells demonstrated that Kupffer cell depletion exacerbated hepatic necrosis at 8 and 24 hours after an acute dose of APAP (Ju, 2002). This was associated with a reduction in the anti-inflammatory cytokine, IL-10 (Ju, 2002). In subsequent studies, it was demonstrated that IL-10 knockout mice have increased liver toxicity and mortality after APAP overdose (Bourdi, 2002). Collectively, it was concluded that IL-10, released from Kupffer cells, protected the liver from toxicity after APAP overdose. Although these studies demonstrate that Kupffer cells are an important source of anti-inflammatory cytokines (e.g., IL-10) after APAP overdose, studies have also shown that Kupffer cells are an important source of proinflammatory mediators (Su, 2000) (Wu, 2010). In support of this, a recent study using a murine model of APAP-induced liver injury, demonstrated that Kupffer cells release

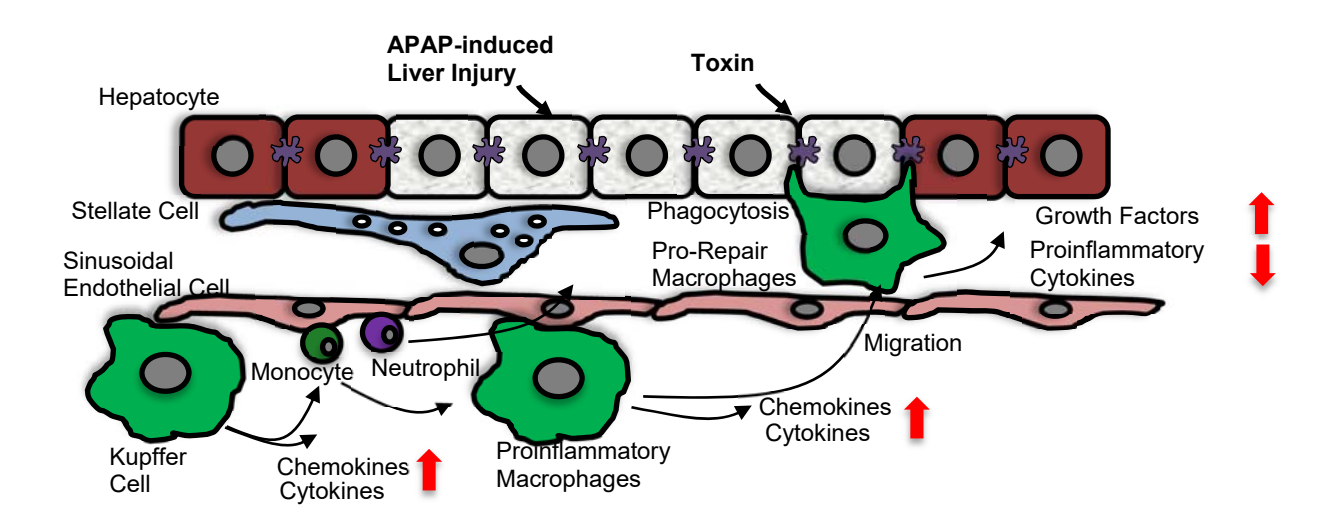


Figure 1.1 APAP-induced Liver Injury. Diagram of hepatic cell types and relative locations in the hepatic sinusoids. A general overview of known macrophage functions following acute liver injury are also shown, in which Kupffer cells become activated and secrete proinflammatory cytokines/chemokines that recruit several immune cells types to the liver. Monocytes migrate to the site of injury and traffic into the necrotic lesions, where they produce cytokines that amplify the immune response. During resolution of injury, the macrophages phagocytose dead cells and differentiate into pro-repair macrophages that produce anti-inflammatory cytokines and growth factors.

proinflammatory cytokines, including IL-1β, TNF-α, and IL-6, by 6 hours after APAP challenge (Fisher, 2013). The mechanism by which Kupffer cells are stimulated to produce proinflammatory cytokines after APAP overdose is not fully known, although our recent studies indicate that this process requires the fibrinolytic enzyme, plasmin, and the damage-associated molecular pattern molecule (DAMP), high-mobility group protein B1 (HMGB1). Interestingly, although Kupffer cells are important for early cytokine induction after APAP overdose, by 24 hours after APAP treatment, the population of resident Kupffer cells is substantially reduced by mechanisms that remain unclear (Dambach, 2002) (Zigmond, 2014). A similar phenomenon, called the "macrophage disappearance reaction" occurs in other tissues after injury (Barth, 1995). Although the importance of this to the pathogenesis of liver injury after APAP overdose is not known, Kupffer cell numbers return to baseline levels, through the local proliferation of remaining Kupffer cells, by 72 hours (Zigmond, 2014).

Injury. Studies have shown that a population of monocyte-derived macrophages, distinct from Kupffer cells, rapidly infiltrates the liver after APAP overdose (Fig. 1.1) (Holt, 2008). Kupffer cells and monocyte-derived macrophages can be distinguished by flow cytometry based upon their expression levels of F4/80 and CD11b (Leenen, 1994) (Holt, 2008). In APAP-treated mice, Kupffer cells are identified as a CD11b^{low} F4/80^{hi} population whereas monocyte-derived macrophages are identified as a CD11b^{hi} F4/80^{low} population that transiently appears in the liver 12 hours after APAP challenge (Holt, 2008). While Kupffer cells are resident to the liver, monocyte-derived macrophages are recruited to the liver in a chemokine-dependent manner.

Immunomodulatory chemokines are chemotactic mediators that stimulate trafficking of immune cells to sites of injury (Rossi, 2000). The chemokine (C-C motif) ligand 2 (CCL2), which acts by binding to its receptor C-C chemokine receptor type 2 (CCR2), is one of the most potent chemokines involved in the migration of monocytes and macrophages to tissues (Kurihara, 1997). After APAP overdose, hepatic expression of *Ccl2* is increased by 12

hours, consistent with the accumulation of CCR2-positive monocyte-derived macrophages (Dambach, 2002). A role for CCL2 in the recruitment of monocyte-derived macrophages to the liver after APAP overdose was shown by using *Ccr2* knockout mice. In these studies, there was a substantial reduction in monocyte-derived macrophages in the livers of *Ccr2* knockout mice when compared to wild-type controls (Holt, 2008) (Zigmond, 2014) (Yang, 2014). Interestingly, although similar levels of injury were observed in wild-type and *Ccr2* knockout mice following APAP challenge, there was a failure to clear necrotic cells from the livers of *Ccr2* knockout mice, indicating an important role for monocyte-derived macrophages in the clearance of dead cells from the liver (Holt, 2008).

Further studies identifying macrophage subsets in the livers of mice following APAP challenge have demonstrated the dynamic presence of three distinct macrophage subsets (Zigmond, 2014). In these studies, Ly6C and the chemokine (C-X3-C motif) receptor 1 (CX3CR1) were used to characterize different macrophage subsets (Lee, 2018). Kupffer cells, which are Ly6Clo CX₃CR1-, were significantly reduced at 24 hours after APAP challenge (i.e., macrophage disappearance reaction), while there was a dramatic increase in Ly6Chi CX₃CR1⁺ macrophages that were recruited to the liver in a CCR2- and M-CSF-dependent manner. By 72 hours, the dominant macrophage population in the liver was Ly6Clo CX3CR1+, which was distinct from the Kupffer cell population (Ly6Clo CX₃CR1-). Adoptive transfer experiments using green fluorescent protein- (GFP)-labeled monocytes determined that the infiltrating Ly6Chi CX3CR1+ macrophages ultimately gave rise to the Ly6CloCX₃CR1⁺ macrophage subset. Molecular profiling using microarray analysis revealed that the Ly6Chi CX3CR1+ macrophages expressed high levels of proinflammatory genes, indicating an M1-like phenotype, while the Ly6CloCX₃CR1⁺ macrophages expressed high levels of pro-restorative genes, indicating an M2like phenotype. The gene expression profile of Ly6CloCX₃CR1⁺ macrophages was distinct from Kupffer cells, which showed variable expression levels of different pro-restorative genes, including scavenger receptors and matrix metalloproteinases (MMPs) (Zigmond, 2014).

Although the various myeloid populations that enter the liver after APAP overdose have been well defined and some of their functions elucidated, the mechanisms that regulate macrophage dynamics in the context of APAP-induced liver injury, including trafficking, cytokine secretion, and phagocytosis, are not well understood and are a main focus of the studies in this dissertation. Elucidation of these mechanisms is important, as our studies indicate that these key functions of macrophages are disrupted in ALF and may contribute to a poor outcome in some ALF patients.

1.3.4 Impaired Macrophage Function in APAP-induced ALF Patients. ALF shares many similarities with septic shock, including the development of systemic inflammatory shock syndrome (SIRS), a debilitating condition that can progress to multi-organ failure and death. Approximately 60% of ALF patients develop SIRS, and studies have revealed that SIRS in APAP-induced ALF is associated with a high morbidity and mortality (Rolando, 2000) (Vaquero, 2003). SIRS is defined as a widespread abnormal inflammatory state occurring throughout the body (Antoniades, 2008). Patients with SIRS present with elevated body temperature, increased heart rate, increased respiratory rate, and/or increased white blood cell counts (Bone, 1992). SIRS develops when local inflammatory mediators, produced at the site of injury, "spill over" into the systemic circulation, producing widespread inflammation. In ALF patients with SIRS, several macrophage-derived pro-inflammatory cytokines, including TNF-α and IL-6, have been detected at high levels in the blood (Fig. 1.2) (Calandra, 1991) (Martin, 1994). In addition to SIRS, many ALF patients develop compensatory anti-inflammatory response syndrome (CARS) which is characterized by an increase in the circulating levels of anti-inflammatory cytokines, such as IL-10 and IL-4 (Friedman, 1997) (Antoniades, 2008). CARS can dampen the antigenpresenting and pathogen-killing capabilities of immune cells, including macrophages, putting ALF patients at high-risk of developing life-threatening infections (Antoniades, 2008). Paradoxically, CARS can occur simultaneously with SIRS in many ALF patients. In fact, ALF patients with elevated systemic levels of both proinflammatory and anti-inflammatory cytokines

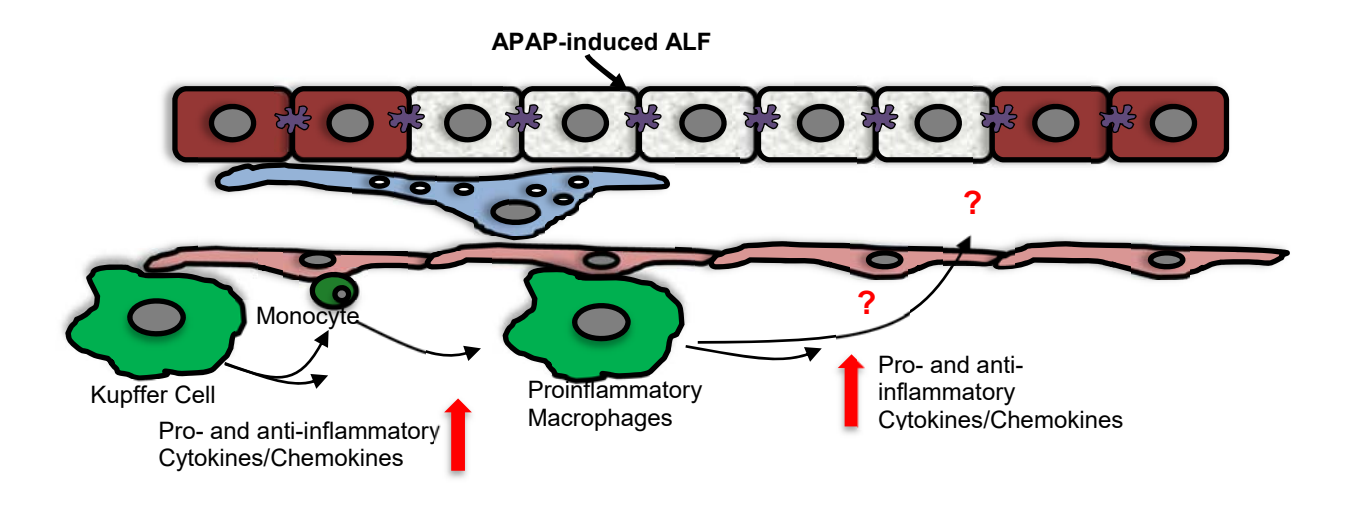


Figure 1.2 APAP-induced ALF. Features of macrophage dysregulation following APAP-induced ALF. In ALF, both pro- and anti-inflammatory cytokines and chemokines are produced at highly elevated, persistent levels. The effect on macrophage trafficking and phenotype remains unknown.

have the poorest prognosis (Berry, 2010). Because macrophages are the primary source of proand anti-inflammatory cytokines that are aberrantly produced in ALF patients, it has been
proposed that macrophage dysregulation is a common feature in the most critically ill ALF
patients (Antoniades, 2006) (Antoniades, 2008). Further, based upon the direct correlation
between cytokine levels and outcome in ALF patients, it has been proposed that macrophage
dysfunction contributes to the pathogenesis of ALF (Berry, 2010) (Antoniades, 2012) (Moore,
2017). While these conclusions are intriguing, they are largely based on correlative clinical
studies that do not mechanistically define how macrophage dysregulation occurs or whether it
contributes directly to the pathogenesis of ALF. To elucidate these mechanisms, studies must
be conducted in animal models of ALF. To date, only one study has provided insight into
whether macrophage dysfunction occurs in ALF and whether it impacts hepatic repair
(Bhushan, 2014).

1.3.5 Impaired Macrophage Function in an Animal Model of APAP-induced ALF.

Nearly every study that has assessed macrophage function in APAP overdose has used a dose of APAP that produces liver injury which is fully repaired. In other words, mice treated with these doses of APAP fully recover and do not develop features of ALF. This is in stark contrast to APAP overdose patients that develop ALF, where approximately one-third of these patients require a liver transplant or die (Lee, 2017). Because of this, it is not surprising that macrophage dysfunction has not been described previously in animal models of APAP overdose. A recent study, though, provided evidence that macrophage dysfunction may occur in mice given a dose of APAP that recapitulates many of the features of ALF in patients, including impaired liver regeneration (Bhushan, 2014). In this study, mice were treated with either a low dose of APAP (300 mg/kg) that is associated with normal repair and recovery, or a high dose of APAP (600 mg/kg). Surprisingly, the maximal area of necrosis produced by these two doses of APAP was identical. However, whereas necrotic cells were cleared from the livers of mice treated with 300 mg/kg APAP, clearance of dead cells from the liver was completely

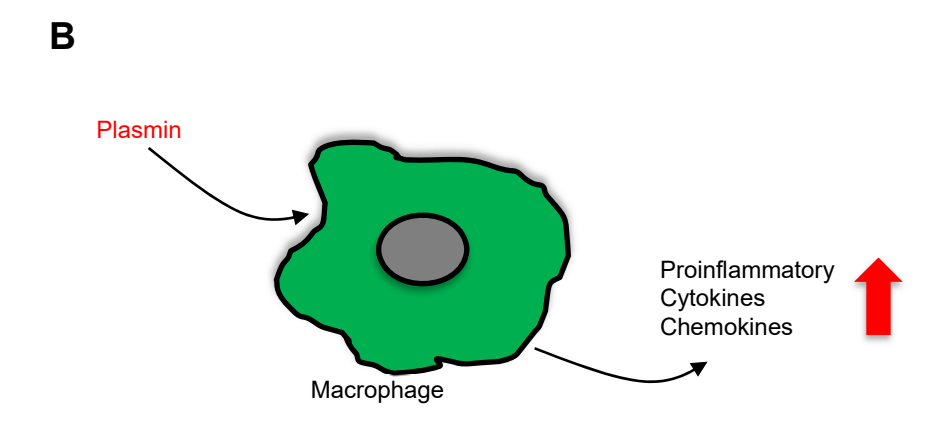
absent in mice treated with 600 mg/kg APAP. Because monocyte-derived macrophages are essential for the clearance of necrotic cells from the liver, this indicated that either macrophage recruitment and/or function was impaired in these mice (Holt, 2008). In addition, IL-6 levels were greater in mice treated with the high dose of APAP when compared to mice treated with the low dose. This is similar to what has been observed in ALF patients with the poorest prognosis (Fig. 1.2). Unfortunately, no additional analysis of macrophage function was conducted in these animal studies. Accordingly, as part of the studies in this dissertation, we evaluated macrophage function further in this animal model of APAP-induced ALF.

1.4 Plasmin Regulation of Macrophage Activation.

Plasminogen, the zymogen form of the proteolytic enzyme plasmin, is a 90 kDa plasma glycoprotein that is produced in the liver and circulates in the blood (Raum, 1980) (Law, 2013). Plasmin is a serine protease that cleaves several blood plasma proteins, extracellular matrix proteins and cellular proteins (Fig. 1.3). Plasmin is most well-known, however, for its role in fibrin degradation and clot removal. Plasminogen can exist in either a closed or an open conformation. Glu-plasminogen is a closed conformation that cannot be readily activated until it binds to fibrin or interacts with a cell surface. Glu-plasminogen can also be cleaved by plasmin during pre-activation to the alternative open conformation, Lys-plasminogen (Miles, 2003). Lysplasminogen has a more accessible activation loop that can be more readily activated. Plasminogen is converted to its active form, plasmin, through cleavage in the activation loop between residues Arg561 and Val562, resulting in a two-chain plasmin molecule (Robbins, 1967) (Law, 2013). The two main physiological plasmin activators are tissue-type plasminogen activator (tPA) and urokinase-type plasminogen activator (uPA). tPA enzyme activity is substantially increased in the presence of fibrin, which allows for the selective activation of plasminogen at sites of fibrin deposition (Cesarman-Maus, 2005). uPA activity occurs independent of fibrin and relies on binding of uPA to the uPA receptor or integrin $\alpha_{\rm M}\beta_2$ on the cell surface (Pluskota, 2004). In addition to these receptors, other receptors, including Annexin Plasminogen

PAIs \longrightarrow uPA \longrightarrow Fibrin α 2-antiplasmin \longrightarrow Plasmin

Fibrin



Degradation Products

Figure 1.3 Plasmin Activity and Regulation of Macrophages. (A) Diagram of important activators and inhibitors of plasminogen and plasmin activities. (B) Illustration of plasmin-mediated effects on macrophages.

A2, enolase-1, and the plasminogen receptor Plg-R(KT) bind plasminogen on the cell surface which enhances its activation by uPA (Godier and Hunt, 2013). Two major inhibitory pathways have been identified that regulate plasmin generation and activity. uPA and tPA are inhibited by the plasminogen activator inhibitors (PAI)-1 and (PAI)-2, and plasmin is inhibited by α 2-antiplasmin in the blood as well as other antiproteases, such as α 2-macroglobulin (Cesarman-Maus, 2005).

In addition to binding to fibrinogen, plasminogen also binds to a variety of cell surface molecules referred to as plasminogen receptors. Binding of plasminogen to fibrinogen and its receptors greatly enhances and localizes plasmin generation. In addition, interaction of plasmin with a few of these receptors has been shown to activate intracellular signaling pathways. (Gong, 2001). Although several putative plasminogen receptors have been identified, only a few of these have been implicated in inflammatory processes (Godier and Hunt, 2013). The heterotetrameric complex annexin A2-S100A10 is made up of a dimer of S100A10 molecules bound to two molecules of annexin A2. Studies have shown that in monocyte-derived macrophages, annexin A2-S100A10 functions as a receptor for plasmin and is required for plasmin-induced signaling (Laumonnier, 2006). Signaling through annexin A2 has been shown to stimulate upregulation of several proinflammatory cytokines in human monocyte-derived macrophages. Upregulation of these cytokines required activation of mitogen-activated protein kinases (MAPKs) and NF-κB (Swisher, 2007). Studies have also demonstrated that plasmin activates protease-activated receptor-1(PAR-1). PAR-1 is a G-protein coupled receptor that is activated by several proteases. Cleavage of PAR-1 produces a tethered ligand that binds to the receptor and activates signaling (Coughlin, 1999). Studies have shown that treatment of mice with selective PAR-1 antagonists prevents the plasmin-mediated migration of leukocytes into the pleural cavity, an effect that was dependent upon MAPK- and NF-κB-dependent release of Ccl2 (Carmo, 2014). Additional plasmin receptors known to facilitate signaling in macrophages

include enolase-1, histone H2B, and Plg-Rkt (Wygrecka, 2009) (Miles, 1991) (Miles, 2017) (Lighvani, 2011) (Godier and Hunt, 2013).

Several studies have shown that plasmin can regulate various functions of monocytes and macrophages, including migration, phagocytosis, and cytokine production. Plasminogen has been shown to promote macrophage migration and recruitment to the lungs and peritoneal cavity during inflammation (Ploplis, 1998) (Wygrecka, 2009). In the liver, plasminogen deficiency impairs the recruitment of macrophages to the liver after a stab injury (Kawao, 2010). Furthermore, studies have demonstrated that plasmin stimulates macrophage phagocytosis (Rosenwald, 2012) (Das, 2014), and in the liver, deficiency in plasminogen prevents the clearance of dead cells after acute carbon tetrachloride-induced injury (Bezerra, 1999). Lastly, several studies have demonstrated plasmin's ability to increase expression of cytokines, including TNF-α, IL-6, IL-1α/β, and chemokines, including CCL2, in monocyte-derived macrophages (Weide, 1996) (Syrovets, 2001) (Burysek, 2002). This enhanced expression occurs through activation of various signaling pathways and transcription factors, including MAP kinases, JAK/STAT, NF-κB, and AP-1 (De Sousa, 2005) (Burysek, 2002) (Syrovets, 2001). While these studies demonstrate an important role for plasmin in regulating macrophage activation, it is not yet known whether plasmin regulates macrophage function after APAPinduced liver injury.

1.5 Purpose

ALF remains a severe and often unpredictable disease with a high mortality rate (Bernal, 2013). In the United States, APAP overdose is the most common cause of ALF, with around 50% of ALF cases caused by APAP overdose (Lee, 2013) (Bernal, 2013). At present, administration of NAC is the only effective treatment option for APAP-induced ALF in patients, although it requires dosing soon after APAP overdose in order to be efficacious (Smilkstein, 1988) (Saito, 2010). Therefore, it is imperative that we investigate the mechanisms involved in the pathogenesis of ALF in order to uncover better treatment options.

Clinical studies have revealed that macrophage dysregulation is a common feature in ALF patients, especially those with the poorest outcome (Antoniades, 2008) (Bhushan, 2014). It has been proposed that macrophage dysregulation leads to high systemic levels of both proand anti-inflammatory cytokines in ALF patients (Antoniades, 2008). While it is well established that this is associated with a poor prognosis in ALF patients, the cause of macrophage dysregulation and excessive cytokine production remains unknown. Further, whether macrophage dysregulation impacts liver repair and the progression of ALF remains unknown. Before these questions can be answered, though, the mechanisms that regulate macrophage functions in the liver during conditions of normal repair need to be better characterized. Only then, will it be possible to determine how macrophage dysregulation occurs in ALF, a condition where liver repair fails to occur. Therefore, the goals of the present studies were to investigate macrophage function in mice given a dose of APAP associated with normal liver repair and then to determine how macrophage function was affected in mice given a dose of APAP that produces many features of ALF, including failed liver repair. The ultimate goal from these studies is to identify ways to reverse macrophage dysregulation in APAP-induced ALF such that liver repair and function is fully restored.

Chapter 2

Dichotomous Role of Plasmin in Regulation of Macrophage Function after Acetaminophen Overdose

2.1 Abstract

Kupffer cells and monocyte-derived macrophages are critical for liver repair after acetaminophen (APAP) overdose. These cells produce pro-mitogenic cytokines and growth factors, and phagocytose dead cell debris, a process that is critical for resolution of inflammation. The factors that regulate these dynamic functions of macrophages after APAP overdose, however, are not fully understood. The hypothesis was tested that the fibrinolytic enzyme, plasmin, is a key regulator of macrophage function after APAP-induced liver injury. In these studies, inhibition of plasmin in mice with tranexamic acid delayed upregulation of proinflammatory cytokines after APAP overdose. In culture, plasmin directly, and in synergy with high-mobility group B1 (HMGB1), stimulated Kupffer cells and bone marrow-derived macrophages to produce cytokines by a mechanism that required NF-κB. Inhibition of plasmin in vivo also prevented trafficking of monocyte-derived macrophages into necrotic lesions after APAP overdose. This prevented phagocytic removal of dead cells, prevented maturation of monocyte-derived macrophages into F4/80-expressing macrophages, and prevented termination of proinflammatory cytokine production. Our studies reveal further that phagocytosis is an important stimulus for cessation of pro-inflammatory cytokine production as treatment of proinflammatory, monocyte-derived macrophages, isolated from APAP-treated mice, with necrotic hepatocytes decreased expression of pro-inflammatory cytokines. Collectively, these studies demonstrate that plasmin is an important regulator of macrophage function after APAP overdose.

2.2 Introduction

Acetaminophen (APAP) is a commonly used over-the-counter analgesic and antipyretic that is safe when taken as directed. Unfortunately, though, thousands of hospitalizations and hundreds of deaths occur each year due to either intentional or accidental overdose (Nourjah, 2006). When taken at high doses, APAP produces hepatocellular injury that can rapidly progress to acute liver failure (ALF), a condition with a high rate of mortality (Lee, 2008).

Pharmacological therapies for APAP overdose are limited to N-acetyl-cysteine (NAC) which is highly efficacious when administered early after APAP ingestion (Rumack, 1981) (Smilkstein, 1988). Unfortunately, many patients do not seek medical attention until liver injury is extensive and NAC is no longer effective.

Monocytes and macrophages play a key role in liver repair after APAP overdose. Early after the onset of liver injury, Kupffer cells, the resident macrophages of the liver, become activated and secrete proinflammatory cytokines that recruit several immune cell types, including proinflammatory monocytes, to the liver (Fisher, 2013). The recruited monocytes migrate within the hepatic sinusoids and ultimately traffic into the necrotic lesions where they produce cytokines that amplify the immune response and produce toxic molecules aimed at killing invading pathogens (Holt, 2008) (Dambach, 2002) (Zigmond, 2014). Upon resolution of the injury, the proinflammatory monocytes phagocytose dead cells and differentiate into prorepair macrophages that produce anti-inflammatory cytokines and pro-regenerative growth factors (Holt, 2008) (Zigmond, 2014). The mechanisms that regulate monocyte/macrophage trafficking, cytokine secretion, and phagocytosis in the context of APAP-induced liver injury are not fully understood. A full understanding of these mechanisms is important, as recent studies in patients and in mouse models indicate that cytokine production and phagocytosis are dysregulated in ALF (Berry, 2010) (Antoniades, 2008) (Bhushan, 2014). These studies raise the intriguing possibility that monocyte/macrophage dysfunction may contribute to failed recovery of liver function in some APAP overdose patients. Accordingly, greater insight into the mechanisms that regulate monocyte/macrophage function could provide insight into the cause of monocyte/macrophage dysregulation and failed liver regeneration in certain ALF patients.

Several studies have demonstrated that the fibrinolytic enzyme, plasmin, regulates various monocyte and macrophage functions. For instance, plasmin regulates macrophage recruitment to the lungs and peritoneum during inflammatory episodes (Ploplis, 1998)

(Wygrecka, 2009), and plasmin stimulates macrophage phagocytosis and cytokine production *in*

vitro (Das, 2014) (Borg, 2015) (Sugimoto, 2017). In the liver, deficiency in plasminogen, the zymogen for plasmin, impairs macrophage recruitment after stab injury and prevents clearance of dead cells after carbon tetrachloride-induced liver injury (Bezerra, 1999) (Kawao, 2010). While these studies indicate a key role for plasmin in regulation of macrophage function, it is not known whether plasmin regulates macrophage function after APAP overdose. Accordingly, in the following studies, the hypothesis was tested that plasmin is critical for regulation of macrophage function after APAP overdose.

2.3 Materials and Methods

2.3.1 Animal Treatments. 6-12 week old male C57BL/6 (Jackson Laboratories, Bar Harbor, ME), Annexin A2 knockout, protease-activated receptor-1 (PAR-1) knockout mice, and hepatocyte-specific HMGB1 knockout mice were used for all studies. Annexin A2 knockout and PAR-1 knockout mice were described previously (Ling, 2004) (Griffin, 2001). Hepatocyte-specific HMGB1 knockout mice were described previously (Deng, 2018). Mice were housed in a 12 hr light/dark cycle under controlled temperature (18-21°C) and humidity. Food (Rodent Chow; Harlan-Teklad) and tap water were allowed *ad libitum*.

For *in vivo* treatment, mice were fasted for approximately 16 hours prior to APAP injection. Mice were injected with 300 mg/kg APAP (Sigma-Aldrich, St. Louis, MO) or sterile saline by intraperitoneal injection and food returned immediately after APAP challenge. For studies using tranexamic acid, mice were injected with 1200 mg/kg Tranexamic Acid (Spectrum Chemical, New Brunswick, NJ) or endotoxin-free water vehicle (G Biosciences, St. Louis, MO) beginning 2 hours after APAP treatment. Tranexamic acid was administered twice daily following the initial treatment.

2.3.2 Sample Collection. Mice were anesthetized using Fatal-Plus Solution (Vortech Pharmaceuticals, Dearborn, MI). Blood was collected from the inferior vena cava and serum collected. The activity of alanine aminotransferase was measured in the serum by using the Infinity ALT (GPT) Liquid Reagent (Thermo-Fisher Scientific, Waltham, MA). The livers were

removed, and a portion was fixed 10% neutral-buffered formalin. The tissues were embedded in paraffin and sections of liver were stained with either hematoxylin and eosin, PCNA, or Ly6G antibody. The area of necrosis was quantified as described by us previously (Mochizuki, 2014). Additional pieces of liver were homogenized in TRIzol Reagent (Thermo-Fisher Scientific) for RNA isolation.

2.3.3 Isolation and Culture of Cells. To isolate Kupffer cells, livers from C57BL/6 mice (Jackson Laboratories) were perfused and digested with collagenase (Collagenase H, Sigma-Aldrich) as described previously (Kim, 2006). Following removal of hepatocytes by centrifugation, the non-parenchymal cells were centrifuged at 300 g for 10 minutes. 1 X 10⁸ cells nonparenchymal cells were resuspended in 60 μl of MACS Buffer (2.5 g bovine serum albumin, 0.416 g EDTA, and 500 mL PBS) containing 12 μl biotinylated anti-F4/80 antibody (Miltenyi Biotec, Bergisch Gladbach, Germany). The cell suspension was incubated for 10 minutes at 4°C and then washed by adding 10 ml of MACS buffer and centrifugation (300 g for 10 minutes). Streptavidin microbeads (Miltenyi Biotec), diluted 1:10 in 60 μl of MACs buffer, were added to the non-parenchymal pellet. Cells were resuspended and incubated at 4 °C for 10 mins and then washed by adding 10 ml of MACS buffer and centrifugation (300 g for 10 minutes). The pellet was resuspended with 500 μl MACS Buffer and applied to MACS LS columns (Miltenyi Biotec). The column was rinsed 3 times with 3 ml MACS buffer. Kupffer cells were collected by removing the column from the midiMACS Separator and rinsing the column with 5 ml of MACS buffer.

For generation of bone marrow-derived macrophages, bone marrow was isolated from the femurs of mice and cultured in RPMI media containing 10% fetal bovine serum (FBS), Penicillin/Streptomycin, and 10 ng/ml recombinant mouse macrophage colony-stimulating factor (M-CSF) (Biolegend, San Diego, CA). On day 4 of culture, the media was replaced with fresh plating medium. Cells were harvested 7 days after plating.

Kupffer cells and bone marrow derived macrophages were plated in serum-free RPMI media. The cells were treated with 100 nM mouse plasmin (Haematologic Technologies, Essex Junction, VT) or human plasma-derived plasminogen (R&D Systems, Minneapolis, MN, <1.0 EU endotoxin per mg of protein). For studies in which cells were cultured with both plasmin and HMGB1, cells were treated with plasmin for 10 minutes followed by addition of 100 ng/ml recombinant human HMGB1 (R&D Systems, <1.0 EU endotoxin per mg of protein). For in vitro studies with tranexamic acid, cells were treated with 1 mM tranexamic acid followed by treatment with plasmin. For inactivation of plasmin, plasmin was incubated with 1 µM D-Val-Phe-Lys chloromethyl ketone (Sigma-Aldrich) for 30 minutes at 37°C prior to addition to cells. Ly6Chi monocytes were isolated from the livers of mice treated with 300 mg/kg APAP for 24 hours. Following removal of hepatocytes, non-parenchymal cells were centrifuged at 300 g for 10 minutes. ACK Buffer (Lonza, Basel, Switzerland) was used to lyse red blood cells. The nonparenchymal fraction was centrifuged at 300 g for 5 mins and resuspended in 60 µl of biotin labeled anti-Ly6c mouse antibody (Miltenyi Biotec) diluted 1:10 in MACs buffer and incubated at 4 °C for 10 minutes. Next, the cells were rinsed using 10 mL MACs buffer and centrifuged at 300 x g for 10 mins. Streptavidin microbeads (Miltenyi Biotec), diluted 1:10 in 60 µl of MACs buffer, were added to the non-parenchymal cell pellet. Cells were resuspended and incubated at 4 °C for 10 mins. Following incubation, the cells were added to MACS LS columns as described above. Ly6chi monocytes, collected from the column, were cultured in serum free Williams' Medium E containing penicillin/streptomycin.

Hepatocytes were isolated from the livers of C57BL/6 mice as described by us previously (Kim, 2006). The cells were diluted to 2.5 X 10⁵ in serum free Williams' Medium E and then made necrotic by 3 cycles of freeze thaw at -80°C. Cell lysis was confirmed by trypan blue staining and was 100%.

- 2.3.4 LAL Assay. Endotoxin was measured in the plasmin, RPMI media (Sigma-Aldrich) and phosphate buffered saline (Sigm-Aldrich) by using the LAL assay following the manufacturer's recommendations (Thermo-Fisher Scientific). The following concentrations of endotoxin were measured: RPMI media: 0.16 EU/mI; PBS: 0.11 EU/mI; Plasmin: 0.13 EU/mI. These concentrations of endotoxin are below those needed to stimulate upregulation of tumor necrosis factor-α (TNF-α) in monocytes and macrophages (Schwarz, 2014).
- 2.3.5 Immunohistochemistry. Immunofluorescence was used to detect F4/80 and CD68 as described by us previously (Mochizuki, 2014). Briefly, 8 μm frozen liver sections were fixed in 4% formalin for 10 minutes followed by blocking in 10% goat serum. The sections were then incubated with rat anti-F4/80 antibody (Bio-Rad) diluted 1:500 or rat anti-CD68 antibody (Bio-Rad, Hercules, CA) diluted 1:500. The sections were then incubated with goat anti-rat secondary antibodies conjugated to Alexa Fluor 488 or 594 (diluted 1:500, Thermo-Fisher Scientific).

Immunofluorescence was also used to detect Ly6C (green) and F4/80 (red) in cultured Ly6Chi F4/80neg monocytes. The cells were fixed in 10% formalin followed by incubation with Fc blocking buffer (BD Biosciences, San Jose, CA; diluted 1:20) for 10 mins at 4 °C. The cells were then incubated overnight at 4°C with either anti-Ly6c antibody conjugated to Alexa 488 or anti-F4/80 antibody conjugated to Alexa 594 antibodies (diluted 1:50, BioLegend).

Neutrophils were detected in sections of formalin-fixed, paraffin-embedded liver by detecting Ly6G (BioXCell, Clone 1A8, West Lebanon, NH). Proliferating hepatocytes were quantified by detecting proliferating cell nuclear antigen (PCNA, antibody from Abcam, Cambridge, United Kingdom).

2.3.6 Western Blot. Macrophages were lysed with RIPA buffer. Protein was separated on a 4-20% polyacrylamide gel (Bio-Rad) and transferred to PVDF membrane. The membranes were incubated with anti-phospho p38, anti-total p38, anti-phospho ERK1/2, anti-total ERK1/2,

anti-phospho IkB, anti- total IkB, anti-phospho JNK, anti-total JNK, anti-phospho AKT, or anti-total AKT using the recommended dilutions (all antibodies from Cell Signaling Technology, Danvers, MA). Membranes were incubated with secondary antibody conjugated with horseradish peroxidase (Sigma-Aldrich) and protein bands were detected using Clarity Western ECL Substrate (Bio-Rad) on a LI-COR Odyssey Fc (LI-COR Biosciences, Lincoln, NE).

2.3.7 Flow Cytometry. Non-parenchymal cells and purified Ly6chi monocytes were isolated using protocols described above. Following isolation, cells were washed and resuspended with FACs buffer (PBS, 1% FBS). The cells were then incubated with Fc blocking buffer (BD Biosciences; diluted 1:20) for 10 mins at 4 °C. Next, cells rinsed were centrifuged at 300 x g for 5 mins to pellet. The cells were then incubated with anti-F4/80/Alexafluor-488 and anti-Ly6c/PE for 30 minutes at 4 °C. In a separate study, the cells were incubated with anti-CD45/PE/Cy7 anti-CD68/Alexafluor-594, and anti-F4/80/Alexafluor 488 for 30 minutes at 4 °C. All antibodies were purchased from Biolegend. Following incubation, cells were washed twice and fixed in formalin (Sigma-Aldrich) for 15 mins at 4 °C. After cells were fixed, they were washed twice and resuspended using FACs buffer. The fluorescence was then detected using an Attune NxT flow cytometer from Life Technologies and the signal was quantified using Attune NxT software (Life Technologies, Carlsbad, CA).

2.3.8 Real-Time PCR. RNA was isolated from liver samples using TRIzol Reagent (Thermo-Fisher Scientific) or from cell culture samples by using the E.Z.N.A Total RNA Kit I (Omega Bio-Tek) according to manufacturer's instructions. Real-time PCR was performed as described by us previously (Kim, 2006). The following primer sequences were used: TNF-α: Forward- 5'-AGGGTCTGGGCCATAGAACT-3', Reverse- 5'-CCACCACGCTCTTCTGTCTAC-3'; Cxcl1: Forward- 5'-TGGCTGGGATTCACCTCAAG-3', Reverse- 5'-CTCAGACAGCGAGGCACATC-3', Reverse- 5'-CTCAGACAGCGAGGCACATC-3', Reverse- 5'-CCTCAACGGAAGAACCAAAGAG-3'; Ccl2: Forward- 5'-CTCAGACAGCGAGGCACATC-3',

CCTGCTGTTCACAGTTGCC-3', Reverse- 5'-ATTGGGATCATCTTGCTGGT-3'; Rpl13a: Forward- 5'-GACCTCCTCCTTTCCCAGGC-3', Reverse- 5'-AAGTACCTGCTTGGCCACAA-3'.

- 2.3.9 Luminex Immunoassay. Protein levels were measured in cell culture supernatants and serum samples by using the Bio-Plex Pro assay Kit (Bio-Rad). The samples were analyzed on a Luminex 200 System.
- **2.3.10 Statistical Analysis.** Results are presented as the mean + SEM. Data were analyzed by a one-way or two-way Analysis of Variance (ANOVA) where appropriate. Data expressed as a percentage were transformed by arcsine square root prior to analysis. Comparisons among group means were made using the Student-Newman-Keuls test. The criterion for significance was p < 0.05 for all studies. A minimum of an n=5 per group were used for *in vivo* studies. *In vitro* studies were repeated a minimum of three times with cells isolated from separate groups of mice.

2.4 Results

2.4.1 Plasmin inhibition suppresses early cytokine induction after APAP overdose.

To investigate the role of plasmin in regulation of monocyte and macrophage function after APAP overdose, plasmin was inhibited with the FDA approved plasmin inhibitor, tranexamic acid. Mice were treated with tranexamic acid beginning 2 hours after APAP administration to prevent interference with APAP metabolism. Treatment of mice with APAP and vehicle caused a time-dependent increase in serum ALT activity that was unaffected by cotreatment with tranexamic acid (Fig. 2.1A). By 8 hours after treatment with APAP, mRNA levels of the proinflammatory cytokines and chemokines, TNF- α , Cxcl1, and Cxcl2, were increased (Fig. 2.1B-D). Cotreatment with tranexamic acid completely prevented upregulation of all three cytokine/chemokines (Fig. 2.1B-D). Similarly, serum levels of Ccl2 protein, a monocyte/macrophage chemokine, were lower in mice treated with APAP and tranexamic acid.

2.4.2 Plasmin stimulates proinflammatory cytokine production by Kupffer cells and bone marrow-derived macrophages. To determine the mechanism by which plasmin

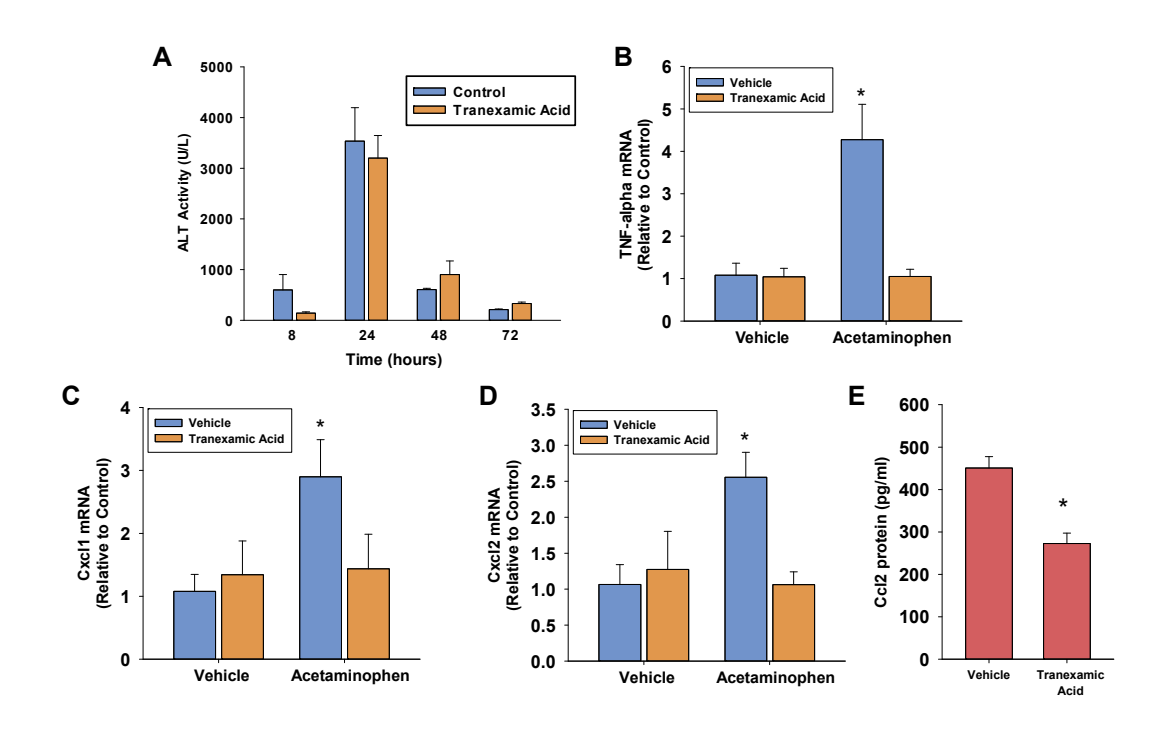


Figure 2.1: Plasmin Inhibition Suppresses Early Cytokine Induction after APAP

Overdose. Mice were treated with 300 mg/kg APAP followed by treatment with tranexamic acid as detailed in the methods. (A) ALT activity was measured at the indicated times. mRNA levels of (B) TNF-a, (C) Cxcl1, and (D) Cxcl2 were measured 8 hours after APAP treatment. (E) Ccl2 protein was measured in the serum. Data are expressed as mean \pm SEM; n = 5 mice per group. *Significantly different from vehicle-treated mice.

stimulates cytokine induction after APAP overdose, we first investigated whether plasmin directly increases expression of cytokines in macrophages. To investigate this, Kupffer cells and bone marrow-derived macrophages (BMMs) were isolated from wild-type C57BL/6 mice and treated with 100 nM plasmin. This concentration of plasmin is pathologically relevant as the plasma concentration of plasminogen, the zymogen for plasmin, is approximately 1.4 μM in mice. Treatment of Kupffer cells (Fig. 2.2A-C) and BMMs (Fig. 2.2E-F) with plasmin increased expression of TNF-α, Cxcl1, and Cxcl2. In addition, plasmin increased production of Ccl2 protein by BMMs (Fig. 2.2G), and stimulated the formation of extensive pseudopodia, a characteristic of activated macrophages (Fig. 2.2D). Upregulation of cytokines (Fig. 2.2H and I) and formation of pseudopodia (data not shown) were inhibited by the plasmin inhibitors, D-Val-Phe-Lys chloromethyl ketone (Fig. 2.2H) and tranexamic acid (Fig. 2.2I), indicating a need for plasmin enzyme activity. Similar to plasmin, plasminogen caused a dose-dependent increase in cytokine mRNA levels (Fig. 2.2J-L).

2.4.3 Activation of signal transduction pathways in plasmin-treated macrophages.

Plasmin activated p38, Erk1/2, and Jnk in BMMs at 2 hrs (Fig. 2.3A). Further, plasmin treatment increased phosphorylation of IκB, indicating activation of NF-κB (Fig. 2.3A). Interestingly, plasmin decreased Akt phosphorylation in BMMs (Fig. 2.3A). Pretreatment of BMMs with the IκB kinase 2 inhibitor, TPCA1, completely prevented upregulation of TNF- α by plasmin (Fig. 2.3B). By contrast, inhibition of p38 signaling (SB203580, Fig. 2.3C), Jnk signaling (SP600125, Fig. 2.3D), or Erk1/2 signaling (PD98059, Fig. 2.3E) did not affect induction of TNF- α by plasmin. Similar results were observed for Cxcl1 and Cxcl2 (data not shown).

Studies have indicated that plasmin may stimulate signaling in cells by activation of either annexin A2 or protease-activated receptor-1 (PAR-1) (Carmo, 2014) (Laumonnier, 2006). To investigate this in macrophages, BMMs were isolated from either annexin A2 or PAR-1

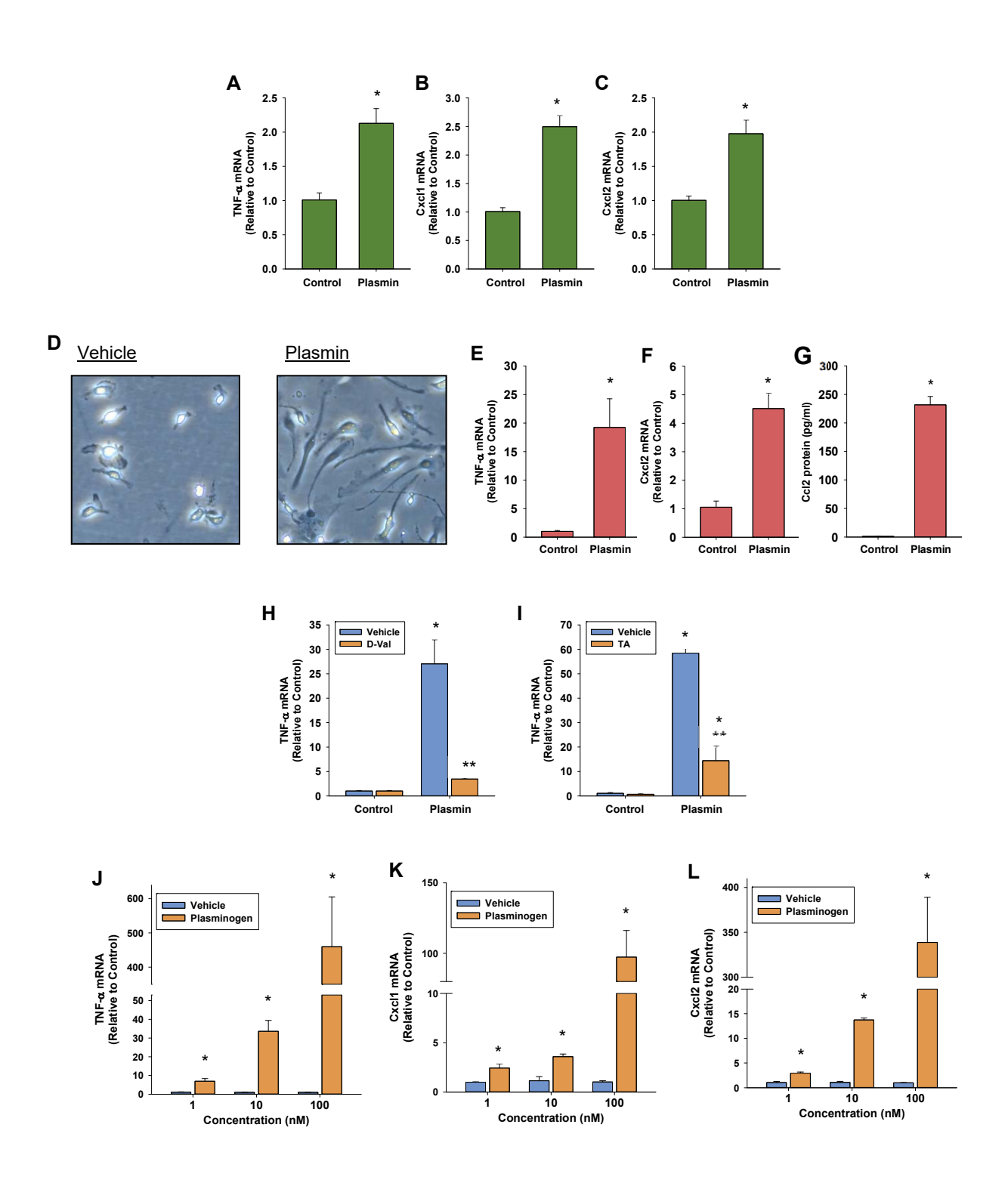


Figure 2.2: Plasmin Stimulates Proinflammatory Cytokine Production by Macrophages.

(A-C) Kupffer cells and (E-G) BMMs were treated with 100 nM plasmin. mRNA levels of the indicated cytokines were measured 6 hours later. (D) Photomicrographs of BMMs treated

Figure 2.2 (cont'd)

with vehicle or plasmin for 18 hours. BMMs were treated with 100 nM plasmin in the presence or absence of (H) D-Val-Phe-Lys chloromethyl ketone or (I) tranexamic acid. TNF- α mRNA levels were quantified. (J-L) BMMs were treated with vehicle or the indicated concentration of plasminogen. mRNA levels of the indicated cytokines were measured 6 hours later. *Significantly different from vehicle-treated cells. **Significantly different from cells treated with plasmin and vehicle. Data are expressed as mean \pm SEM; n = 3.

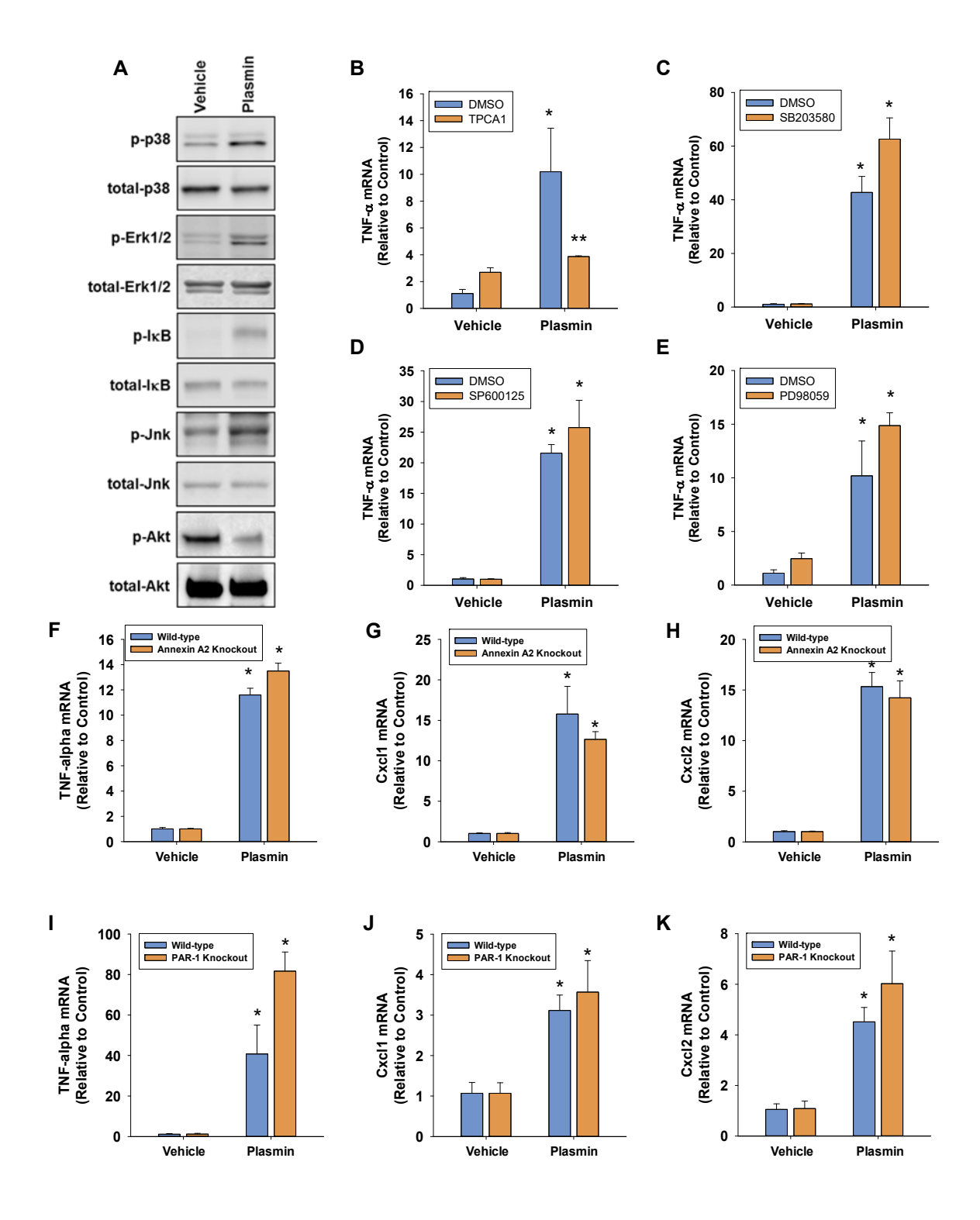


Figure 2.3: Plasmin-activated Signaling Pathways in Macrophages. (A) BMMs were treated with plasmin for 1 hour. Various signaling pathways were quantified by western blot. (B-E) BMMs were treated with the indicated inhibitor or DMSO followed by treatment with

Figure 2.3 (cont'd)

plasmin 30 minutes later. TNF-a mRNA levels were measured 6 hours later. BMMs were isolated from (F-H) wild-type and annexin A2 knockout mice or (I-K) wild-type and PAR-1 knockout mice and treated with plasmin. mRNA levels of the indicated cytokines were measured 6 hours later. *Significantly different from vehicle-treated cells. **Significantly different from cells treated with plasmin and vehicle in (B) or significantly different from wild-type cells treated with plasmin in (I). Data are expressed as mean \pm SEM; n = 3.

knockout mice. As shown in Figs. 2.3F-K, neither loss of annexin A2 nor PAR-1 affected upregulation of cytokines by plasmin.

2.4.4 HMGB1 enhances activation of macrophages by plasmin. Recent studies have revealed that the damage-associated molecular pattern molecule (DAMP), high mobility group box 1 (HMGB1), contributes to macrophage activation in the liver after APAP overdose (Huebener, 2015). To examine this further, Kupffer cells and BMMs were isolated and treated with either recombinant HMGB1 or necrotic primary mouse hepatocytes, which contain HMGB1. As shown in Fig. 2.4A and B, neither HMGB1 nor necrotic hepatocytes increased expression of TNF- α in Kupffer cells or BMMs. As demonstrated earlier, though, plasmin increased expression of TNF- α in both cell types. Next, we treated Kupffer cells with increasing concentrations of HMGB1. As shown in Fig. 2.4C, concentrations of HMGB1 as high as 500 ng/ml did not increase expression of TNF-α. By comparison, blood levels of HMGB1 are approximately 4 ng/ml in APAP-induced ALF patients and approximately 175 ng/ml in mice treated with a high dose of APAP (530 mg/kg) (Antoine, 2009). Because of the apparent importance of both plasmin and HMGB1 in macrophage activation in vivo, we tested the hypothesis that these two mediators interact to fully activate macrophages. As shown in Fig. 2.4D-E, plasmin increased TNF- α and Cxcl1 mRNA levels, whereas, HMGB1 alone did not. Interestingly, HMGB1 synergistically enhanced upregulation of these cytokines by plasmin, supporting an interaction between these inflammatory mediators. In addition to mRNA levels, Ccl2 protein levels were synergistically increased by the combination of plasmin and HMGB1 (Fig. 2.4F). Similar to recombinant HMGB1, necrotic hepatocytes from wild-type mice, which did not activate macrophages directly (Fig. 2.4A and B), enhanced upregulation of proinflammatory cytokines by plasmin, whereas necrotic hepatocytes from hepatocyte-specific HMGB1 knockout mice did not (Fig. 2.4G-I). Because NF-kB activation was required for upregulation of cytokines by plasmin, we investigated whether it was also required for the

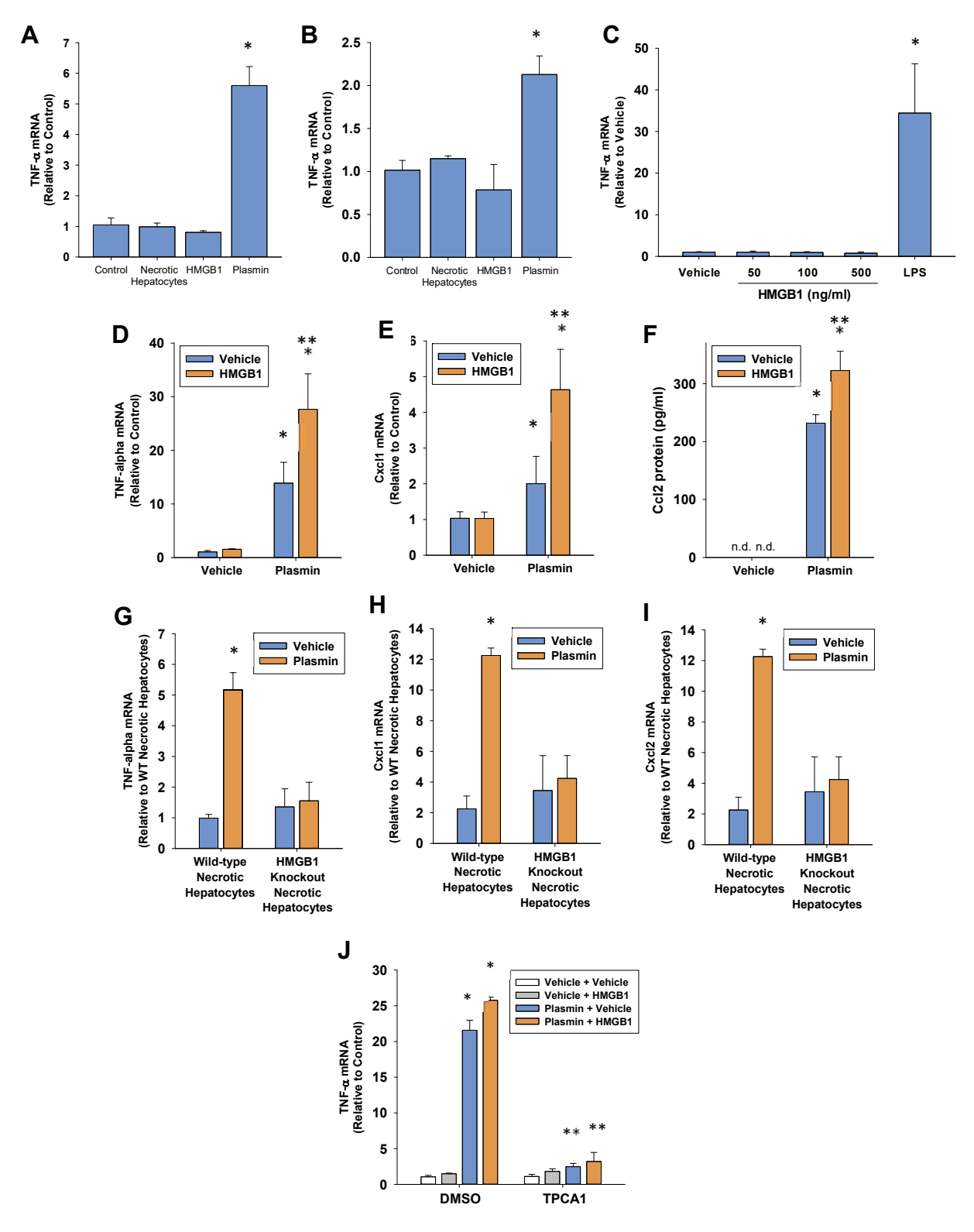


Figure 2.4: HMGB1 Enhances Activation of Macrophages by Plasmin. (A) BMMs and (B)

Kupffer cells were treated with necrotic hepatocytes, 100 ng/ml HMGB1, or 100 nM plasmin

Figure 2.4 (cont'd)

for 6 hours. (C) BMMs were treated with the indicated for 6 hours. (C) BMMs were treated with the indicated concentrations of HMGB1. TNF-a mRNA was measured by real-time PCR. *Significantly different from control (n=3). (D-F) BMMs were treated with plasmin in the presence or absence of HMGB1 for 6 hours. Cytokine mRNAs and Ccl2 protein were quantified. *Significantly different from vehicle treated BMMs. **Significantly different from plasmin treated BMMs (n=3). (G-I) BMMs were treated with plasmin followed by treatment with necrotic hepatocytes from wild-type or hepatocyte-specific HMGB1 knockout mice. *Significantly different from vehicle treated BMMs (n=3). (J) BMMs were treated with TPCA1 or DMSO for 30 minutes followed by treatment with plasmin with and without HMGB1. TNF-a mRNA was measured. *Significantly different from vehicle + vehicle or vehicle + DMSO. **Significantly different from DMSO + plasmin + vehicle or DMSO + plasmin + HMGB1. Data are expressed as mean ± SEM; *n* = 3.

interaction between plasmin and HMGB1. As shown in Fig. 2.4J, TPCA1 substantially prevented upregulation of TNF-α by the combination of plasmin and HMGB1.

2.4.5 Plasmin inhibition prevents removal of necrotic cells from the liver after APAP overdose. Next, we determined the impact of plasmin inhibition on macrophage function at later times after APAP overdose. In mice treated with APAP and vehicle, necrotic cells were cleared from the liver between 48 and 72 hours (Fig. 2.5A, B and E). As shown in Fig. 2.5B, very few necrotic cells remained in the liver 72 hours after treatment with APAP and vehicle. In striking contrast, inhibition of plasmin with tranexamic acid prevented clearance of necrotic cells from the liver at 72 hours, as indicated by extensive necrosis remaining in the liver (Fig. 2.5D and E). Interestingly, despite the impact on clearance of necrotic cells, the numbers of PCNA-positive hepatocytes were not affected (Fig. 2.6).

It was previously reported that the complement system is needed for removal of necrotic cells from the liver after carbon tetrachloride (Cresci, 2015). Accordingly, we determined whether inhibition of plasmin affected complement deposition in the liver. As shown in Fig. 2.7A, fragments of C3 cleavage were deposited in necrotic regions of liver after APAP overdose. By 72 hours, the complement-coated necrotic cells were completely removed from the liver (Fig. 2.7B and E). In mice treated with APAP and tranexamic acid, C3 cleavage products deposited in necrotic regions similar to mice treated with APAP and vehicle, indicating no role for plasmin in activation of the complement system. By contrast, however, the complement coated necrotic cells were not removed from the livers of mice treated with APAP and tranexamic acid (Fig. 2.7D and E).

2.4.6 Plasmin inhibition prevents trafficking of macrophages into necrotic lesions after APAP overdose. By 48 hours after treatment of mice with APAP and vehicle, CD68 positive monocytes/macrophages filled the necrotic lesions (Fig. 2.8A, necrotic region outlined by a dashed line). In mice treated with APAP and tranexamic acid, however, very few CD68 positive monocytes/macrophages trafficked into the necrotic lesions (Fig. 2.8B). In these mice,

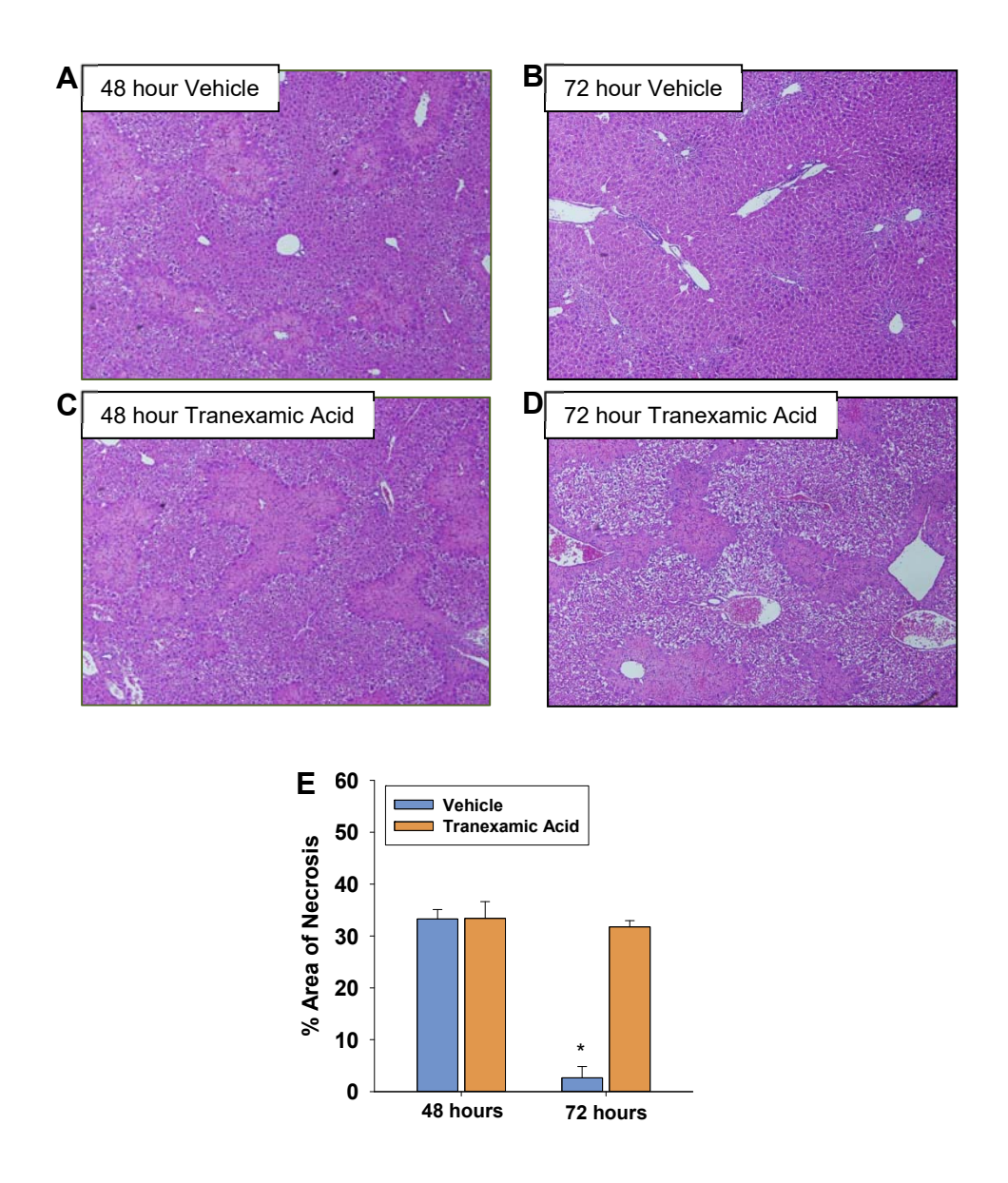


Figure 2.5: Plasmin Inhibition Prevents Removal of Necrotic Cells. Mice were treated with 300 mg/kg APAP followed by treatment with tranexamic acid as detailed in the methods. (A-D) Photomicrographs of sections of H&E stained liver sections. (E) Area of necrosis was quantified in sections of liver. *Significantly different from vehicle-treated mice at 48hrs. Data are expressed as mean \pm SEM; n = 5 mice per group.

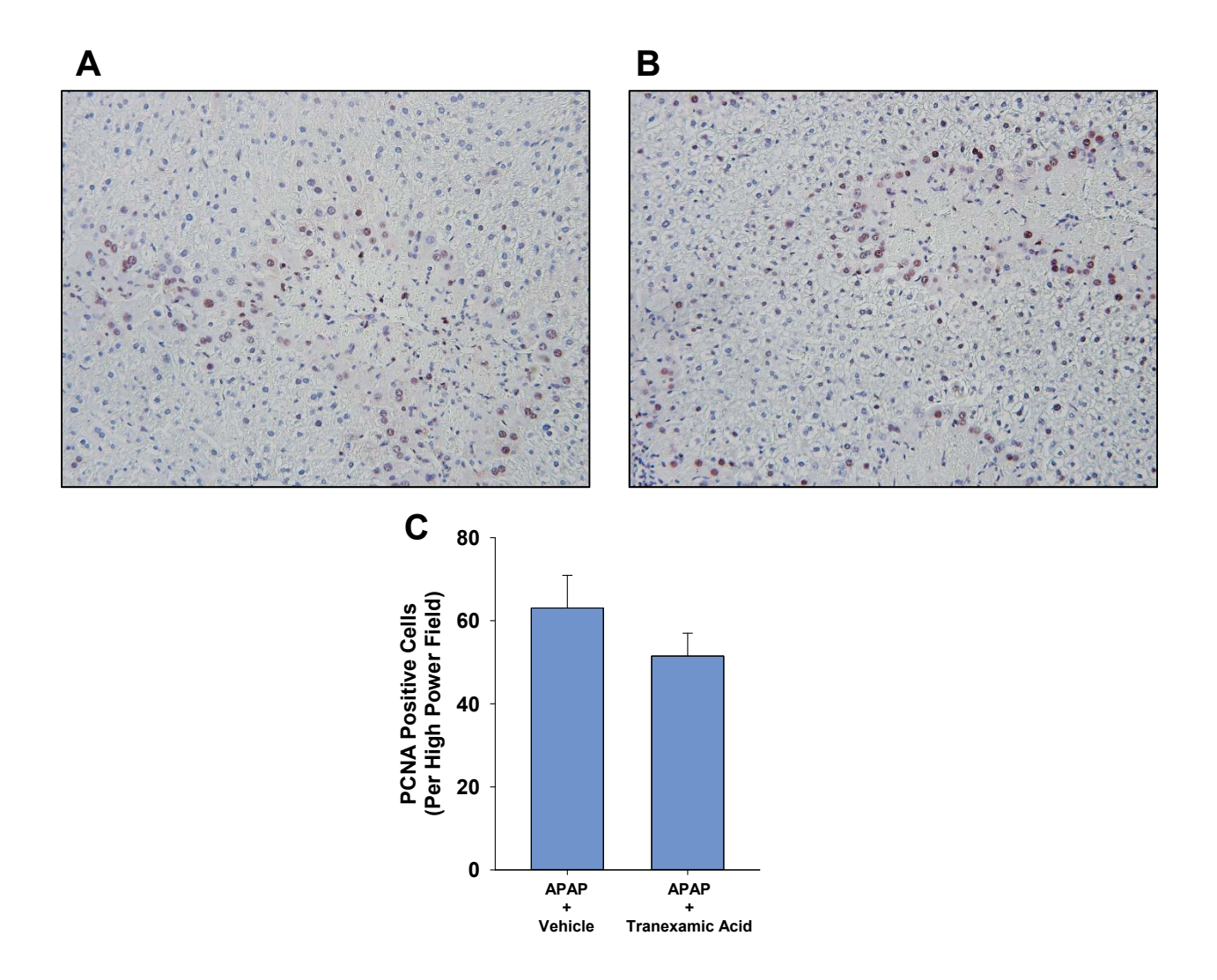


Figure 2.6: Effect of Plasmin Inhibition on Proliferation after APAP Overdose. Mice were treated with 300 mg/kg APAP followed by treatment with tranexamic acid for 48 hours as detailed in the methods. PCNA was detected in liver sections from mice treated with either (A) APAP and water or (B) APAP and tranexamic acid. Positive staining appears brown in the photomicrographs. (C) The number of PCNA-positive hepatocytes was quantified. Data are expressed as mean ± SEM; n = 5 mice per group.

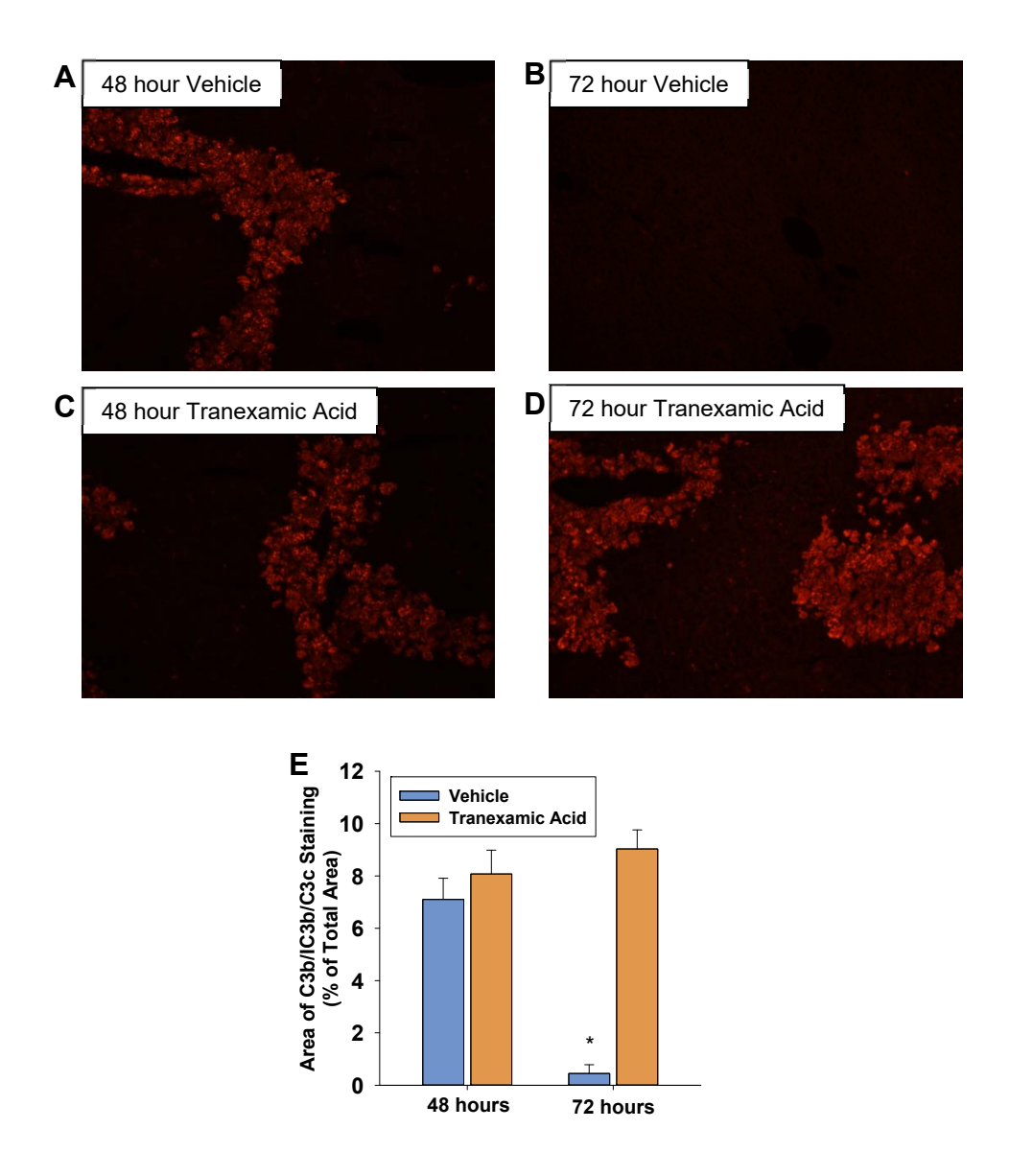


Figure 2.7: Effect of Plasmin Inhibition on Complement after APAP Overdose. Mice were treated with 300 mg/kg APAP followed by treatment with tranexamic acid as detailed in the methods. C3b/iC3b/C3c was detected by immunofluorescence. (A-D) Representative photomicrographs of sections of H&E stained liver sections. (E) Area of C3b/iC3b/C3c immunostaining was quantified in sections of liver. *Significantly different from mice treated with APAP and tranexamic acid mice. Data are expressed as mean ± SEM; n = 5 mice per group.

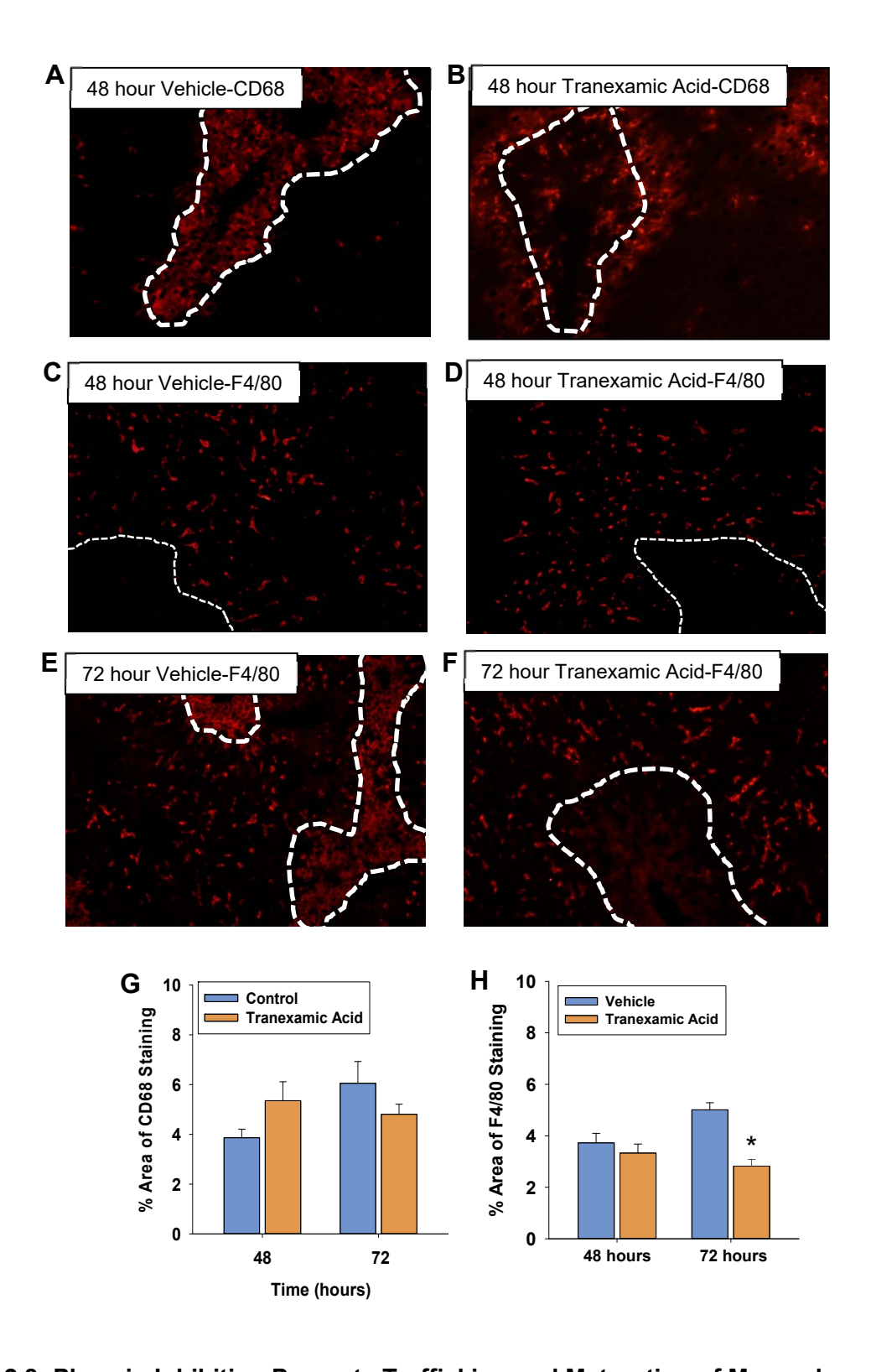


Figure 2.8: Plasmin Inhibition Prevents Trafficking and Maturation of Macrophages.

Mice were treated with 300 mg/kg APAP followed by treatment with tranexamic

Figure 2.8 (cont'd)

acid as detailed in the methods. (A and B) CD68 was detected by immunofluorescence. The necrotic lesions are demarcated by a dashed line. (C-F) F4/80 was detected by immunofluorescence. (G) Area of CD68 fluorescence was quantified in sections of liver. (H) Area of F4/80 immunostaining was quantified in sections of liver. *Significantly different from mice treated with APAP and vehicle. Data are expressed as mean ± SEM; n = 5 mice per group.

CD68 positive monocytes/macrophages remained at the periphery of the necrotic lesions.

Quantitatively, though, there was no difference in the numbers of CD68 positive monocytes/macrophages in the livers of mice treated with either APAP and vehicle or APAP and tranexamic acid (Fig. 2.8C).

F4/80 positive macrophages were primarily located outside of the necrotic lesions at 48 hours after treatment with either APAP and vehicle or APAP and tranexamic acid (Fig. 2.8D and E). By 72 hours after treatment with APAP and vehicle, macrophages within the necrotic lesions began to express F4/80 (Fig. 2.8F). By contrast, at 72 hours after treatment with APAP and tranexamic acid, no macrophages expressing F4/80 were detected within necrotic lesions (Fig. 2.8G). To confirm these findings, flow cytometry was used to quantify F4/80 on CD68+ macrophages. For these studies, liver nonparenchymal cells were isolated from livers and stained for CD45, CD68, and F4/80. F4/80 was quantified on liver nonparenchymal cells that were positive for CD45 and CD68 (gating strategy illustrated in Fig. 2.9A). As shown in Figure 2.9, both the intensity of F4/80 staining and the percentage of F4/80+ cells were lower in the CD45+ CD68+ population of macrophages in the livers of mice treated with APAP and tranexamic acid when compared to mice treated with APAP and vehicle.

2.4.7 Effect of plasmin inhibition on neutrophil accumulation after APAP overdose.
Since plasmin inhibition impacted the accumulation of macrophages into the necrotic lesions,
we determined whether this impacted accumulation of another immune cell type, neutrophils.
As shown in Figure 2.10, neutrophil accumulation into necrotic lesions was not affected by inhibition of plasmin.

2.4.8 Impact of plasmin inhibition on expression of cytokines late after APAP overdose. Studies have suggested that phagocytosis of dead cells by proinflammatory macrophages decreases expression of proinflammatory cytokines, a step that is critical for resolution of inflammation (Holt, 2008) (Arnold, 2007) (Odaka, 2003) (Fadok, 1998). Because there was a failure of monocytes/macrophages to phagocytose dead cells in mice treated with

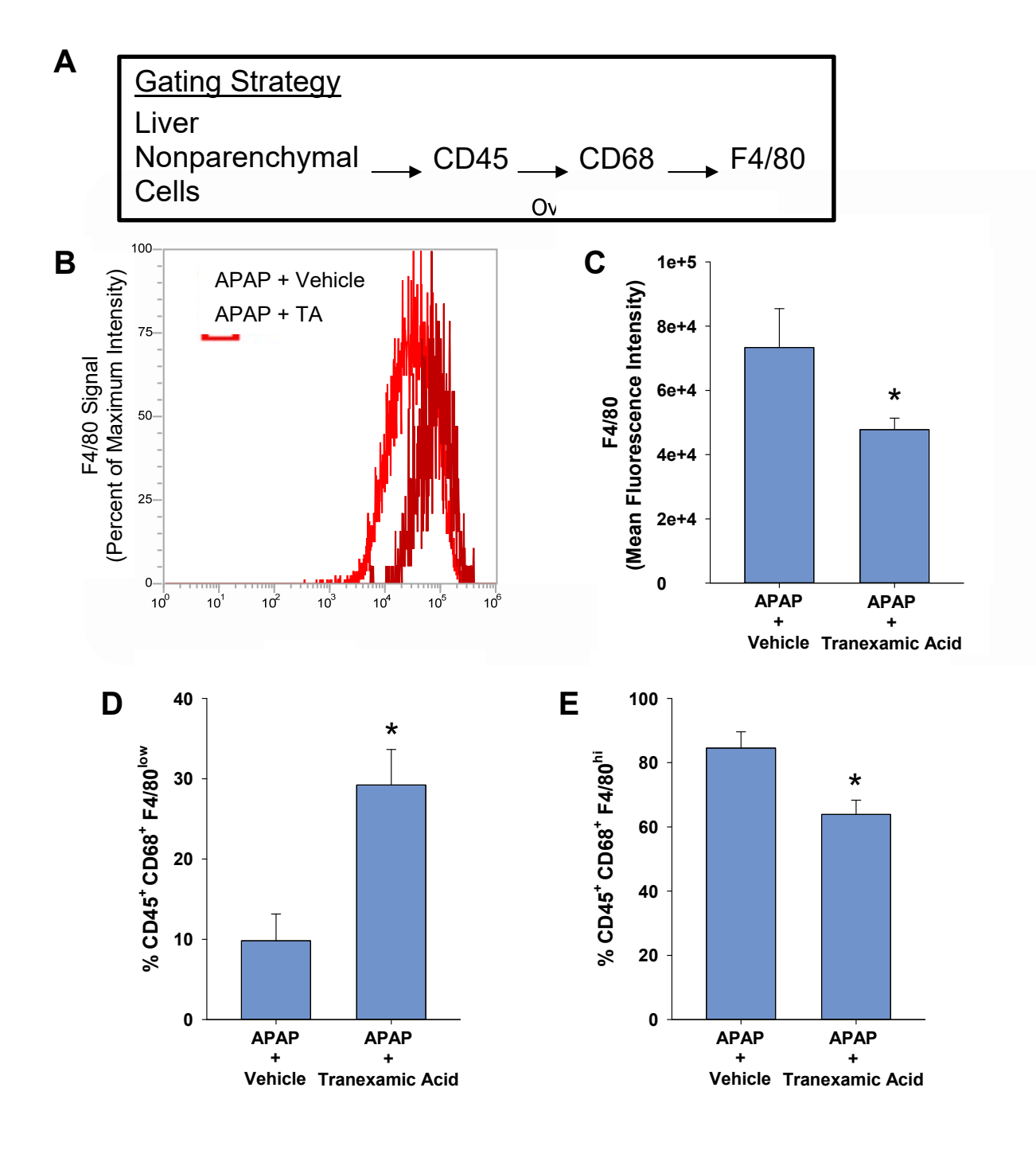


Figure 2.9: Effect of Plasmin Inhibition on Macrophage Phenotype. Mice were treated with 300 mg/kg APAP followed by treatment with tranexamic acid as detailed in the methods. After 72 hours, the livers were digested and CD45, CD68, and F4/80 were detected in the nonparenchymal cell fraction by flow cytometry. (A) The gating strategy used for flow cytometry. (B and C) The intensity of F4/80 staining within the CD45⁺CD68⁺

Figure 2.9 (cont'd)

population was quantified. (D and E) The percentage of F4/80^{low} and F4/80^{hi} macrophages within the CD45 $^+$ CD68 $^+$ population was quantified. *Significantly different from mice treated with APAP and vehicle. Data are expressed as mean \pm SEM; n = 3 mice per group.

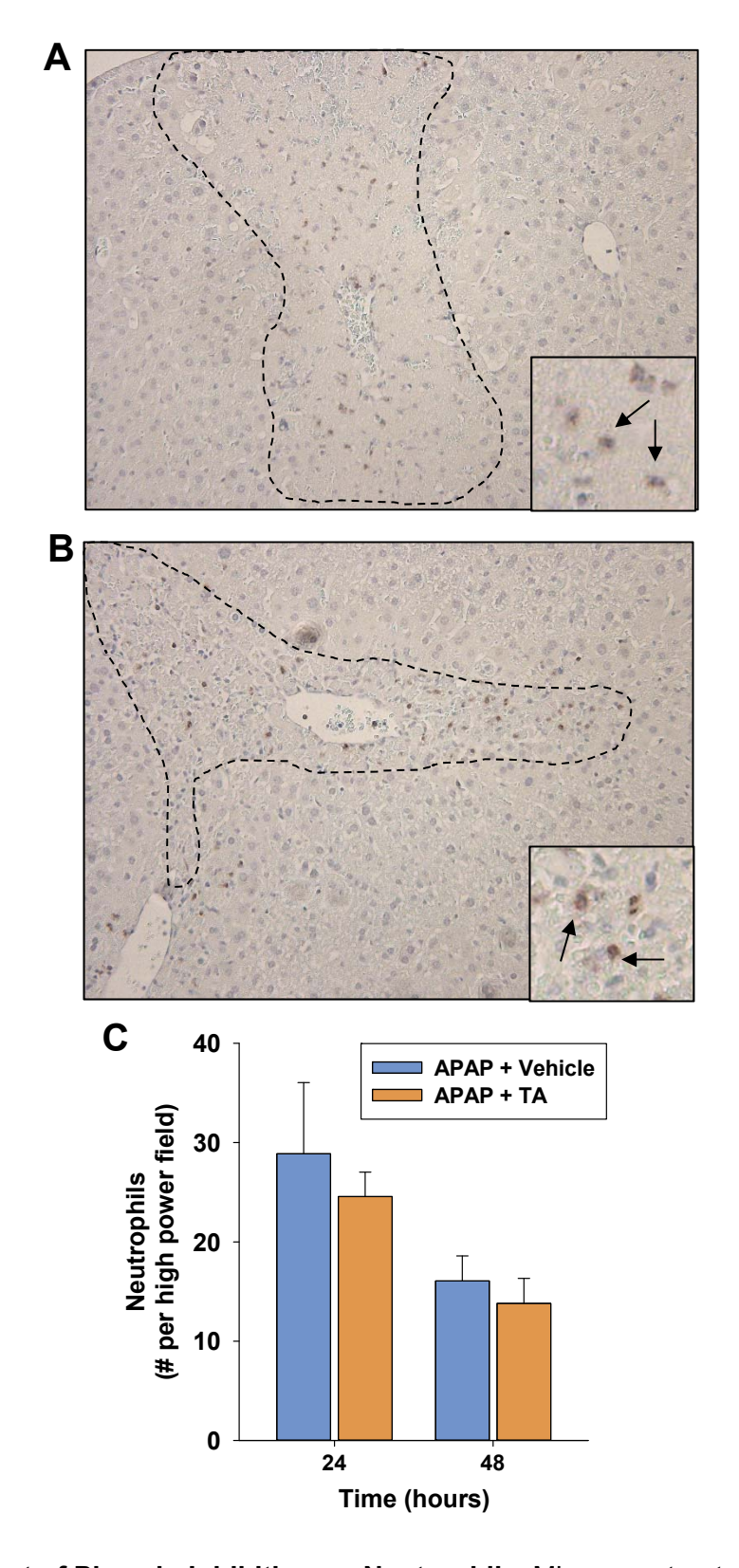


Figure 2.10: Effect of Plasmin Inhibition on Neutrophils. Mice were treated with 300

Figure 2.10 (cont'd)

mg/kg APAP followed by treatment with tranexamic for 24 and 48 hours as detailed in the methods. Ly6 G^{\dagger} neutrophils were detected in liver sections from mice treated 24 hours earlier with either (A) APAP and water or (B) APAP and tranexamic acid. The necrotic lesions are demarcated by a dashed line. Inset shows a higher power image. Neutrophils are indicated by arrows. (C) The number of neutrophils was quantified. Data are expressed as mean \pm SEM; n = 5 mice per group.

APAP and tranexamic acid, we determined whether there was a similar failure to terminate inflammatory cytokine production. In mice treated with APAP and vehicle, mRNA levels of TNF-α and Ccl2 were substantially increased in the liver by 24 hours after treatment (Fig. 2.11). By 72 hours mRNA levels of both cytokines returned to baseline levels (Fig. 2.11). In mice treated with APAP and tranexamic acid, mRNA levels of TNF-α and Ccl2 were elevated at 24 hours and remained elevated at 72 hours (Fig. 2.11). Similar results were observed for blood levels of Ccl2 protein (Fig. 2.11C).

2.4.9 Necrotic hepatocytes decrease cytokine expression in proinflammatory monocytes. Our studies above demonstrated that tranexamic acid prevented phagocytosis of dead cells and prevented downregulation of proinflammatory cytokines (Figs. 2.5 and 2.11). This suggested that phagocytosis may be a stimulus for decreasing cytokine expression in proinflammatory monocytes. To investigate this further in vitro, we used immunomagnetic bead purification to isolate proinflammatory monocytes (Ly6Chi F4/80low) from the livers of APAPtreated mice. Proinflammatory monocytes rapidly infiltrate the liver after APAP overdose, and studies indicate that these cells are responsible for the clearance of dead cells (Holt, 2008). To isolate these cells, we used an antibody against Ly6C, which is expressed at high levels on the surface of proinflammatory monocytes (Yang, 2014). These cells were isolated from the livers of mice treated 24 hours earlier with APAP, a time where cytokines are highly expressed (Fig. 2.11) and a time before phagocytosis of dead cells begins (Fig. 2.5). Using anti-Ly6C labeled immunomagnetic beads, Ly6Chi F4/80low proinflammatory monocytes were enriched by approximately 92% from liver homogenates (Fig. 2.12A and B). Immunocytochemistry confirmed that these cells expressed Ly6C but not F4/80 (Fig. 2.12C and D). Treatment of these cells with hepatocytes made necrotic by 3 cycles of freeze thaw, decreased expression of the proinflammatory monocyte/macrophage marker, inducible nitric oxide synthase iNOS, and decreased expression of the proinflammatory cytokines, TNF- α and Ccl2 (Fig. 2.12E-G).

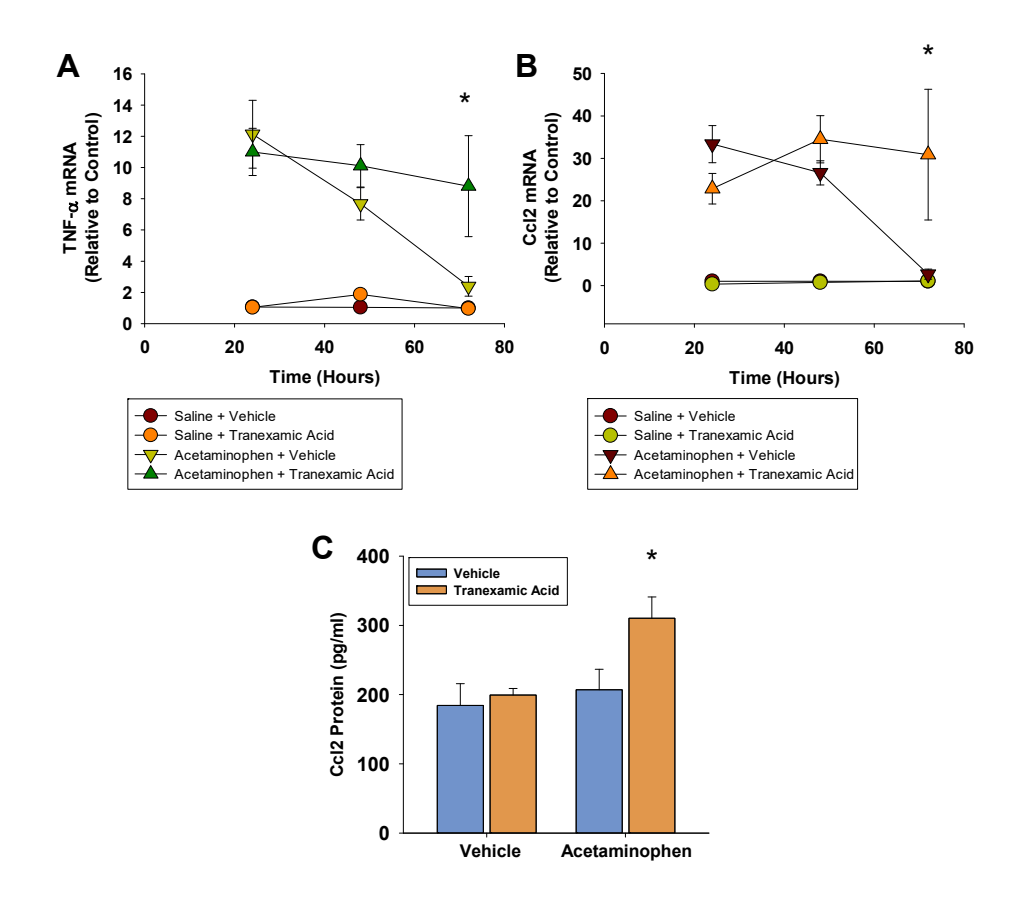


Figure 2.11: Impact of Plasmin Inhibition on Cytokine Expression Late after APAP **Overdose.** Mice were treated with 300 mg/kg APAP followed by treatment with tranexamic acid as detailed in the methods. (A and B) TNF- α and Ccl2 mRNAs were quantified in the liver. (C) Ccl2 protein was quantified in the serum. *Significantly different from mice treated with APAP and vehicle. Data are expressed as mean \pm SEM; n = 5 mice per group.

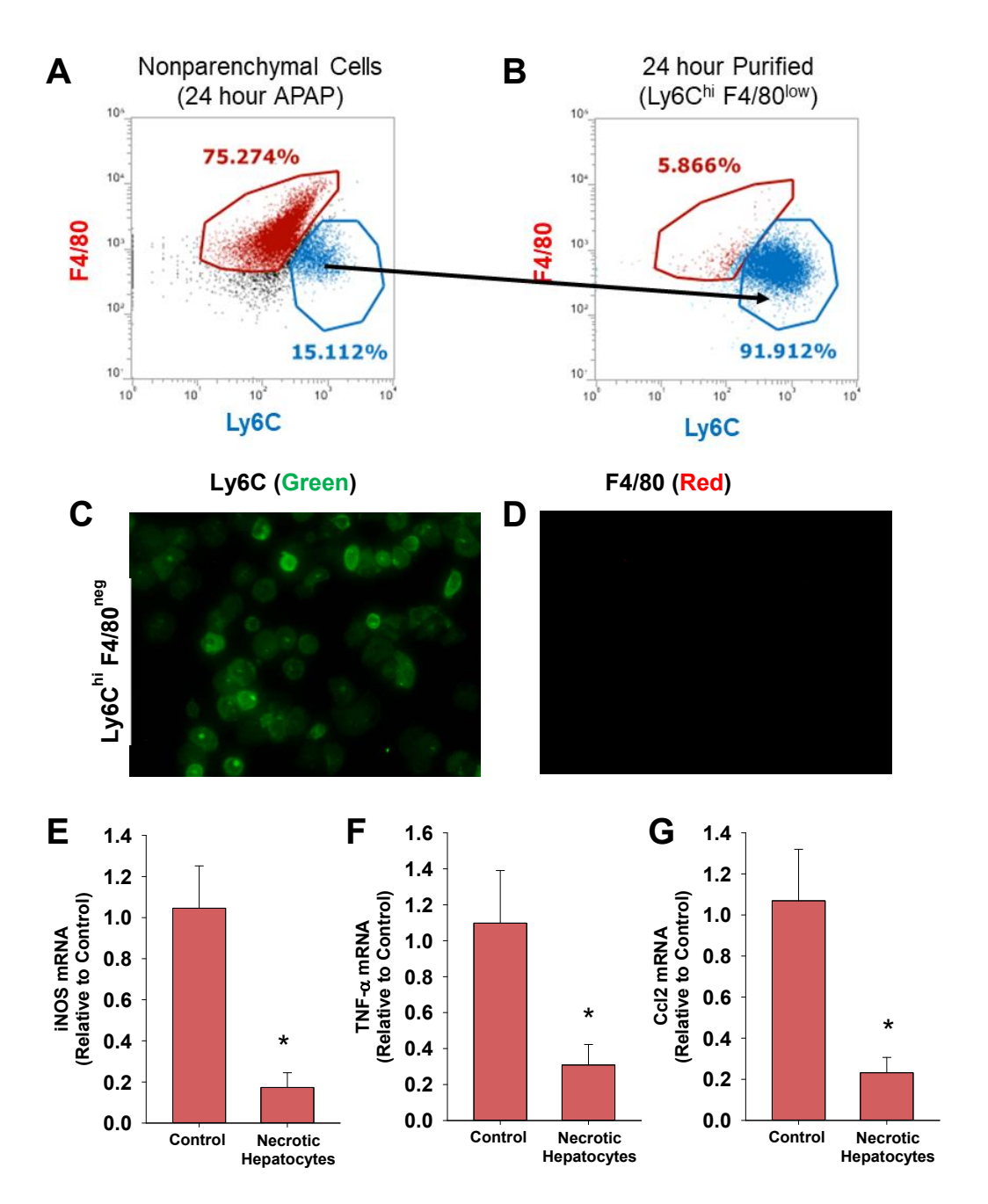


Figure 2.12: Necrotic Hepatocytes Decrease Cytokine Expression in Proinflammatory

Monocytes. Mice were treated with 300 mg/kg APAP. After 24 hours, Ly6C^{hi} F4/80^{neg} monocytes were isolated from the livers of mice by using immunomagnetic beads. (A)

Nonparenchymal cells and (B) purified Ly6C^{hi} F4/80^{neg} were analyzed by flow cytometry. (C)

Immunofluorescence was used to detect Ly6C (green) and F4/80 (red) in cultured Ly6C^{hi}

Figure 2.12 (cont'd)

containing necrotic hepatocytes. *Significantly different from cells treated with control media.

Data are expressed as mean \pm SEM; n = 3.

2.5 Discussion

Macrophages perform several key functions in the liver after APAP overdose, including production of immunomodulatory cytokines, phagocytosis of dead cell debris, and production of pro-mitogenic growth factors. Proper regulation of these pathways is critical for repair of the liver and restoration of liver function. Studies over the last two decades have indicated that macrophage dysregulation occurs in a subset of ALF patients, leading to aberrant cytokine production and, potentially, multiorgan failure (Berry, 2010) (Antoniades, 2008). Similarly, in an animal model of ALF, there is evidence that macrophage-dependent clearance of dead cells from the liver is impaired (Bhushan, 2014). Collectively, these studies highlight the importance of understanding the pathways that regulate macrophage function after ALF. Our studies indicate that plasmin is a central regulator of macrophage function after APAP overdose, and that plasmin not only stimulates macrophage activation during the inflammatory phase, but it also stimulates resolution of inflammation during the regenerative phase.

Gao and colleagues recently demonstrated that plasmin activity is increased in the liver within 6 hours after APAP treatment (Gao, 2018). At this time, Kupffer cells, the resident macrophages of the liver, become activated and secrete proinflammatory cytokines that recruit various immune cell types to the liver (Fisher, 2013). Several recent studies have revealed that plasmin is critical for induction of cytokines and initiation of inflammation in the peritoneum, lungs and brain (Gong, 2008) (Swaisgood, 2007) (Hultman, 2014). Based upon these findings, we examined whether plasmin is similarly required for early cytokine induction after APAP overdose. Our studies revealed that inhibition of plasmin prevented upregulation of TNF- α , Cxcl1, Cxcl2, and Ccl2 by 6 hours after APAP treatment. Interestingly, this effect was lost by 24 hours after APAP treatment, indicating that additional factors maintain cytokine production at later times. Alternatively, it is possible that plasmin-dependent activation of Kupffer cells produces the initial wave of cytokines, whereas proinflammatory monocytes recruited to the liver at later times maintain cytokine production, an effect that may occur independent of plasmin.

Studies using RAW264.7 cells and monocyte-derived macrophages have revealed that plasmin directly stimulates macrophage activation (Laumonnier, 2006) (Syrovets, 2001) (Weide, 1996). Based upon these findings, we tested the hypothesis that plasmin directly activates Kupffer cells. Treatment of Kupffer cells or bone marrow-derived macrophages with plasmin increased production of several cytokines. Upregulation of these cytokines required NF-κB and plasmin enzyme activity similar to what was reported in monocyte-derived macrophages (Syrovets, 2001). By contrast to monocyte-derived macrophages (Laumonnier, 2006), however, this occurred independent of annexin A2, a putative receptor for plasmin. While it is not fully clear why this difference exists, it is possible that the mechanism by which plasmin activates macrophages may depend upon the source of macrophages. Studies have also suggested that PAR-1 is activated on macrophages by plasmin (Carmo, 2014). Our studies revealed, however, that PAR-1 was dispensable for macrophage activation by plasmin after APAP overdose. In addition to annexin A2 and PAR-1, the receptors enolase-1 and Plg-Rkt bind to plasmin and facilitate signaling in macrophages (Wygrecka, 2009) (Miles, 1991) (Miles, 2017) (Lighvani, 2011). It is possible that plasmin stimulates production of proinflammatory cytokines after APAP overdose through activation of one of these receptors.

It has been proposed that HMGB1 is critical for triggering macrophage activation after tissue injury. In support of this, deficiency in HMGB1 reduces proinflammatory cytokine induction in the liver after ischemia-reperfusion or APAP overdose (Huebener, 2015). Surprisingly, though, in our studies, treatment of bone marrow-derived macrophages or Kupffer cells with recombinant HMGB1, ranging in concentration from 50-500 ng/ml, or necrotic hepatocytes did not increase expression of TNF-α. These concentrations of HMGB1 are within or above the range reported *in vivo*. Blood levels of HMGB1 are approximately 4 ng/ml in APAP-induced acute liver failure patients and approximately 175 ng/ml in mice treated with a high dose of APAP (i.e., 530 mg/kg) (Antoine, 2009). It is possible that HMGB1 concentrations are higher in the liver where Kupffer cells reside and that the concentrations tested in our

studies were below this level. Studies have shown that HMGB1 does activate macrophages in the µg/ml range (Abraham, 2000) (Andersson, 2000). Alternatively, it is possible that specific post-translational modifications occur on HMGB1 that modifies its potency after APAP overdose. Studies have shown that the redox status of HMGB1 heavily dictates the bioactivity of this protein (Yang, 2013). Further, studies have demonstrated that HMGB1 can be acetylated and phosphorylated (Ge, 2014). These aspects of HMGB1 biology were not investigated in our studies. An additional possibility, revealed by our studies, is that HMGB1 synergistically enhances activation of Kupffer cells by plasmin, and that both mediators are needed to fully activate macrophages.

Our studies showed that plasmin activation of macrophages was greatly enhanced by concentrations of HMGB1 that were without effect alone. Similar to our studies, it was reported that HMGB1 synergistically enhances LPS-induced cytokine production by macrophages (Youn, 2008) (Qin, 2009). In this context, HMGB1 delivers extracellular LPS to the cytosol of cells where it stimulates pyroptosis by a caspase-11-dependent manner (Deng, 2018). Similarly, HMGB1 has been shown to interact with extracellular DNA and CXCL12 to enhance signaling through TLR9 and CXCR4, respectively (Tian, 2007) (Schiraldi, 2012). Our studies did not fully elucidate the molecular mechanism by which HMGB1 enhances activation of macrophages by plasmin. One intriguing possibility, though, is that plasmin cleaves HMGB1 which modifies its potency. It was previously reported that plasmin cleaves HMGB1, however, whether this affected its ability to activate either Tlr4 or RAGE was not investigated (Parkkinen, 1991). Others have identified proteases that cleave HMGB1, however, in these instances, cleavage of HMGB1 decreased its activity (Ito, 2008) (Roy, 2014) (Marchetti, 2012).

Paradoxically, although plasmin was critical for early cytokine induction, it was also important for resolution of inflammation at later times. A similarly important role for plasmin was recently reported in a mouse model of peritonitis, where plasmin was critical for induction of the anti-inflammatory protein, annexin A1 (Sugimoto, 2017). Our studies suggest that plasmin

stimulated resolution of inflammation after APAP overdose indirectly through the modulation of macrophage trafficking. After APAP treatment, necrotic lesions fill with CD68* monocytes/macrophages by 48 hours (Fig. 2.8A). While inhibition of plasmin did not affect accumulation of these cells in the liver, it did prevent trafficking of these cells into the necrotic lesions. This was reported previously in plasminogen knockout mice subjected to a stab wound in the liver (Kawao, 2010). One possible explanation for failed trafficking of macrophages is that fibrin, localized within the lesions, produces a physical barrier that prevents macrophage penetration into the lesion. It was recently demonstrated, though, that fibrinogen-deficient mice show a similar defect in the removal of necrotic cells from the liver after APAP overdose, suggesting that impaired clearance of fibrin is not the cause of impaired macrophage trafficking (Kopec, 2017). Another possible explanation is that plasmin activates matrix metalloproteinases (MMPs) that are needed for macrophage migration through the cellular debris and extracellular matrix within necrotic lesions. Plasmin activates several MMPs, including MMP2, MMP9, and MMP12, and the hepatic activity of these MMPs is increased in APAP-treated mice (Gong, 2008) (Monea, 2002) (Ito, 2005). Furthermore, it was previously shown by Gao et al. that excessive plasmin activity following APAP overdose in mice results in compromised sinusoidal vascular integrity through the detachment of sinusoidal endothelial cells (Gao, 2018). This was prevented by inhibition of plasmin with tranexamic acid (Gao, 2018). It is possible that the loss of sinusoidal integrity is important for trafficking macrophages into the necrotic lesions and for the direct physical interaction between macrophages and necrotic hepatocytes. Interestingly, although macrophage trafficking was impaired, neutrophil trafficking into the necrotic lesions was unaffected by plasmin inhibition.

Diminished trafficking of monocytes/macrophages into the lesions prevented phagocytic clearance of dead cell debris, which our results indicate, allowed for the persistence of proinflammatory monocytes/macrophages. After APAP overdose, proinflammatory monocytes are rapidly recruited to the liver. As necrotic cell debris is removed from the liver, these cells

mature into Ly6C^{low} F4/80^{hi} macrophages that express reduced levels of proinflammatory cytokines. Although the factors that stimulate differentiation of proinflammatory monocytes into Ly6C^{low} F4/80^{hi} macrophages in the liver after APAP overdose are not known, our studies suggest that phagocytosis of necrotic hepatocytes stimulates this process. In support of this, incubation of Ly6C^{hi} F4/80^{low} monocytes, isolated from the livers of APAP-treated mice, with necrotic hepatocytes was sufficient to decrease expression of proinflammatory cytokines. This would explain the lack of F4/80 induction on macrophages and the persistence of cytokine expression in mice co-treated with APAP and the plasmin inhibitor, tranexamic acid. In other words, when plasmin was inhibited, monocytes were incapable of entering the lesions and phagocytosing dead cell debris, which prevented maturation of these cells into F4/80-expressing macrophages that express reduced levels of cytokines.

As mentioned, several studies have indicated that macrophage dysfunction occurs in ALF, which in patients, leads to sustained cytokine production, and in animal models, leads to the failed clearance of necrotic cells. Interestingly, it was recently reported that plasminogen deficiency occurs in patients with ALF (Lisman, 2012). Based upon our findings, it is possible that plasminogen deficiency could explain, in part, sustained cytokine production and failed phagocytosis in ALF. Therefore, restoration of plasminogen levels in these patients may restore macrophage function leading to enhanced phagocytosis and diminished cytokine production. Additional studies are needed, however, to test this possibility.

Collectively, our studies indicate that plasmin not only stimulates cytokine production by Kupffer cells, but it also promotes resolution of inflammation after APAP overdose. It promotes resolution of inflammation by promoting trafficking of monocytes/macrophages into necrotic lesions where these cells phagocytose dead cell debris, a process that stimulates their maturation and differentiation.

2.6 Acknowledgements

We thank Dr. Russell S. Taichman from the Department of Periodontic and Oral Medicine at the University of Michigan for the generous gift of Annexin A2 knockout mice.

Chapter 3

Impaired Macrophage Function in Mice with Acetaminophen-induced Acute Liver Failure

3.1 Abstract

Acetaminophen (APAP) overdose is the leading cause of acute liver failure (ALF) in the United States. Clinical studies have revealed that systemic levels of pro- and anti-inflammatory cytokines are highest in ALF patients with the poorest prognosis. Although the underlying cause remains unknown, it has been proposed that cytokine dysregulation results from impaired macrophage function in ALF. To investigate this further, we determined whether macrophage dysregulation occurs in a mouse model of ALF and determined whether it impacts liver repair. In these studies, mice were treated with either 300 mg/kg APAP, a dose that produces moderate liver injury that is fully repaired, or with 600 mg/kg acetaminophen, a dose of APAP that recapitulates many of the features of ALF in patients, including failed liver repair. In mice given 300 mg/kg APAP, levels of proinflammatory cytokines were rapidly increased in the liver. Proinflammatory monocyte-derived macrophages accumulated in the liver and trafficked into the necrotic lesions. Coincident with the clearance of necrotic hepatocytes, the proinflammatory macrophages shifted phenotype to pro-reparative macrophages, a process that terminated production of proinflammatory cytokines. In mice treated with 600 mg/kg APAP, however, proinflammatory monocyte-derived macrophages accumulated in the liver but failed to traffic into the necrotic lesions and failed to remove dead cell debris. Further, the proinflammatory macrophages did not switch phenotype leading to the sustained production of several proinflammatory cytokines. Similar to ALF patients, systemic IL-10 concentrations were also higher in mice treated with 600 mg/kg APAP. Remarkably, administration of an IL-10 neutralizing antibody, 24 hours after treatment of mice with APAP, fully restored macrophage trafficking into the necrotic lesions. It did not, however, stimulate macrophage-dependent clearance of dead cells from the liver. Collectively, these studies demonstrate that macrophage dysregulation in ALF impairs intrahepatic macrophage trafficking, phagocytic clearance of dead cells, and macrophage phenotype switching, resulting in the sustained production of proinflammatory cytokines.

3.2 Introduction

In severe cases of acetaminophen (APAP) overdose, acute liver injury rapidly progresses to acute liver failure (ALF), producing life threatening cardiac instability, hepatic encephalopathy, and multiorgan failure (Lee, 2008) (Bernal and Wendon, 2013). The first line of therapy for APAP overdose is N-acetyl cysteine (NAC) which is most efficacious when administered during the active phase of injury (Smilkstein, 1988) (Saito, 2010). If NAC fails to impact the progression of ALF, supportive medical care and liver transplantation are the only remaining modes of therapy. Unfortunately, despite significant improvements in clinical care and emergency liver transplantation, mortality remains at approximately 40% (Bernal, 2013). This highlights the importance of studies aimed at understanding the pathogenesis of ALF, such that new targets of therapy can be identified.

After liver injury, monocyte-derived macrophages accumulate in the liver and perform several key functions in liver repair, including production of pro-mitogenic cytokines and growth factors, recruitment of additional immune cell types, and clearance of excess extracellular matrix and dead cell debris (Holt, 2008)⁶ (Zigmond, 2014) (Ju and Tacke, 2016). Simultaneous with the clearance of necrotic cells, recruited macrophages switch from a proinflammatory phenotype to a pro-reparative, anti-inflammatory phenotype by a mechanism that may involve hydrogen peroxide released from neutrophils (Yang, 2019). This phenotypic switch is associated with a decrease in the levels of proinflammatory cytokines. Interestingly, several clinical studies have indicated that macrophage dysregulation is a common feature in ALF, and that the degree of dysregulation is a key determinant of outcome in these patients (Antoniades, 2008). In support of this, several macrophage-derived, proinflammatory cytokines, including interleukin-1 (IL-1), IL-6, tumor necrosis factor-α (TNF-α), and CCL2, are persistently elevated in ALF patients (Calandra, 1991) (Martin, 1994) (Roth, 2009) (Berry, 2010). Further, there is a direct association between high cytokine levels and increased risk of multi-organ failure and death in ALF patients (Calandra, 1990) (Berry, 2010) (Antoniades, 2008). Paradoxically, blood

concentrations of the anti-inflammatory cytokine, IL-10, are also highest in ALF patients with the poorest outcome (Friedman, 1997) (Berry, 2010). In fact, recent studies identified a population of blood monocytes in ALF and acute on chronic liver failure patients that express markers of myeloid-derived suppressor cells (MDSCs) which are an immune suppressive myeloid cell type that produces high levels of IL-10 (Bernsmeier, 2018) (Huang, 2006). While it is well established that macrophage function is compromised in ALF, it remains unclear whether this contributes to the pathogenesis of ALF.

In the present studies, we determined whether macrophage dysregulation occurs in a mouse model of ALF. To examine this, we used a model of APAP overdose, established by Bhushan and colleagues, that recapitulates many of the features of ALF in patients, including failed liver repair (Bhushan, 2014). Our studies reveal that similar to ALF patients, proinflammatory cytokines and IL-10 are highly elevated in these mice when compared to mice given a dose of APAP associated with normal liver repair. We show further that IL-10 contributes to macrophage dysfunction by preventing trafficking of macrophages into necrotic lesions.

3.3 Materials and Methods

3.3.1 Animal Treatments. 6-12 week old male C57BL/6J (Jackson Laboratories) were used for all studies. Mice were housed in a 12 hr light/dark cycle under controlled temperature (18-21°C) and humidity. Food (Rodent Chow; Harlan-Teklad) and tap water were allowed *ad libitum*.

For treatment with 300 mg/kg APAP, mice were fasted for approximately 16 hours prior to APAP injection. Mice were then injected with 300 mg/kg APAP (Sigma-Aldrich) or sterile saline by intraperitoneal injection. For treatment with 600 mg/kg APAP, mice were fasted for approximately 12 hours prior to APAP injection. Mice were then injected with 600 mg/kg APAP or sterile saline by intraperitoneal injection. Food was returned to the mice immediately after APAP challenge.

For IL-10 neutralization studies, mice were injected with 0.5 mg *InVivo*MAb anti-mouse IL-10 antibody (Bio X Cell, clone JES5-2A5) or 0.5 mg isotype control antibody (Innovative Research, Rat IgG) at 24 hours after APAP treatment. Liver and blood were collected at 72 hours after APAP treatment.

For recombinant IL-10 studies, mice were injected with 5 μ g IL-10 (Biolegend, San Diego, CA) or sterile saline at 24 hours after APAP treatment. Liver and blood were collected at 48 hours after APAP treatment.

- 3.3.2 Sample Collection. Mice were anesthetized using Fatal-Plus Solution (Vortech Pharmaceuticals). Blood was collected from the inferior vena cava and the livers were removed. A portion of each liver was fixed in 10% neutral-buffered formalin. The livers were embedded in paraffin, sectioned, and stained with hematoxylin and eosin. The area of necrosis was quantified as described by us previously (Mochizuki, 2014). Additional portions of the liver were homogenized in TRIzol Reagent (Thermo-Fisher Scientific) for RNA isolation or were snap-frozen in liquid nitrogen for sectioning and immunofluorescence staining.
- **3.3.3 Immunofluorescence.** Immunofluorescence was used to detect F4/80 and CD68 as described by us previously (Mochizuki, 2014). Briefly, 8 μm sections were cut from frozen livers and fixed for 10 minutes in 4% formalin. The sections were then incubated in blocking buffer (10% goat serum) followed by incubation with either rat anti-F4/80 antibody (Bio-Rad) diluted 1:500 or rat anti-CD68 antibody (Bio-Rad) diluted 1:500. After washing, the sections were incubated with goat anti-rat secondary antibody conjugated to Alexa Fluor 594 (diluted 1:500, Thermo Fisher Scientific).
- **3.3.4 Luminex Immunoassay.** Protein levels were measured in blood serum samples by using the Bio-Plex Pro assay kit (Bio-Rad) according to manufacturer's instructions. Bead fluorescent readings were obtained using a Luminex 200 system.

- 3.3.5 Flow Cytometry. To isolate non-parenchymal cells, mouse livers were perfused and digested with collagenase (Collagenase H, Sigma Chemical Company) as described previously (Kim, 2006). Hepatocytes were removed by centrifugation and non-parenchymal cells were collected after centrifugation at 300 x g for 10 minutes. Non-parenchymal cells were washed and resuspended in FACs buffer (PBS, 1% FBS). The cells were then incubated with Fc blocking buffer (BD Biosciences; diluted 1:20) for 10 mins at 4 °C, rinsed, and then pelleted by centrifugation at 300 g for 5 minutes. The cells were incubated with anti-F4/80 conjugated to Alexa-488 and anti-Ly6c conjugated to PE for 30 minutes at 4°C. All antibodies were purchased from Biolegend. Following incubation, cells were washed twice and fixed in formalin (Sigma) for 15 minutes at 4°C. The fixed cells were washed twice and resuspended in FACs buffer. An Attune NxT flow cytometer (Life Technologies) was then used to measure fluorescence. Signal was quantified using Attune NxT software.
- **3.3.6 Real-Time PCR.** Total RNA was isolated from liver samples using TRIzol Reagent (Thermo-Fisher) and reverse transcribed into cDNA as described previously (Kim, 2006). Real-time PCR was performed on a QuantStudio 7 Flex Real-Time PCR System (Thermo-Fisher) using the iTaq Universal SYBR green Supermix (Bio-Rad). The following primer sequences were used: Tnf-α: Forward- 5'-AGGGTCTGGGCCATAGAACT-3', Reverse- 5'-CCACCACGCTCTTCTGTCTAC-3'; Ccl2: Forward- 5'-CCTGCTGTTCACAGTTGCC-3', Reverse- 5'-ATTGGGATCATCTTGCTGGT-3'; Il-10: Forward- 5'-TGTCAAATTCATTCATGGCCT-3', Reverse- 5'-ATCGATTTCTCCCCTGTGAA-3': Rpl13a: Forward- 5'-GACCTCCTCCTTTCCCAGGC-3', Reverse- 5'-AAGTACCTGCTTGGCCACAA-3'.
- **3.3.7 Statistical Analysis.** Results are presented as the mean + SEM. Data were analyzed by a one-way or two-way Analysis of Variance (ANOVA) where appropriate. Data expressed as a percentage were transformed by arcsine square root prior to analysis.

Comparisons among group means were made using the Student-Newman-Keuls test. The criterion for significance was p < 0.05 for all studies.

3.4 Results

3.4.1 Impaired clearance of necrotic cells from the livers of mice with APAPinduced ALF. To determine the impact of ALF on hepatic macrophage function after APAP
overdose, groups of mice were treated with either 300 mg/kg of APAP, a dose of APAP that
produces moderate liver injury that is fully repaired, or 600 mg/kg of APAP, a dose of APAP that
recapitulates many of the features of ALF in patients, including failed liver regeneration
(Bhushan, 2014). Treatment of mice with 300 mg/kg APAP produced liver necrosis that was
maximal by 24 hours after treatment (Fig. 3.1A and 1E). Extensive inflammatory infiltrates,
consisting of macrophages and neutrophils were present within the necrotic lesions of these
mice (Fig. 3.1F). By 72 hours, the necrotic cells were largely cleared from the livers (Fig. 3.1C
and 1E). Treatment of mice with 600 mg/kg APAP produced necrotic lesions that were similar
in size to mice treated with 300 mg/kg APAP (Fig. 3.1B and 1E). By contrast, though, the
necrotic lesions were largely devoid of inflammatory cells (Fig. 3.1G), and the necrotic cells
were not cleared from the livers of these mice by 72 hours (Fig. 3.1D and 1E).

3.4.2 Reduced accumulation of neutrophils and failed trafficking of macrophages into necrotic lesions in mice with ALF. Histopathological analysis above indicated reduced inflammatory cell infiltrates in the necrotic lesions of mice treated with 600 mg/kg APAP (Fig. 3.1G). To examine this further, we first quantified Ly6G+ neutrophils by flow cytometry. As shown in Figure 3.1H, reduced numbers of neutrophils were present in the livers of mice treated with 600 mg/kg APAP. Next, we detected CD68+ macrophages in sections of liver by immunofluorescence staining. Prior studies revealed that CD68+ macrophages accumulate in the livers of patients with APAP-induced ALF (Antoniades, 2012) (Mossanen, 2016). In mice treated with 300 mg/kg APAP, CD68+ macrophages began to accumulate in the liver and traffic into the necrotic lesions by 24 hours (Fig. 3.2A, necrotic lesions demarcated by white dotted

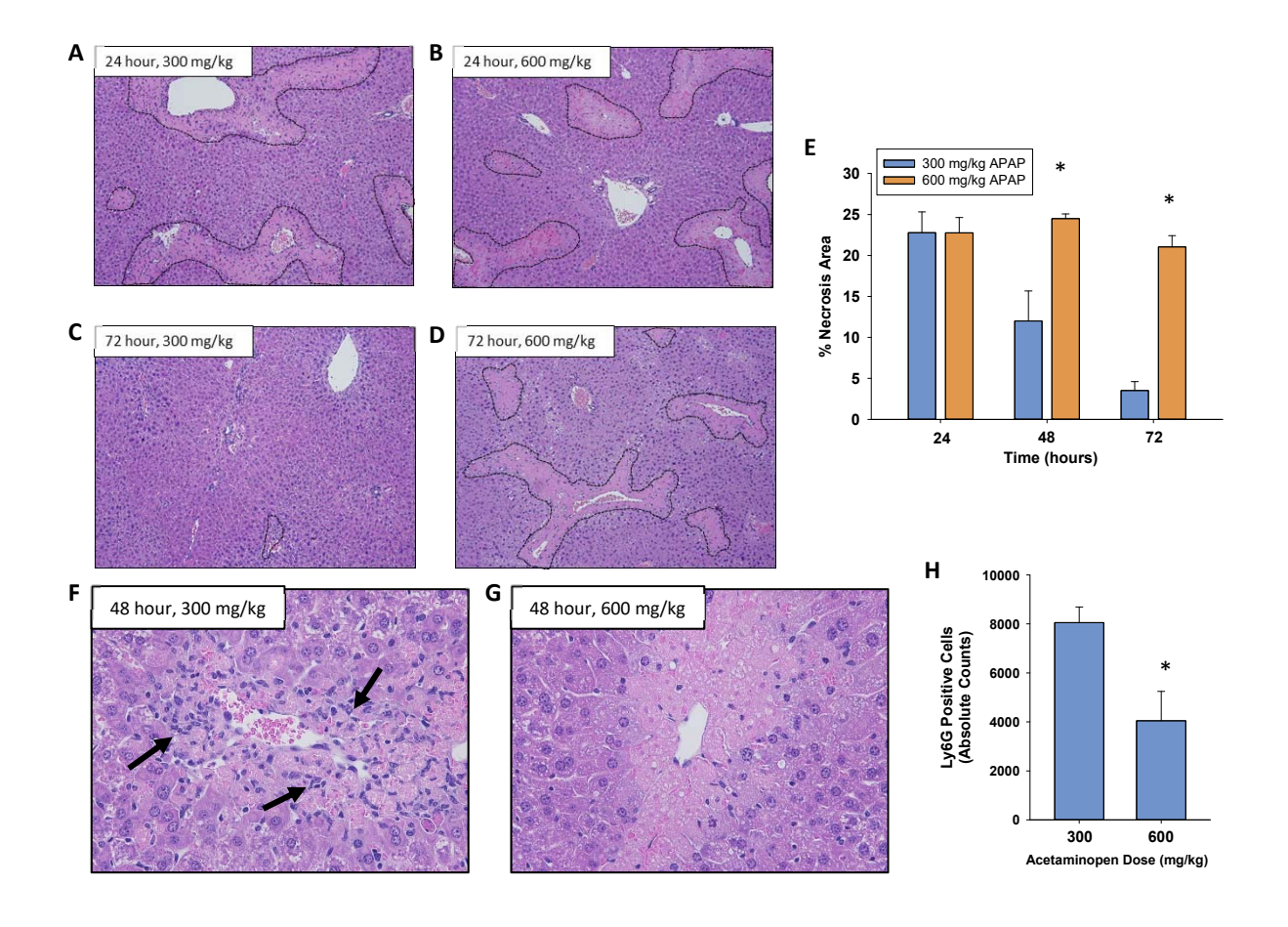


Figure 3.1: Impaired Clearance of Necrotic Cells after APAP-induced ALF. Mice were treated with either 300 mg/kg APAP or 600 mg/kg APAP as detailed in the methods. (A-D) Photomicrographs of H&E stained liver sections. The necrotic lesions are demarcated by a dashed line. (E) Area of necrosis was quantified in sections of liver. *Significantly different from mice treated with 300 mg/kg APAP. Data are expressed as mean \pm SEM; n = 5 mice per group. (F-G) Photomicrographs of H&E stained liver sections. Arrows indicate inflammatory cells within the lesion. (H) Neutrophils (Ly6G $^+$) were quantified by flow cytometry in livers from mice treated with APAP. *Significantly different from mice treated with 300 mg/kg APAP. Data are expressed as mean \pm SEM; n = 3 mice per group.

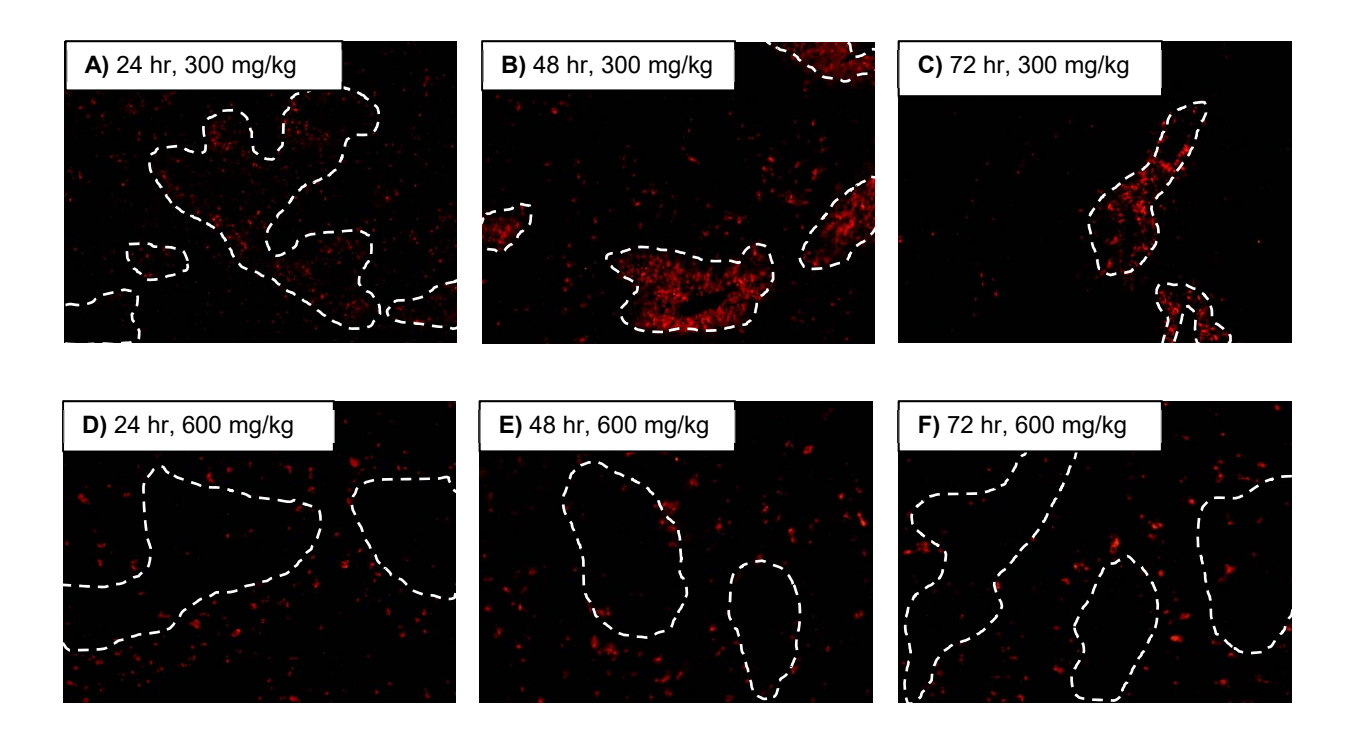


Figure 3.2: Macrophages Fail to Traffic into Necrotic Lesions after APAP-induced ALF.

Mice were treated with either 300 mg/kg APAP or 600 mg/kg APAP. (A-C) CD68 was detected by immunofluorescence in liver sections from mice treated with 300 mg/kg mice. The necrotic lesions are demarcated by a white dashed line. (D-F) CD68 was detected by immunofluorescence in liver sections from mice treated with 600 mg/kg mice. Representative photomicrographs from an n = 5 mice per group.

lines). By 48 hours, the necrotic lesions were filled with CD68⁺ macrophages (Fig. 3.2B). In mice treated with 600 mg/kg APAP, however, CD68⁺ macrophages accumulated in the liver but remained at the periphery of the necrotic lesions at all times examined (Fig. 3.2D-F).

We showed previously in mice treated with 300 mg/kg APAP, that macrophages within the necrotic lesions begin to express the mature tissue macrophage marker, F4/80, as necrotic cells are cleared from the liver (Roth, 2019). Because of the failure to clear necrotic cells from the livers of mice with ALF (Fig. 3.1E), we next determined whether induction of F4/80 was impaired. To examine this, immunofluorescence was used to detect F4/80 in liver sections from mice treated with either 300 mg/kg APAP or 600 mg/kg APAP. In mice treated with 300 mg/kg APAP, F4/80+ macrophages were largely present outside of the necrotic lesions at 24 and 48 hours after treatment (Fig. 3.3A and B). By 72 hours, however, F4/80+ macrophages filled the necrotic lesions as described by us previously (Fig. 3.3C) (Roth, 2019). By contrast, F4/80+ macrophages were not detected in the lesions of mice treated with 600 mg/kg APAP at any time point (Fig. 3.3D-F).

To examine this further, we used flow cytometry to detect the proinflammatory macrophage marker, Ly6C, and the mature tissue macrophage marker, F4/80, in nonparenchymal cell fractions from livers of mice treated with APAP. Lineage tracing studies showed previously that Ly6C+ proinflammatory macrophages accumulate in the liver after APAP overdose and begin to express F4/80 as necrotic cells are cleared from the liver (Zigmond, 2014). This was associated with a shift in macrophage phenotype from proinflammatory to prorestorative, which not only increased F4/80, but also decreased Ly6C (Zigmond, 2014). As shown in Figure 3.4A, macrophages in the livers of vehicle-treated mice were largely F4/80+ Ly6C- (red square). By 24 hours after treatment with 300 mg/kg APAP, however, a population of Ly6C+ F4/80- macrophages appeared in the liver (Fig 3.4B, green circle). By 72 hours, this population of macrophages was no longer present indicating that they had transitioned to Ly6C- F4/80+ macrophages as described previously (Fig. 3.4C) (Zigmond, 2014) (Yang, 2019). Similar

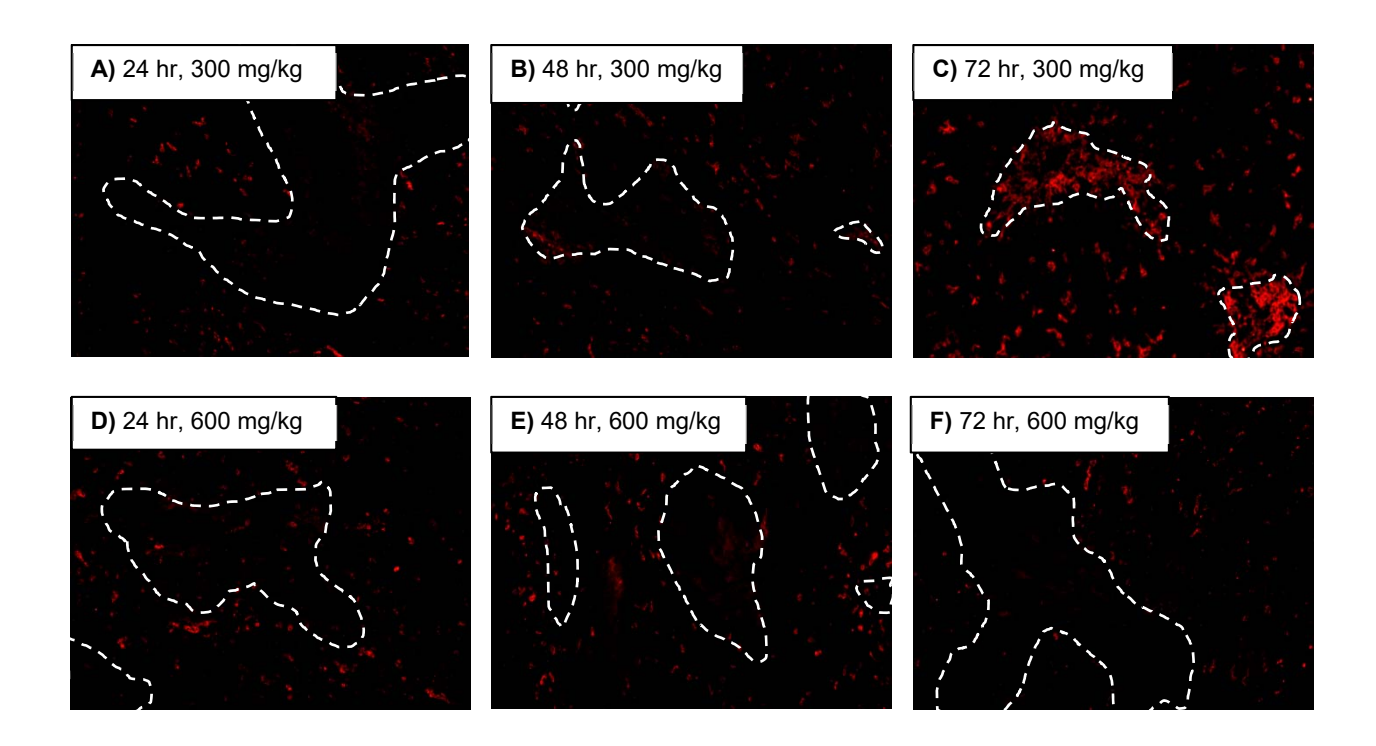


Figure 3.3: Macrophages Fail to Traffic into Necrotic Lesions and Mature. Mice were treated with either 300 mg/kg APAP or 600 mg/kg APAP. (A-C) F4/80 was detected by immunofluorescence in liver sections from mice treated with 300 mg/kg mice. The necrotic lesions are demarcated by a white dashed line. (D-F) F4/80 was detected by immunofluorescence in liver sections from mice treated with 600 mg/kg mice. Representative photomicrographs from an n = 5 mice per group.

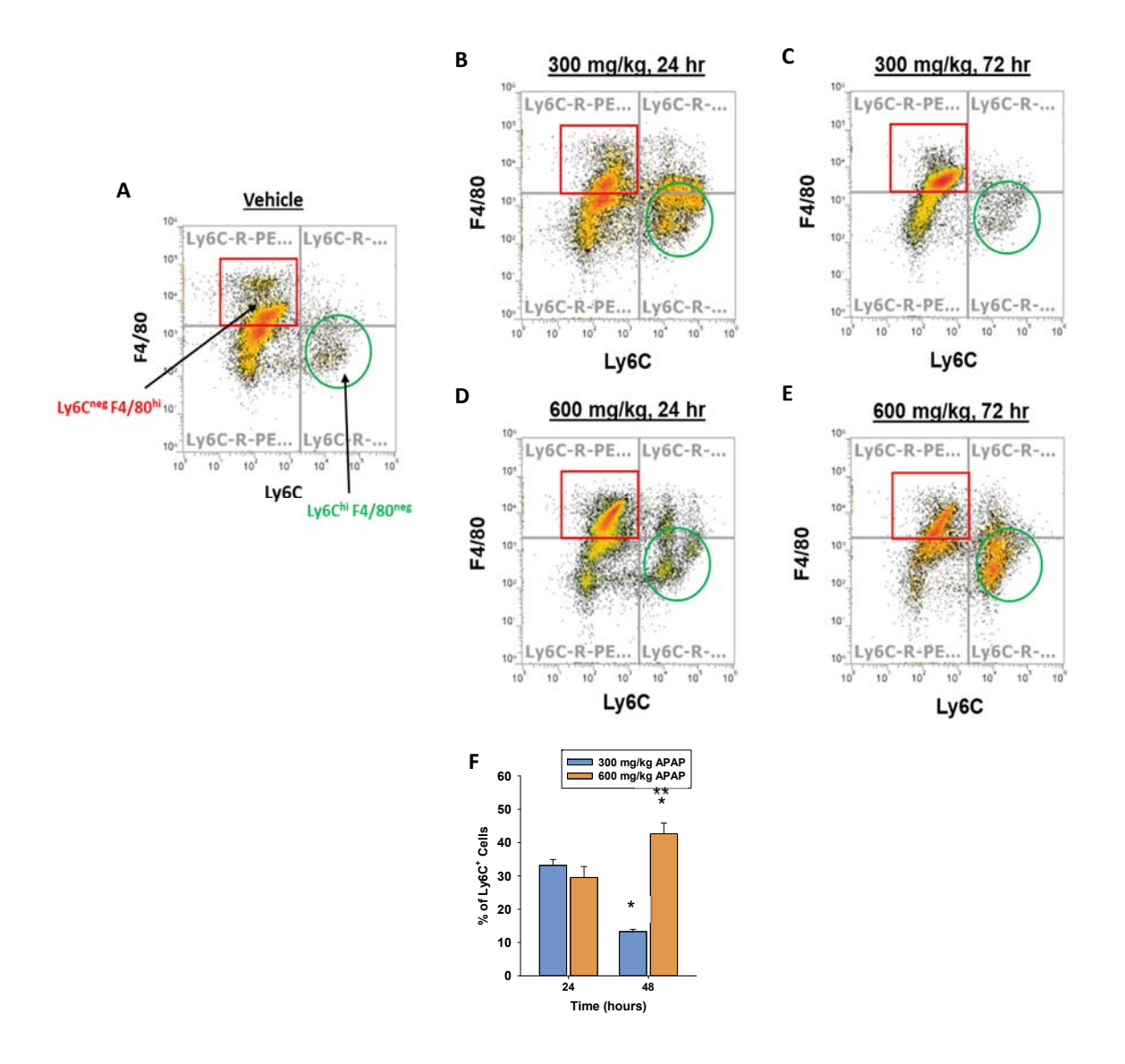


Figure 3.4: Effect on Macrophage Phenotype after APAP-induced ALF. Mice were treated with either vehicle control, 300 mg/kg APAP, or 600 mg/kg APAP. (A) After 24 hours, livers were digested and Ly6C⁺ and F4/80⁺ cells were detected by flow cytometry in the nonparenchymal cell fraction of vehicle-treated mice. After 24 (B) and 72 hours (C) Ly6C⁺ and F4/80⁺ were detected by flow cytometry. After 24 (D) and 72 hours (E) Ly6C⁺ and F4/80⁺ were detected by flow cytometry. (F) The percentage of Ly6C⁺ cells was quantified by flow cytometry. *Significantly different from 24 hours. **Significantly different from mice treated with 300 mg/kg APAP 48 hours earlier. Data are expressed as mean ± SEM; n = 3.

to mice treated with 300 mg/kg APAP, a population of Ly6C⁺ F4/80⁻ macrophages appeared in the liver by 24 hours after treatment with 600 mg/kg APAP (Fig 3.4D, green circle). Interestingly, this population of macrophages remained at 72 hours after treatment with 600 mg/kg APAP (Fig. 3.4E, green circle). Quantification of the flow cytometry showed a similar percentage of Ly6C⁺ macrophages in the livers of mice treated with 300 mg/kg APAP and 600 mg/kg APAP at 24 hours after treatment (Fig. 3.4F). By 72 hours, this population of macrophages was decreased in mice treated with 300 mg/kg APAP (Fig. 3.4F). By contrast, this population of macrophages continued to increase in mice treated with 600 mg/kg APAP (Fig. 3.4F). Collectively, this suggested that the Ly6C⁺ proinflammatory macrophages failed to switch phenotype to anti-inflammatory, pro-restorative macrophages in mice treated with 600 mg/kg APAP. To examine this further, we next determined whether this impacted levels of proinflammatory cytokines.

3.4.3 Sustained cytokine production in mice with APAP-induced ALF. In mice treated with 300 mg/kg APAP, mRNA levels of the proinflammatory cytokines, Ccl2 and Tnf- α , peaked at 24 hours and returned to baseline by 72 hours after treatment (Fig. 3.5A and B). By contrast, mRNA levels of Ccl2 and Tnf- α were increased at 24 hours after treatment with 600 mg/kg APAP and remained elevated at 72 hours after treatment (Fig. 3.5A and B). In addition, serum levels of CCL2, TNF- α , IL-1 β , IL-6, IFN- γ , and IL-4 protein were greater in mice treated with 600 mg/kg APAP at 72 hours after treatment when compared to mice treated with 300 mg/kg APAP (Fig. 3.5C-5H).

Clinical studies have revealed that levels of anti-inflammatory cytokines, such as IL-10, are also paradoxically elevated in ALF patients (Berry, 2010). These studies showed further that high levels of IL-10 were associated with a poor outcome. Similar to ALF patients, mRNA levels of the anti-inflammatory cytokine, IL-10, were substantially elevated in mice treated with 600 mg/kg APAP, and levels of both mRNA in liver and protein in serum remained elevated at

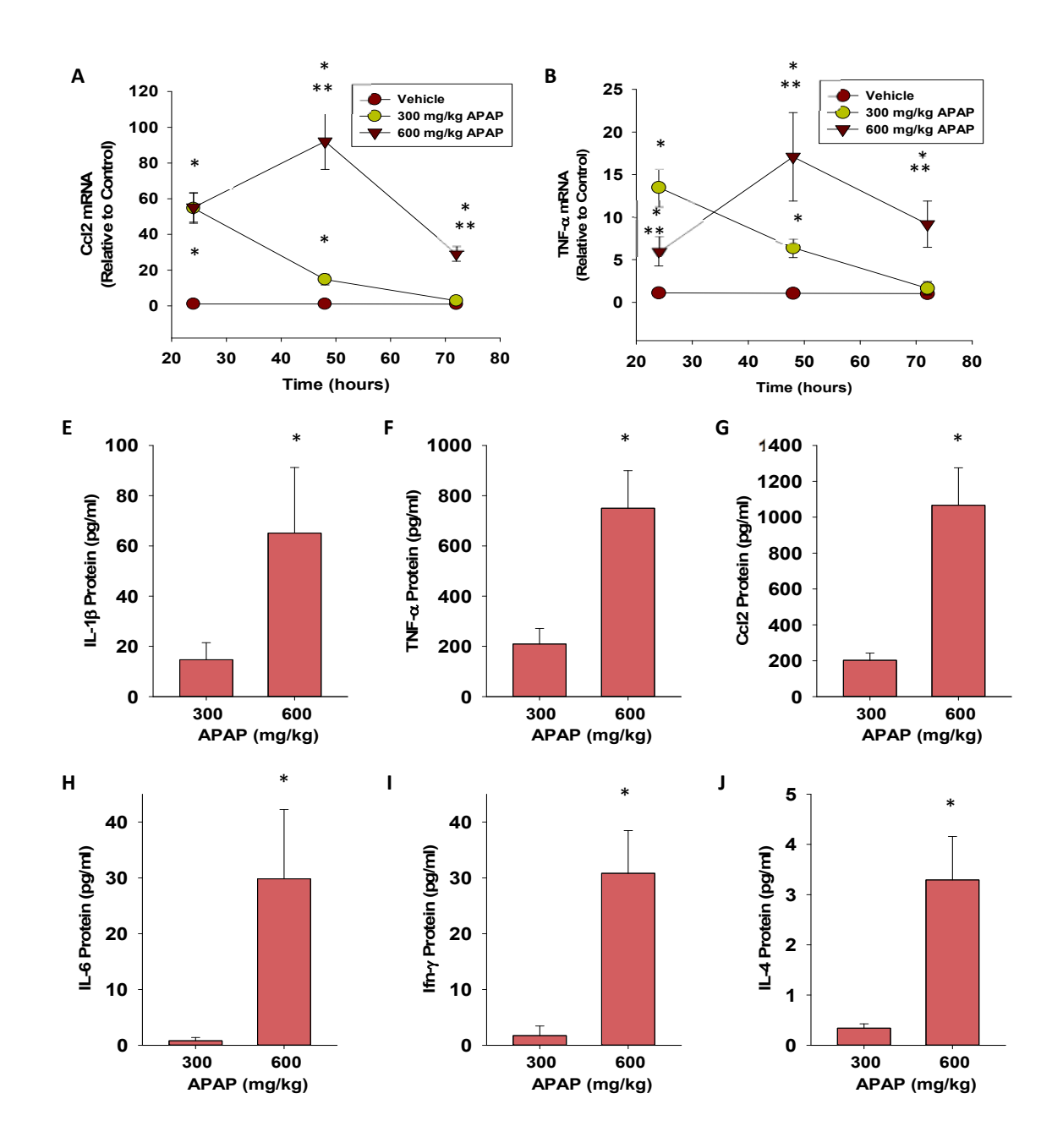


Figure 3.5: Sustained Cytokine Production after APAP-induced ALF. (A) Ccl2 and (B) TNF- α mRNA levels were measured at 24, 48, and 72 hours after APAP treatment. *Significantly different from vehicle-treated mice. **Significantly different from mice treated with 300 mg/kg at the same time point. (C-H) Serum levels of the indicated cytokine were measured at 72 hours after APAP treatment. *Significantly different from mice treated with 300 mg/kg APAP. Data are expressed as mean \pm SEM; n = 5 mice per group.

72 hours (Fig. 3.6). In mice treated with 300 mg/kg APAP, however, mRNA levels of IL-10 were not increased until 72 hours after treatment (Fig. 3.6).

3.4.4 IL-10 prevents trafficking of macrophages into necrotic lesions in mice with APAP-induced ALF. IL-10 is a potent anti-inflammatory cytokine that has multiple effects on macrophage function, including inhibition of macrophage migration (Vicioso, 1998). Because macrophages failed to traffic into necrotic lesions of mice with ALF and levels of IL-10 were highly elevated in these mice, we next tested the hypothesis that IL-10 prevented macrophage trafficking into the necrotic lesions. We took two approaches to test this hypothesis. First, mice treated with 300 mg/kg APAP were treated with vehicle or recombinant IL-10. In the second approach, we neutralized IL-10 in mice treated with 600 mg/kg APAP. As shown earlier, numerous CD68⁺ macrophages accumulated into the necrotic lesions of mice treated with 300 mg/kg APAP and vehicle (Fig. 3.7A, necrotic lesions demarcated by a dotted while line). In mice treated with recombinant IL-10 twenty-four hours after 300 mg/kg APAP treatment, CD68* macrophages accumulated in the liver but were largely confined to the border of the necrotic lesions (Fig. 3.7B) similar to mice treated with 600 mg/kg APAP alone (Fig. 3.2F). Similar to results in Figure 3.2, CD68+ macrophages accumulated at the periphery of the necrotic lesions in mice treated with 600 mg/kg APAP (Fig. 3.7C). Injection of IL-10 neutralizing antibody 24 hours after treatment with 600 mg/kg APAP resulted in the accumulation of numerous CD68* cells within the necrotic lesions, indicating that neutralization of IL-10 restored trafficking of CD68⁺ cells (Fig. 3.7D).

3.4.5 Impact of IL-10 on clearance of necrotic cells from the livers of APAP-treated mice. Since IL-10 impacted macrophage trafficking into the necrotic lesions, we determined whether this restored clearance of necrotic cells. As shown in Figure 3.8, cotreatment of mice with APAP and IL-10 resulted in larger necrotic lesions, suggesting that IL-10 prevented clearance of necrotic cells. Because IL-10 neutralization in mice treated with 600 mg/kg APAP recovered macrophage trafficking into the necrotic lesions (Fig. 3.7D), we would predict that this

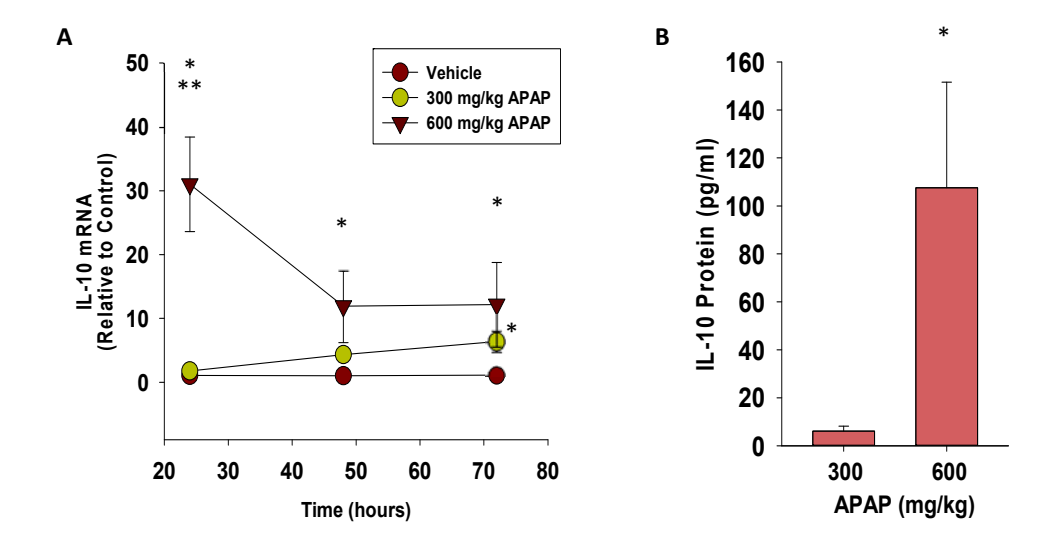


Figure 3.6 High IL-10 Levels after APAP-induced ALF. (A) mRNA levels of IL-10 were measured at 24, 48, and 72 hours after APAP treatment. *Significantly different from vehicle-treated mice. **Significantly different from mice treated with 300mg/kg APAP. Data are expressed as mean \pm SEM; n = 5 mice per group. (B) Serum levels of IL-10 were measured at 72 hours. *Significantly different from mice treated with 300 mg/kg. Data are expressed as mean \pm SEM; n = 5 mice per group.

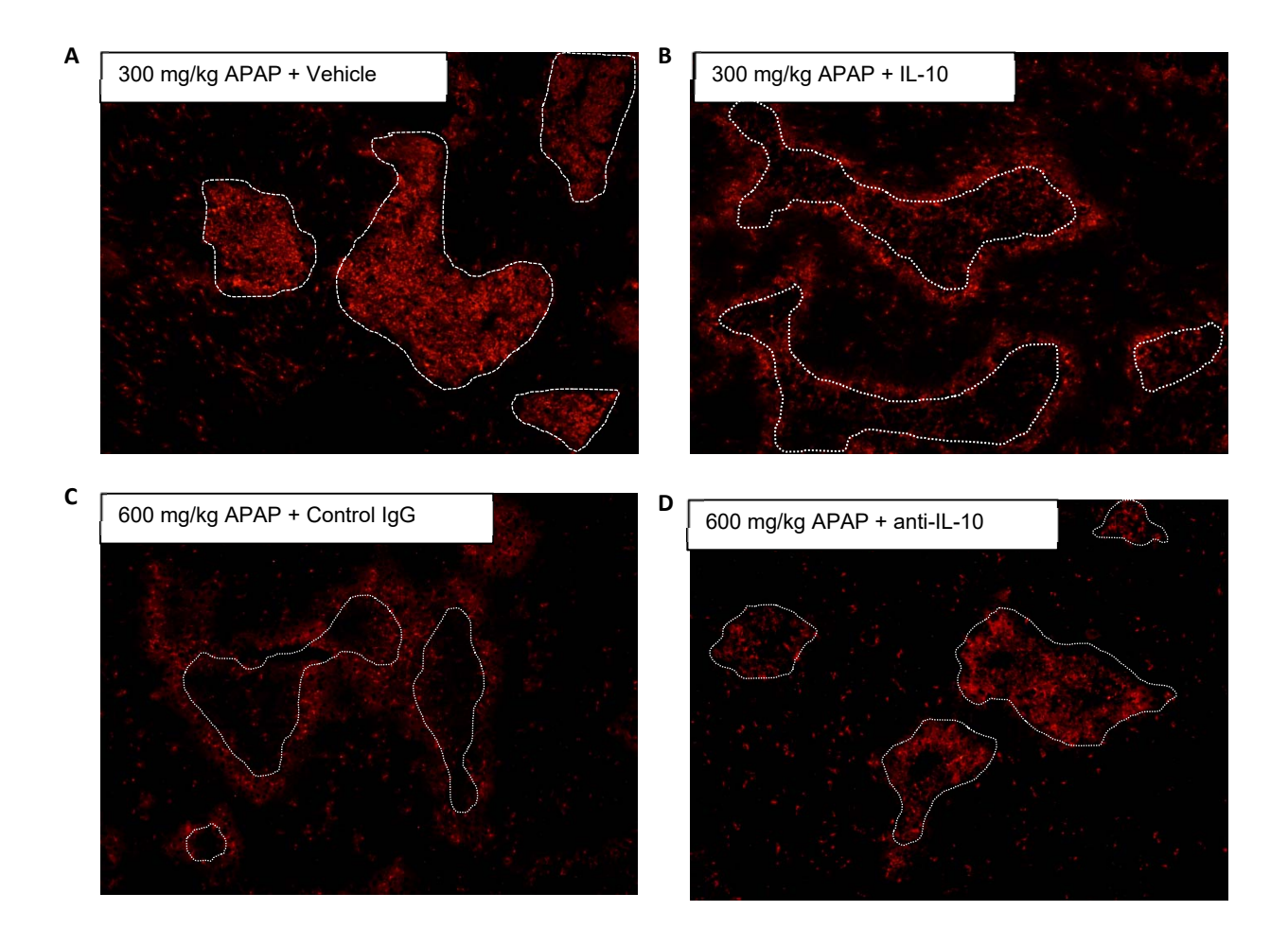


Figure 3.7: High IL-10 Levels Prevents Trafficking of Macrophages into Necrotic

Lesions. CD68 was detected by immunofluorescence in sections of liver from mice treated with (A) 300 mg/kg APAP + vehicle, (B) 300 mg/kg APAP + 5 μg IL-10, (C) 600mg/kg APAP + control IgG, or (D) 600mg/kg APAP + IL-10 neutralizing antibody. The necrotic lesions are demarcated by a dashed line. Representative photomicrographs from an n = 5 mice per group.

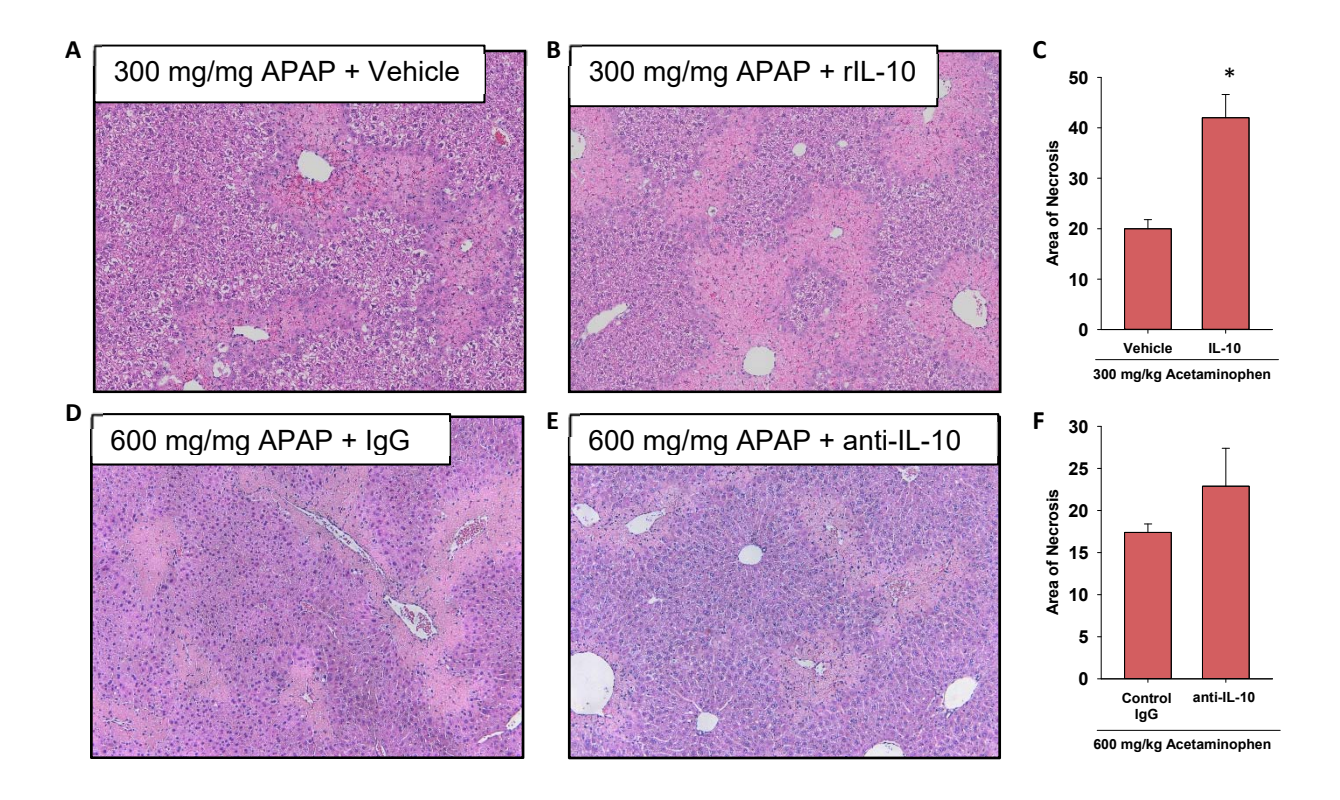


Figure 3.8: Impact of High IL-10 Levels on Clearance of Necrotic Cells. Representative photomicrographs of H&E stained liver sections from mice treated with (A) 300 mg/kg APAP + vehicle, (B) 300 mg/kg APAP + 5 μ g IL-10, (D) 600mg/kg APAP + control IgG, or (E) 600mg/kg APAP + IL-10 neutralizing antibody. (C and F) The area of necrosis was quantified. *Significantly different from mice treated with 300 mg/kg APAP + vehicle. Data are expressed as mean \pm SEM; n = 5 mice per group.

might stimulate clearance of necrotic cells, which fails to occur in mice treated with 600 mg/kg APAP alone (Fig. 3.1D and E). In mice treated with 600 mg/kg APAP, however, neutralization of IL-10 had no impact on the clearance of necrotic cells from the liver (Fig. 3.8D-F).

3.5 Discussion

Clinical studies have revealed that macrophage dysregulation is common in ALF, and that the degree of dysregulation is a predictor of outcome in these patients (Antoniades, 2008). What remains unclear, though, is the mechanism by which macrophage dysregulation occurs in ALF and whether it contributes to failed liver repair in these patients. In the present study, we utilized a mouse model of APAP-induced ALF to determine whether macrophage dysregulation is a feature of ALF in mice and to determine the impact of this condition on repair of the liver (Bhushan, 2014).

In mice treated with a dose of APAP (300 mg/kg) associated with normal liver repair, hepatic levels of proinflammatory cytokines were rapidly increased by 24 hours after treatment. By 72 hours, levels of these cytokines returned to baseline indicating a transition to the resolution phase of inflammation. By contrast, in mice treated with a dose of APAP that produces ALF (i.e., 600 mg/kg), levels of several proinflammatory cytokines remained highly elevated at 72 hours. This suggested that the mechanisms that trigger resolution of inflammation in these mice are impaired. Importantly, the sustained elevation in proinflammatory cytokines observed in these mice mirrored that which occurs in ALF patients (Antoniades, 2008). Although the underlying cause of sustained inflammation is not known, our studies indicate that it may result from a failure of macrophages to properly transition from an M1-like proinflammatory macrophage into an M2-like pro-reparative macrophage, a step that is critical for resolution of inflammation. During normal liver repair (i.e., 300 mg/kg APAP), monocytederived proinflammatory macrophages, characterized as Ly6C^{hi} F4/80^{how}, are rapidly recruited to the liver. Lineage tracing studies have revealed that these cells transition into Ly6C^{low} F4/80^{hi} macrophages as liver injury is resolved and necrotic cell debris is removed. During this process

of "phenotype switching", proinflammatory cytokine production is terminated (Zigmond, 2014). In mice with ALF (i.e., 600 mg/kg APAP), though, a large population of Ly6Chi F4/80low macrophages remained in the liver at 72 hours, suggesting that the process of phenotype switching did not occur, leading to the sustained production of proinflammatory cytokines. Although we did not elucidate the underlying cause, reduced phagocytosis and impaired neutrophil recruitment may be contributing factors. We showed recently that phagocytosis of necrotic hepatocytes by Ly6Chi F4/80low macrophages, isolated from APAP treated mice, decreased expression of proinflammatory cytokines, suggesting that phagocytosis may be an important stimulus of phenotype switching (Roth, 2019). As demonstrated in Figure 3.1, macrophage-mediated phagocytosis of dead cells was completely prevented in mice with ALF. Yang et al. recently demonstrated that hydrogen peroxide released from neutrophils is an important stimulus of the transition of Ly6Chi F4/80low macrophages into Ly6Clow F4/80hi macrophages after APAP overdose (Yang, 2019). In our studies, hepatic neutrophil numbers were substantially reduced in mice treated with 600 mg/kg APAP when compared to mice treated with 300 mg/kg APAP. Although it is not known whether this similarly occurs in ALF patients, systemic neutrophil dysfunction has been reported in ALF patients (Taylor, 2013). It is possible that this could further impact neutrophil-dependent switching of macrophage phenotype in liver (Taylor, 2013).

In addition to high levels of proinflammatory cytokines, ALF patients often present with high circulating levels of anti-inflammatory cytokines, including IL-10 (Friedman, 1997) (Berry, 2010). In our studies we observed a similar phenomenon where IL-10 levels were highly elevated in mice treated with 600 mg/kg APAP at times where IL-10 was not increased in mice treated with 300 mg/kg APAP. Interestingly, our studies revealed further that high levels of IL-10 in these mice severely impacted macrophage function. In mice with ALF, monocyte-derived macrophages accumulated in the liver but failed to traffic into the necrotic lesions, resulting in impaired phagocytic removal of dead cells and sustained cytokine production. Interestingly,

neutralization of IL-10 in mice with APAP-induced ALF restored macrophage trafficking, while, treatment of mice with recombinant IL-10 prevented macrophage trafficking in mice treated with 300 mg/kg APAP. While the mechanism by which IL-10 limits macrophage trafficking in the liver was not elucidated in our studies, it was previously shown that IL-10 inhibits monocyte chemotaxis *in vitro*, an effect that was potentiated by GM-CSF (Viscioso, 1998).

One potential source of IL-10 in ALF may be myeloid-derived suppressor cells (MDSCs), an immune suppressive myeloid cell that produces high levels of IL-10. In support of this, a recent study demonstrated that in acute on chronic liver failure patients and in ALF patients, there is an expanded population of blood monocytes expressing markers of MDSCs (Bernsmeier, 2018). Unfortunately, in our studies, we were unable to determine whether there was an expansion of MDSCs in mice with APAP-induced ALF, as there are currently no selective markers for these cells in mice (Cassetta, 2019). The mechanism(s) that trigger MDSC formation in ALF are not currently known. Although, it was recently reported that in mice expressing a mutant form of fibrin(ogen) incapable of binding leukocyte β_2 integrins, that circulating IL-10 levels were substantially higher after treatment with a dose of APAP associated with normal liver repair (Kopec, 2017). Interestingly, similar to mice with ALF, there was a failure to clear dead cell debris in these mice. This suggests that direct engagement of fibrin(ogen) by monocytes may be a critical determinant of monocyte phenotype, and that disruption of this interaction may stimulate monocytes to transition to MDSCs. Further studies are needed, however, to evaluate this.

Although neutralization of IL-10 rescued hepatic trafficking of monocyte-derived macrophages in mice, it did not restore clearance of necrotic cells by phagocytosis. This suggests that other factors in ALF negatively impact macrophage phagocytic function. One possibility is that the transition of monocytes into MDSCs impaired their ability to phagocytose dead cell debris. Consistent with this, MDSCs isolated from the blood of patients with acute on chronic liver failure or ALF showed a reduced ability to phagocytose *E. coli* (Bernsmeier, 2018).

This suggests that a full reversal of MDSC phenotype may be needed to fully restore macrophage function and liver repair in ALF.

Collectively, our studies demonstrate that macrophage dysregulation is a key feature of ALF in mice similar to patients. In mice this leads to impaired macrophage trafficking, reduced phagocytosis, and sustained cytokine production that severely impacts liver repair. Further investigation into the underlying cause of macrophage dysregulation in mice could highlight ways to prevent or reverse this condition in ALF patients, thereby restoring liver repair and, ultimately, liver function.

Chapter 4

Differential Response of Hepatic Monocytederived Macrophages and Kupffer Cells to Bacterial Lipopolysaccharide

4.1 Abstract

The liver contains two distinct populations of macrophages, monocyte-derived macrophages (MDMs), which primarily reside proximal to the Glisson's capsule and Kupffer cells, which reside within the sinusoids. Kupffer cells infiltrate the liver during embryogenesis and are replenished from local proliferation of mature Kupffer cells. By contrast MDMs arise from hematopoietic stem cells in the bone marrow and are replenished from circulating monocytes. Studies have revealed that these two hepatic macrophage populations possess distinct transcriptomic profiles, suggesting that they may be functionally distinct. In the present study, we tested the hypothesis that MDMs and Kupffer cells are differentially sensitive to bacterial lipopolysaccharide (LPS). MDMs and Kupffer cells were purified to greater than 90% from the livers of mice by using magnetic beads labeled with Cx3cr1 antibody for MDMs and F4/80 antibody for Kupffer cells. Basal levels of tumor necrosis factor- α (TNF- α) mRNA were higher in MDMs when compared to Kupffer cells. After treatment with LPS, mRNA levels of TNF- α , Cxcl1, and Cxcl2 were increased to a greater extent in MDMs when compared to Kupffer cells. To confirm these findings, Kupffer cells and MDMs were isolated from mice in which bone marrow transplantation was used to selectively tag cells arising from hematopoietic stem cells in adult mice. Similar to above, treatment of MDMs with LPS increased TNF-α, Cxcl1, and Cxcl2 to a greater extent when compared to Kupffer cells. Collectively, these results indicate that MDMs exhibit a greater pro-inflammatory phenotype in the liver when exposed to LPS.

4.2 Introduction

Hepatic macrophages arise from two distinct developmental lineages (Varol, 2015). Kupffer cells, the resident tissue macrophages of the liver, develop from progenitor stem cells originating in the fetal yolk-sac (Schulz, 2012) (Epelman, 2014). These cells reside within the lumen of the hepatic sinusoids where they are positioned to detect and clear blood-borne

pathogens, cellular debris, and other foreign material that may enter the portal circulation through the gut (Guillot and Tacke, 2019). Kupffer cells are replenished by local proliferation of mature Kupffer cells under homeostatic conditions and after toxin-induced liver injury (Zigmond, 2014). Under conditions of severe depletion, however, bone marrow-derived monocytes are recruited to the Kupffer cell niche where they ultimately mature into Kupffer cells (Yona, 2013) (Scott, 2016). In addition to Kupffer cells, a second, distinct population of hepatic macrophages exists under steady-state conditions that develops from monocytes arising from hematopoietic stem cells in the bone marrow (Sierro, 2017). These monocyte-derived macrophages (MDMs), also known as liver capsular macrophages, are positioned proximal to the Glisson's capsule, a fibrous layer of connective tissue surrounding the liver (David, 2016) (Abdel-Misih and Bloomston, 2010). They are also located around blood vessels within the liver (Yona, 2013). Studies have revealed that MDMs protect the liver from pathogens that might invade from the peritoneal cavity by extending dendrites through the Glisson's capsule and into the peritoneal cavity (Sierro, 2017).

Recent studies have demonstrated that in addition to being ontogenetically and morphologically distinct, bone marrow-derived and yolk sac-derived resident hepatic macrophages possess distinct transcriptomic profiles (David, 2016) (Beattie, 2016) (Sierro, 2017). While Kupffer cells displayed enhanced expression of phagocytosis-related genes, MDMs displayed enhanced expression of antigen-presenting genes (David, 2016). However, beyond identification of transcriptional differences between the two populations, it remains to be demonstrated whether there are functional differences between these macrophage populations.

Kupffer cells and monocyte-derived MDMs can be distinguished by expression of membrane markers. Whereas Kupffer cells are F4/80^{hi}CD11blowCx3Cr1low, monocyte-derived LCMs are F4/80lowCD11bhighCx3Cr1high under steady-state conditions (Schulz, 2012) (Yona, 2013). In the present study, we exploited differences in these cell surface markers and used bone marrow transplantation to purify these two macrophage populations. Once purified, we

determined the sensitivity of these two macrophage populations to bacterial lipopolysaccharide (LPS) by measuring proinflammatory cytokine expression.

4.3 Materials and Methods

- **4.3.1 Animal Treatments.** 6-12 week old male C57Bl/6 mice (Jackson Laboratories, Bar Harbor, ME) were used for all studies. For bone marrow transplantation, Ptprc^a Pepc^b/BoyJ mice, a congenic C57Bl/6 strain, which expresses the CD45.1 allele were transplanted into C57Bl/6 mice which express the CD45.2 allele. Mice were housed in a 12 hr light/dark cycle under controlled temperature (18-21°C) and humidity. Food (Rodent Chow; Harlan-Teklad) and tap water were allowed *ad libitum*.
- **4.3.2 Bone Marrow Transplant.** Recipient mice (C57Bl/6, CD45.2) were irradiated with 11 Gy as a split dose (2 X 5.5 Gy, 3 hours apart) using a Cs¹³⁷ irradiator (JL Shepherd, San Fernando, CA). For some studies, the midsection of the mouse was covered with 5 mm of lead to protect the liver from irradiation. After 18-24 hours, the irradiated C57Bl/6 (CD45.2) mice were injected (retro-orbital injection) with 2 x 10⁶ bone marrow cells isolated from Ptprc^a Pepc^b/BoyJ (CD45.1) donor mice. MDMs and Kupffer cells were isolated 3-5 months after bone marrow transplant.
- 4.3.3 Isolation of Kupffer cells and monocyte-derived macrophages from C57BI/6 mice. To isolate Kupffer cells and MDMs, livers were perfused with collagenase (Collagenase H, Sigma-Aldrich) as described previously (Kim, 2006). The hepatocytes were removed by centrifugation and the nonparenchymal cells were pelleted by centrifugation at 300g for 10 minutes. 1 X 10⁸ nonparenchymal cells were resuspended in 60 μl of MACS Buffer (2.5 g bovine serum albumin, 0.416 g EDTA, and 500 mL PBS) containing 12 μl anti-CD11c antibody (Miltenyi Biotec, Bergisch Gladbach, Germany). The cell suspension was incubated for 10 minutes in the dark at 4°C and then washed with 10 mL of MACS buffer. The cells were centrifuged at 300g for 10 minutes and the resulting pellet was resuspended with 500 μl MACS

Buffer and applied to MACS LS columns (Miltenyi Biotec). The column was rinsed 3 times with 3 ml of MACS buffer. Unlabeled CD11c-negative cells passing through the column were collected and centrifuged at 300g for 10 minutes. The pellet was resuspended in MACS Buffer containing anti-CX3CR1 antibody (Miltenyi Biotec) (12 µl CX3CR1 antibody in 60 µl MACS buffer per 108 cells). The cell suspension was incubated for 10 minutes in the dark at 4°C and then washed with 10 mL MACS buffer. The cells were centrifuged at 300g for 10 minutes. The cell pellet was resuspended and applied to MACS LS columns (Miltenyi Biotec). Monocytederived CX3CR1-positive macrophages were collected by removing the column from the midiMACS Separator and rinsing the column with 5 ml MACS buffer. The CX3CR1-negative flow-through was collected and centrifuged at 300g for 10 minutes. The pellet was resuspended in MACS Buffer with biotinylated anti-F4/80 antibody (Miltenyi Biotec). The cell suspension was incubated for 10 minutes at 4°C and then washed and centrifuged as above. Streptavidin microbeads (Miltenyi Biotec), diluted 1:10 in 60 µl of MACs buffer, were added to the cell pellet and incubated for 10 minutes at 4°C. The pellet was resuspended in 500 μl MACS Buffer and applied to MACS LS columns. Kupffer cells were collected by removing the column from the midiMACS Separator and rinsing the column with 5 ml of MACS buffer.

4.3.4 Isolation of Kupffer cells and monocyte-derived macrophages from bone-marrow transplanted mice. Livers from bone marrow transplanted mice were perfused and digested with collagenase. Nonparenchymal cells were separated from hepatocytes by centrifugation. To isolate Kupffer cells, half of the nonparenchymal cell fraction were incubated with anti-CD45.2 antibody for 10 minutes at 4°C (Miltenyi Biotec), followed by incubation with Streptavidin beads for 15 minutes at 4°C. The cell suspension was then washed, resuspended in 500 μl MACS Buffer, and applied to MACS LS columns. The CD45.2-positive flow-through cells were then incubated with biotinylated anti-F4/80 antibody for 10 minutes at 4°C, followed by incubation with Streptavidin beads for 15 minutes at 4°C. The cell suspension was then

washed, resuspended in 500 μ l MACS Buffer, and applied to MACS LS columns. Kupffer cells were collected by removing the column from the midiMACS Separator and rinsing the column with 5 ml of MACS buffer.

To isolate MDMs, the remaining half of the nonparenchymal cells were incubated with anti-CD45.1 antibody for 10 minutes at 4°C (Miltenyi Biotec), followed by incubation with Streptavidin beads for 15 minutes at 4°C. The cell suspension was washed, resuspended in 500 μ l MACS Buffer, and applied to MACS LS columns. MDMs were collected by removing the column from the midiMACS Separator and rinsing the column with 5 ml of MACS buffer. The pellet was resuspended in MACS Buffer containing anti-CX3CR1 antibody (Miltenyi Biotec) (12 μ l CX3CR1 antibody in 60 μ l MACS buffer per 10 8 cells), and the CX3CR1 positive MDMs were collected as described above.

4.3.5 Flow Cytometry. The Kupffer cells and MDMs isolated using magnetic bead separation were washed and resuspended in FACS buffer (PBS, 1% FBS). The cells were then incubated with Fc blocking buffer (BD Biosciences; diluted 1:20) for 10 mins at 4 °C. The cells were then rinsed and centrifuged at 300 g for 5 minutes. The cell pellet was then resuspended with anti-F4/80 Alexa Fluor-488 and anti-CD11b APC/Cy7 (BioLegend, San Diego, CA) and incubated for 30 minutes at 4 °C. The cells were then washed twice and fixed in formalin (Sigma) for 15 minutes. After cells were fixed, they were washed twice and resuspended in FACs buffer. Fluorescence was then detected using an Attune NxT flow cytometer (Life Technologies, Carlsbad, CA) and the data were analyzed using Attune NxT software.

4.3.6 LPS Treatment. Cells were seeded in 1 mL Dulbecco's Modified Eagle Medium (DMEM) (Thermo-Fisher Scientific, Waltham, MA) supplemented with 10% FBS and penicillin/streptomycin in each well of a 12-well cell culture plate (Grenier Bio-One, Kremsmunster, Austria) for ~16 hours. The cells were then washed with PBS before adding

1mL serum-free DMEM to each well. The cells were treated with 10 ng/ml lipopolysaccharide (LPS) (Sigma Chemical) for 3 hours at 37°C.

- **4.3.7 Immunohistochemistry.** Immunofluorescence was used to detect F4/80, CD45.1, and CD45.2 as described by us previously (Mochizuki, 2014). Briefly, frozen livers were cut into 8 μm sections, fixed in 4% formalin for 10 minutes, followed by blocking in 10% goat serum. The sections were then incubated with Alexa Fluor-488 anti-mouse CD45.1 antibody (Biolegend) diluted 1:100, Alexa Fluor-488 anti-mouse CD45.2 antibody (Biolegend) diluted 1:100, or rat anti-F4/80 antibody (Bio-Rad, Hercules, CA) diluted 1:500. The sections were then incubated with goat anti-rat secondary antibody conjugated to Alexa Fluor-594 diluted 1:500 (Thermo-Fisher Scientific).
- **4.3.8 Real-Time PCR.** RNA was isolated from cells by using the E.Z.N.A Total RNA Kit I (Omega Bio-Tek) according to manufacturer's instructions. Real-time PCR was performed as described previously (Kim, 2006). Real-time PCR was performed on a QuantStudio 7 Flex Real-Time PCR System (Thermo-Fisher) using the iTaq Universal SYBR green Supermix (Bio-Rad). The following primer sequences were used: TNF-α: Forward- 5'-

AGGGTCTGGGCCATAGAACT-3', Reverse- 5'-CCACCACGCTCTTCTGTCTAC-3'; Cxcl1:
Forward- 5'-TGGCTGGGATTCACCTCAAG-3', Reverse- 5'-GTGGCTATGACTTCGGTTTGG-3';
Cxcl2: Forward- 5'-CTCAGACAGCGAGGCACATC-3', Reverse- 5'-

CCTCAACGGAAGAACCAAAGAG-3'; Rpl13a: Forward- 5'-GACCTCCTCCTTTCCCAGGC-3', Reverse- 5'-AAGTACCTGCTTGGCCACAA-3'.

4.3.9 Statistical Analysis. Results are presented as the mean + SEM. Data were analyzed by two-way Analysis of Variance (ANOVA) where appropriate. Comparisons among group means were made using the Student-Newman-Keuls test, with a criterion for significance of p < 0.05 for all studies.

4.4 Results

- 4.4.1 Purification of Kupffer cells and MDMs from mouse liver. Flow cytometry was used to detect Kupffer cells (F4/80^{high}CD11blow, blue oval) and MDMs (F4/80lowCD11bhigh, red oval) in hepatic nonparenchymal cell fractions from untreated mice (Fig. 4.1). Next, we used antibody-labeled magnetic beads to purify Kupffer cells and MDMs from nonparenchymal cell fractions. Antibody against CD11c, a protein expressed by dendritic cells, was first used to remove dendritic cells from the nonparenchymal cell fraction (Fig. 4.2A) (Lau and Thompson, 2003). Next, antibody against CX3CR1 was used to purify MDMs and antibody against F4/80 was used to purify Kupffer cells (Fig. 4.2A). Flow cytometry was then used to determine the purity of the Kupffer cell and MDM fractions. MDMs, identified as F4/80lowCD11bhigh, were approximately 94.7% pure (Fig. 4.2B), whereas Kupffer cells, identified as F4/80highCD11blow, were approximately 99.2% pure (Fig. 4.2C). Further, basal expression of CD11b, Flt3, and Ccr2 mRNAs was greater in MDMs as reported previously (Fig. 4.3).
- 4.4.2 Differential upregulation of cytokines in Kupffer cells and MDMs by LPS. We next determined the sensitivity of MDMs and Kupffer cells to LPS. Treatment of Kupffer cells with LPS increased Tnf- α , Cxcl1, and Cxcl2 mRNA levels by 15.9, 1.6, and 2.3-fold respectively (Fig. 4.4A-B). Treatment of MDMs with LPS increased Tnf- α ,, Cxcl1, and Cxcl2 by 102.9, 3.2, and 8.2-fold respectively (Fig. 4.4A-C).
- **4.4.3 Generation of chimeric mice.** We next used bone marrow transplantation to generate chimeric mice. To accomplish this, bone marrow was isolated from mice expressing the CD45.1 allele and transplanted into lethally irradiated mice expressing the CD45.2 allele (Fig. 4.5A). Because Kupffer cells are of embryonic origin, they remain CD45.2⁺ after transplant, whereas MDMs, which arise from hematopoietic stem cells in the bone marrow, will be CD45.1⁺. After bone marrow transplant, we first used immunofluorescence staining to confirm that Kupffer cells were F4/80⁺CD45.2⁺ whereas MDMs were F4/80⁻CD45.1⁺. As

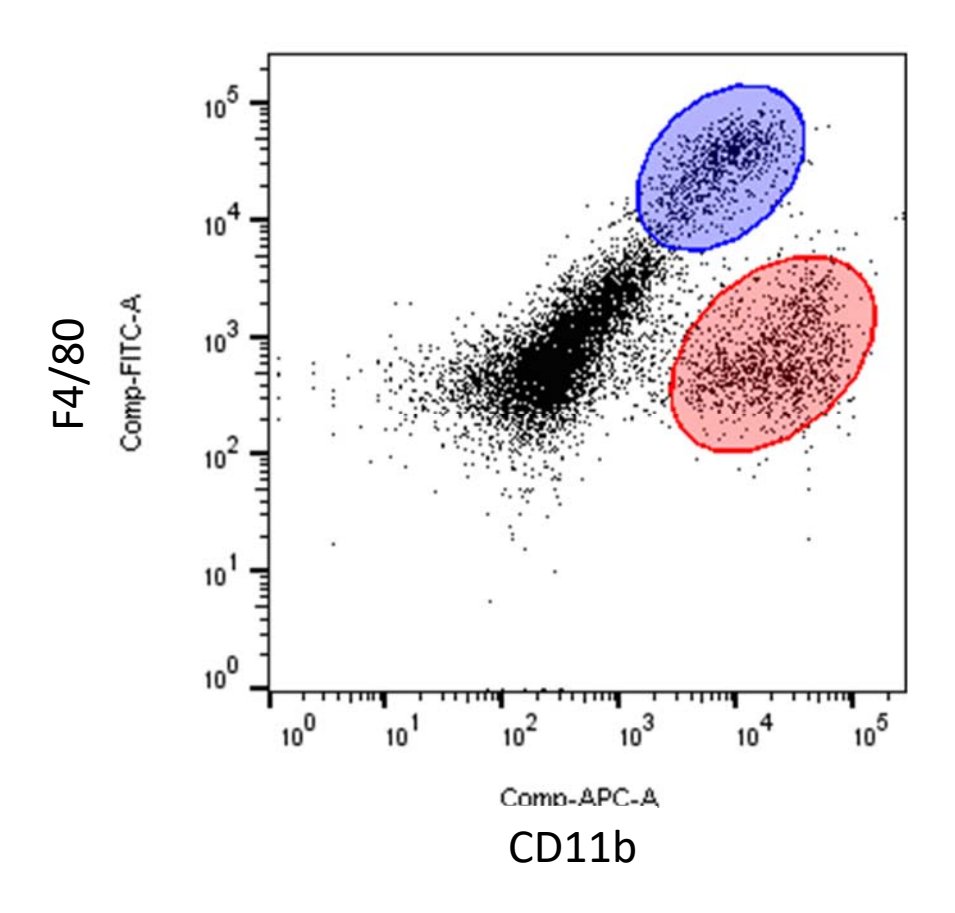


Figure 4.1: Resident Kupffer Cell and MDM Populations in the Liver. The nonparenchymal cell fraction was isolated from untreated mice and flow cytometry was used to detect F4/80 and CD11b. The Kupffer cell population (F4/80^{high}CD11b^{low}) is highlighted in blue, while the MDM population (F4/80^{low}CD11b^{high}) is highlighted in red.

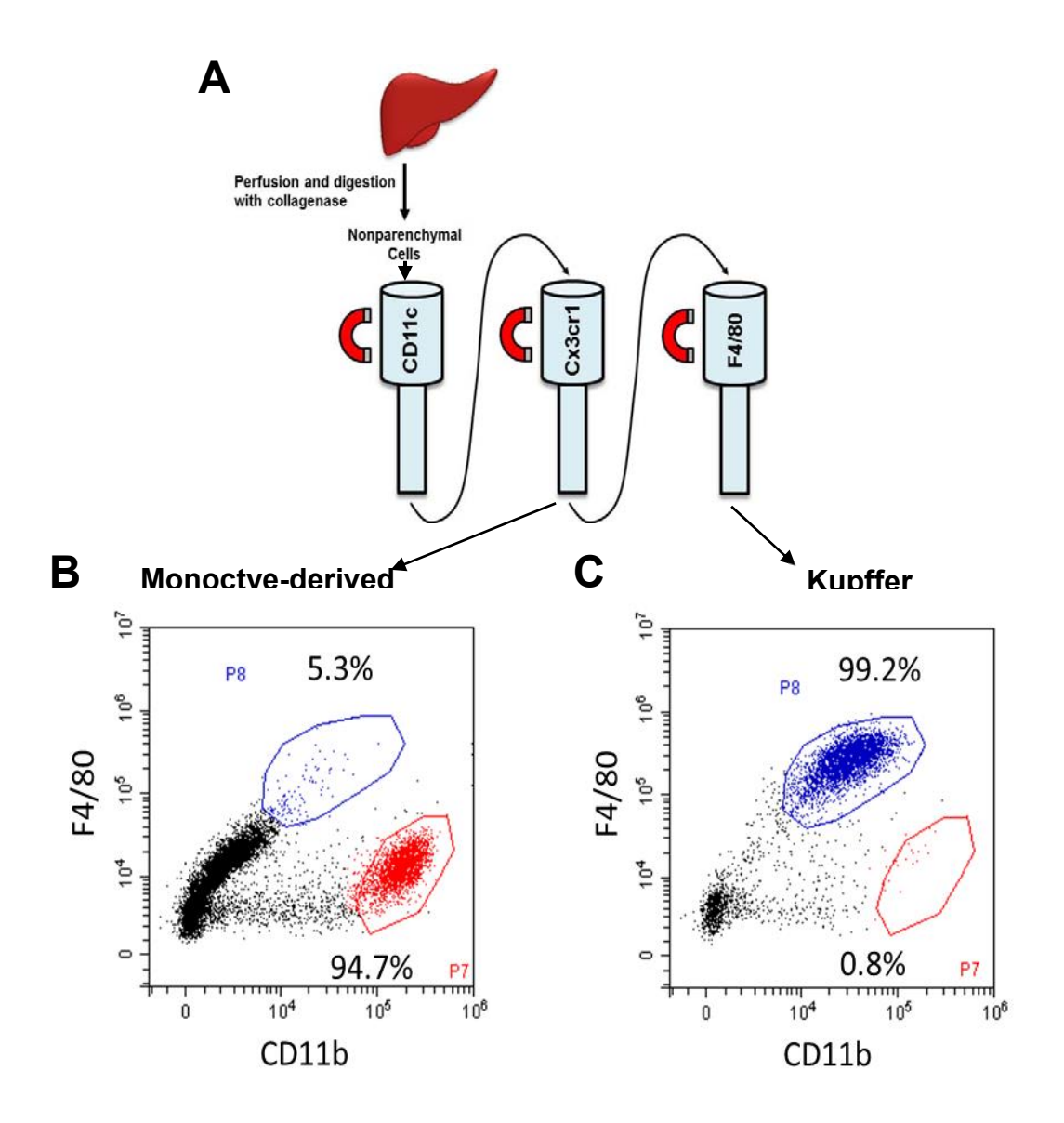


Figure 4.2: Isolation of Kupffer Cells and MDMs from the Liver. Livers from untreated mice were perfused and digested with collagenase. Nonparenchymal cells were separated from hepatocytes by centrifugation. (A) Kupffer cells and monocyte-derived macrophages were purified from the nonparenchymal cell fraction by using immunomagnetic bead separation. (B) MDMs (F4/80^{low}CD11b^{high}) were approximately 94.7% pure, while (C) Kupffer cells (F4/80^{high}CD11b^{low}) were approximately 99.2% pure.

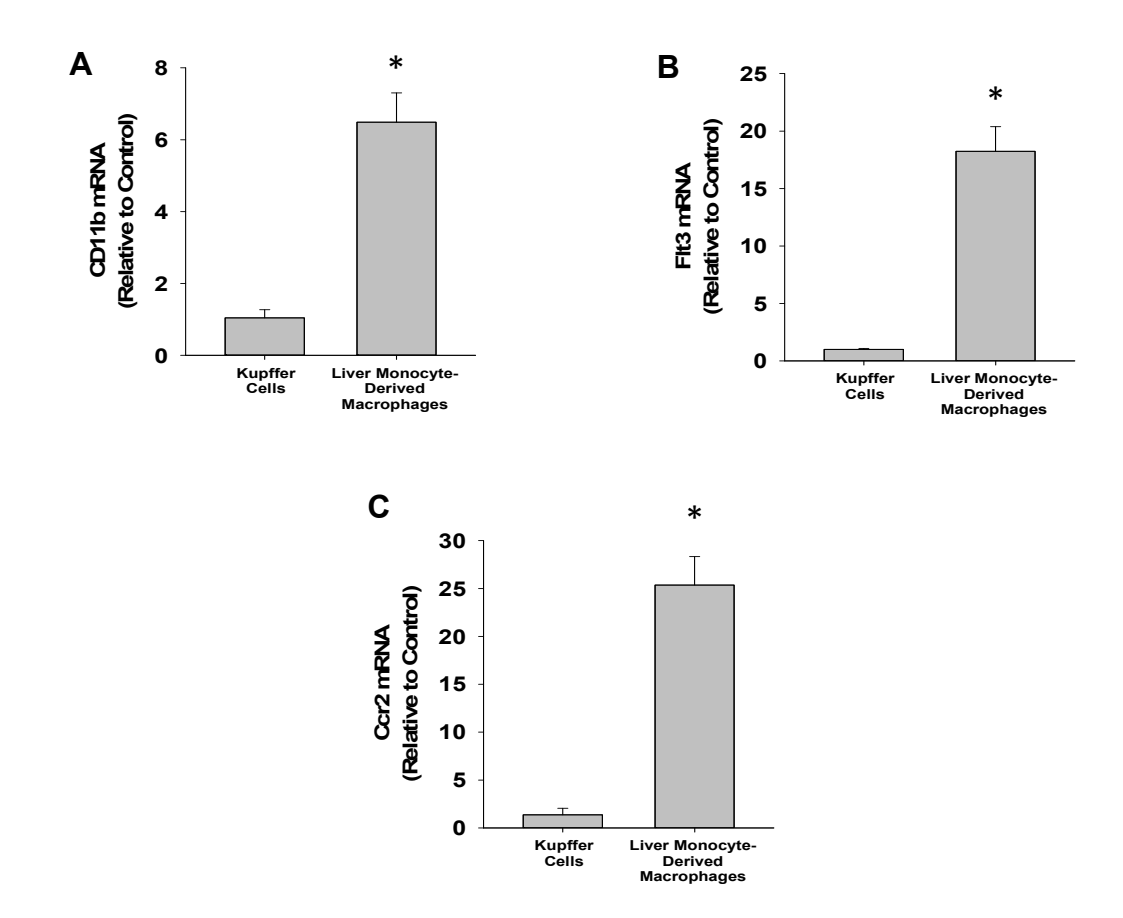


Figure 4.3: Basal Expression Levels of Kupffer Cells and MDMs. Kupffer cells and MDMs were isolated from the liver and separated by immunomagnetic bead separation. RNA was isolated from untreated cell cultures and basal mRNA levels of (A) CD11b, (B) Flt3, and (C) Ccr2 were measured by real-time PCR. Data are expressed as mean +/- SEM. *Significantly different from Kupffer cells at p<0.05.

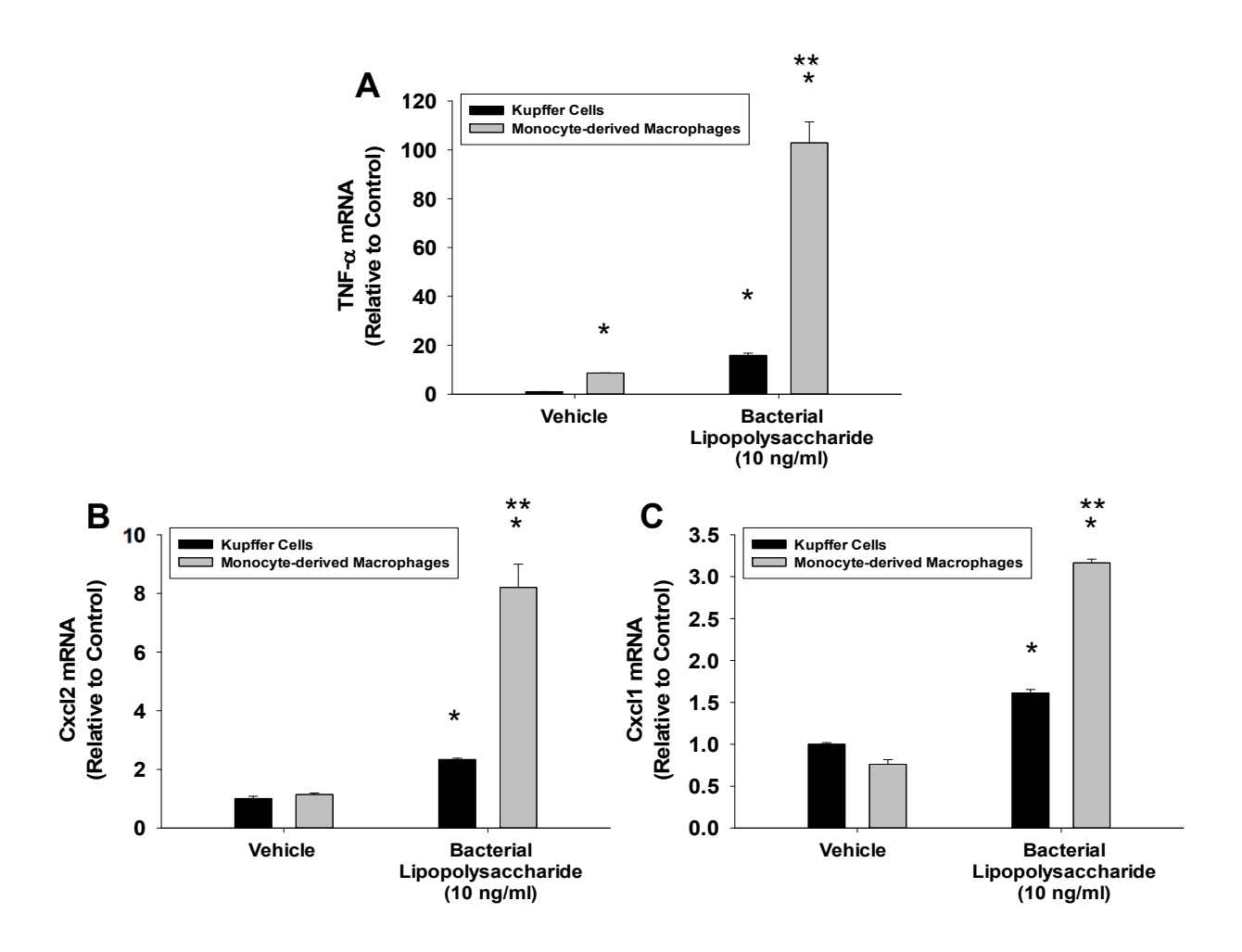


Figure 4.4: Differential Upregulation of Cytokines in Kupffer Cells and MDMs by LPS.

Kupffer cells and MDMs were isolated from the liver and separated by immunomagnetic bead separation. The cells were treated with LPS or vehicle for 3 hours. mRNA levels of (A) TNF- α , (B) Cxcl2, and (C) Cxcl1 were measured by real-time PCR. Data are expressed as mean +/- SEM. *Significantly different from vehicle-treated cells. **Significantly different from LPS-treated Kupffer cells at p<0.05.

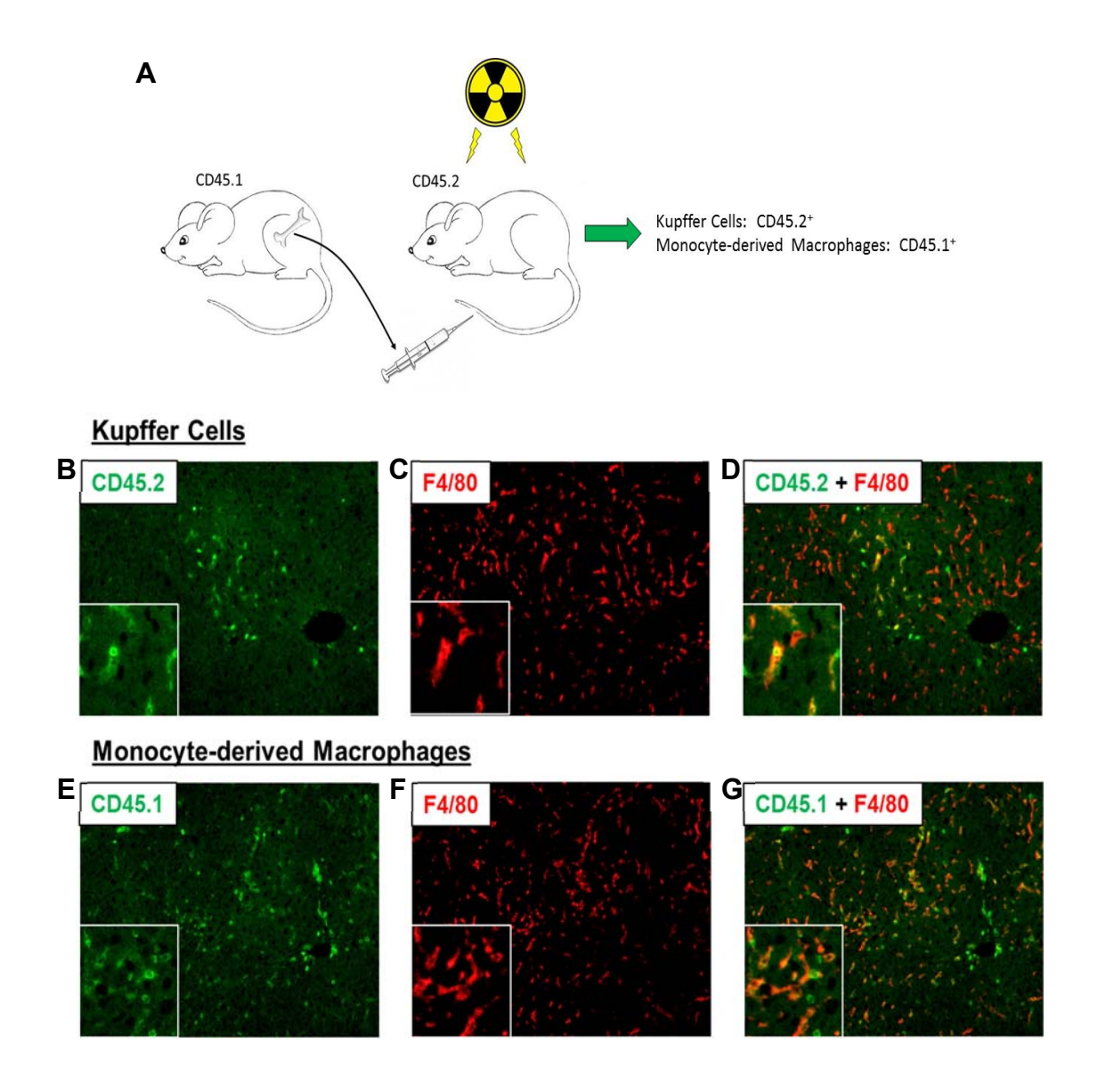


Figure 4.5: Generation of Chimeric Mice after Whole Body Irradiation and Bone Marrow Transplantation. (A) C57BL/6 (i.e., CD45.2) mice were subjected to whole body irradiation followed by transplantation with bone marrow from CD45.1 mice. (B-D) Immunohistochemistry was used to detect CD45.2 (i.e., Kupffer cells) and F4/80. (E-G) Immunohistochemistry was used to detect CD45.1 (i.e., MDMs) and F4/80.

anticipated, CD45.2 positive cells (green) colocalized with F4/80 (red) (Figure 4.5B-5D). Surprisingly, though, there was also substantial colocalization between CD45.1 (green) and F4/80 (red), indicating that many F4/80⁺ Kupffer cells had arose from hematopoietic stem cells in the bone marrow (Figure 4.5E-5G). It is possible that whole body irradiation produced extensive Kupffer cell toxicity that required MDMs recruited from bone marrow to fully recover. To prevent Kupffer cell toxicity, we next shielded the liver with lead prior to lethal irradiation (Fig. 4.6A). As shown in Figure 4.6B-D, after bone marrow transplant, all F4/80⁺ cells were also CD45.2⁺ (Fig. 4.6B-6D) whereas all CD45.1⁺ cells were F4/80⁻ (Fig. 4.6E-G). This indicated that Kupffer cells were CD45.2⁺ whereas MDMs were CD45.1⁺.

4.4.4 Isolation of Kupffer cells and MDMs from chimeric mice and treatment with LPS. Kupffer cells and MDMs were isolated from bone marrow transplanted mice. Magnetic beads labeled with CD45.2 and F4/80 were used to isolate Kupffer cells, whereas magnetic beads labeled with CD45.1 and CX3CR1 were used to isolate MDMs (Fig. 4.7). Treatment of Kupffer cells, isolated in this manner, with LPS increased Tnf-α, Cxcl1, and Cxcl2 mRNA levels by 13.6, 13.4, and 43.1-fold respectively (Fig. 4.8). Treatment of MDMs with LPS increased Tnf-α, Cxcl1, and Cxcl2 by 22.9, 28.7, and 75.9-fold respectively (Fig. 4.8).

4.5 Discussion

Recent studies demonstrated that hepatic MDMs and Kupffer cells possess distinct transcriptomic profiles (David, 2016) (Beattie, 2016) (Sierro, 2017). This suggested that functional differences may exist between these two hepatic macrophage populations. In support of this, our studies revealed that proinflammatory cytokines were upregulated to a greater extent in MDMs when compared to Kupffer cells. In addition, basal levels of Tnf-α were higher in MDMs. These results indicate that MDMs are skewed towards an M1-like proinflammatory phenotype and may produce a greater inflammatory response when exposed to bacteria or potentially other pathogens. It is possible that these phenotypic differences

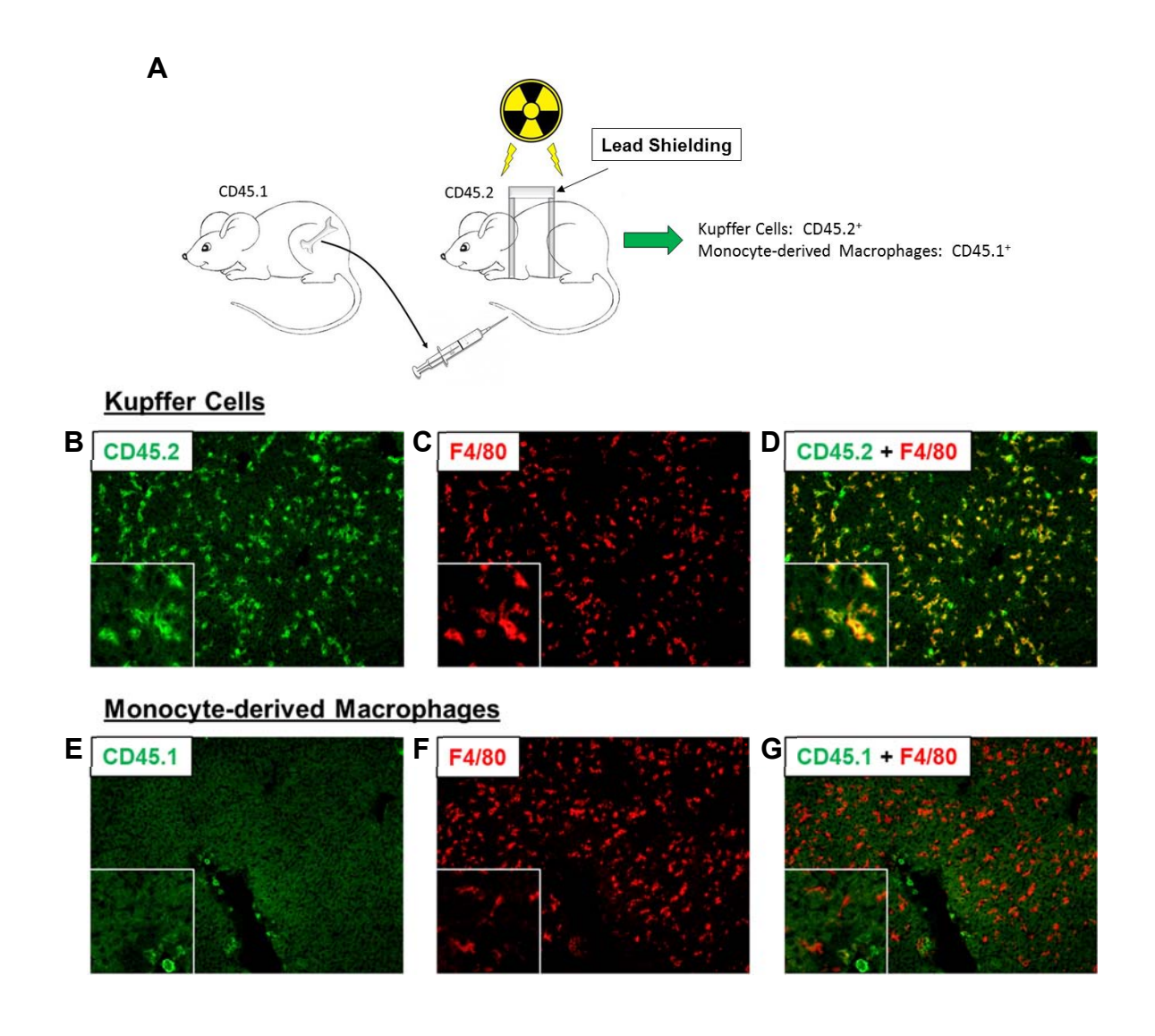


Figure 4.6: Generation of Bone Marrow Transplant Mice after Partial Body Irradiation.

(A) C57BL/6 (i.e., CD45.2) mice were subjected to partial body irradiation followed by transplantation with bone marrow from CD45.1 mice. (B-D) Immunohistochemistry was used to detect CD45.2 (i.e., Kupffer cells) and F4/80. (E-G) Immunohistochemistry was used to detect CD45.1 (i.e., MDMs) and F4/80.

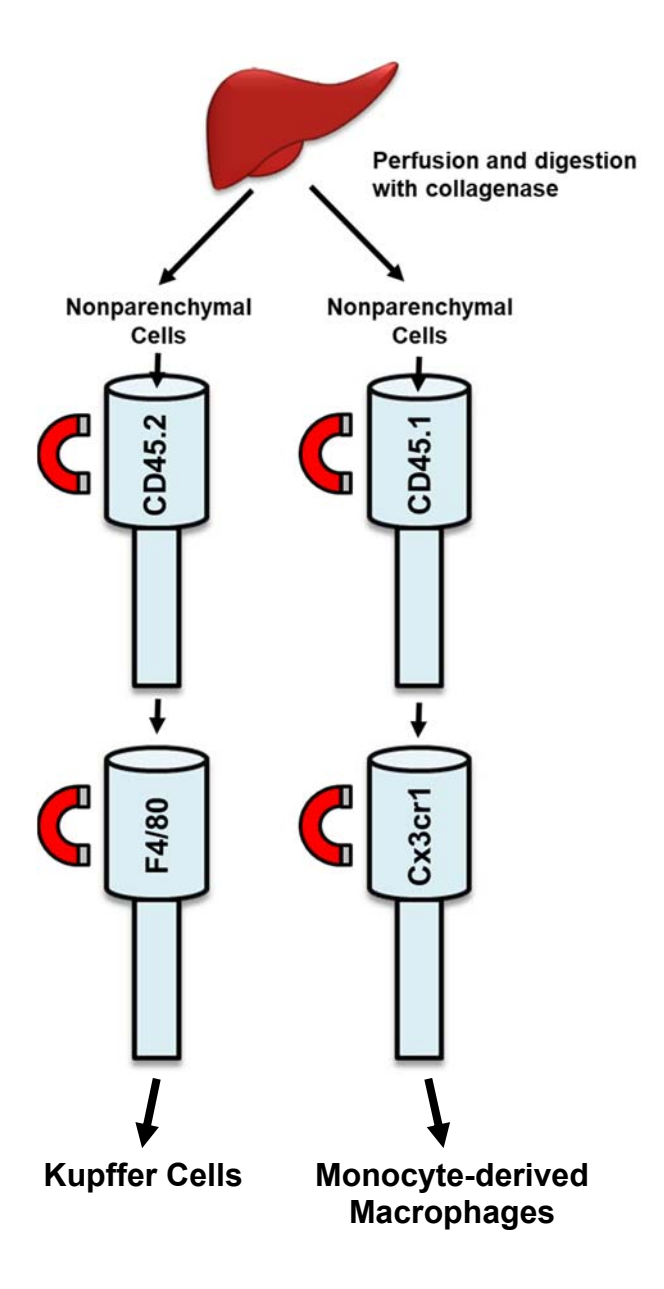


Figure 4.7: Isolation of Kupffer Cells and MDMs from Bone Marrow Transplant Mice.

Livers from bone marrow transplanted mice were perfused and digested with collagenase. Nonparenchymal cells were separated from hepatocytes by centrifugation. Kupffer cells were purified from the nonparenchymal cell fraction via immunomagnetic bead separation using antibodies for CD45.2 and F4/80. MDMs were purified from the nonparenchymal cell fraction via immunomagnetic bead separation using antibodies for CD45.1 and Cx3cr1.

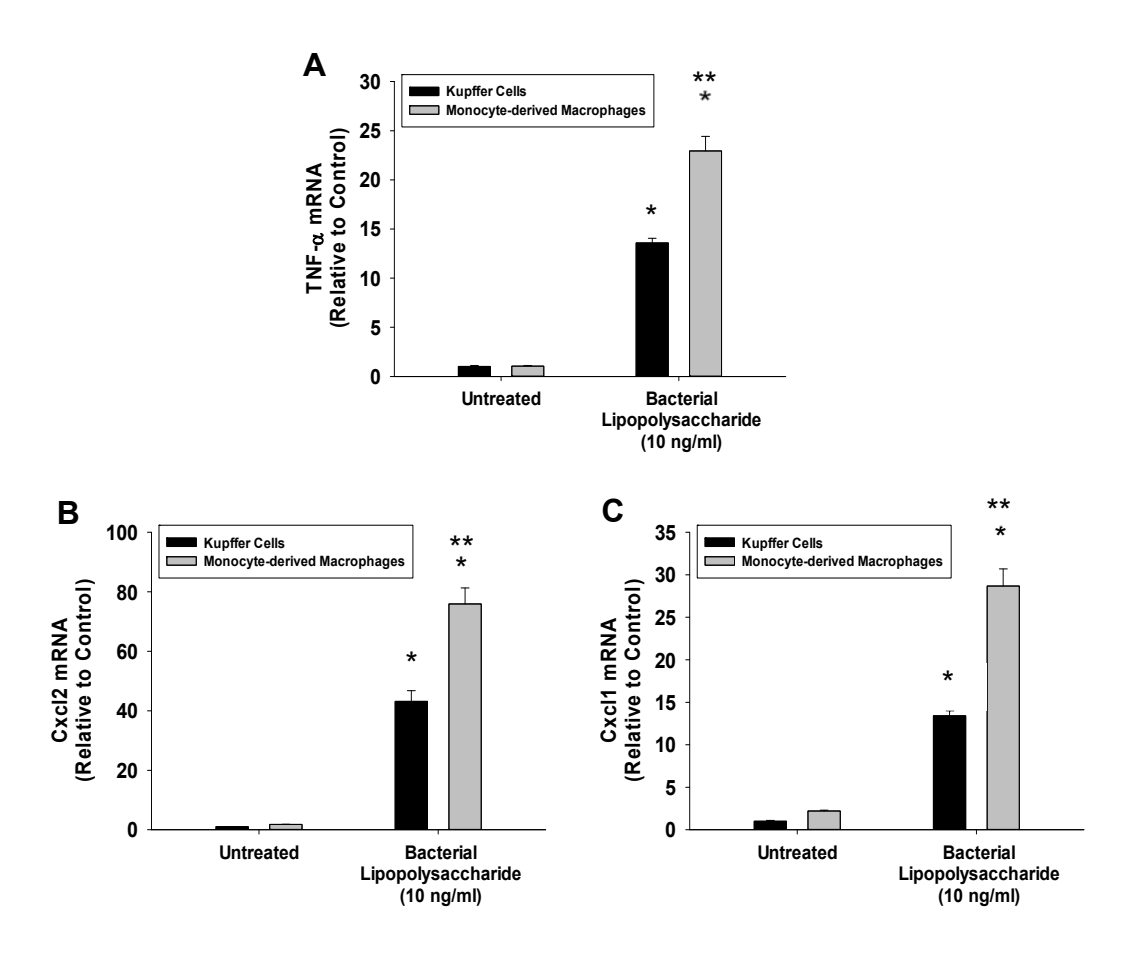


Figure 4.8: Differential Upregulation of Cytokines in Kupffer Cells and MDMs from Bone Marrow Transplant Mice. Kupffer cells and MDMs were isolated from the livers of bone marrow transplanted mice and separated by immunomagnetic bead separation. The cells were treated with LPS or vehicle for 3 hours. mRNA levels of (A) TNF-α, (B) Cxcl2, and (C) Cxcl1 were measured by real-time PCR. Data are expressed as mean +/- SEM.
*Significantly different from vehicle-treated cells. **Significantly different from LPS-treated Kupffer cells at p<0.05.

between MDMs and Kupffer cells stem from differences in their anatomical location within the liver. MDMs reside proximal to the Glisson's capsule putting them in close proximity to the peritoneal cavity (David, 2016). Interestingly, studies have demonstrated that MDMs extend dendrites into the peritoneal cavity where they are able to capture bacteria. Based upon these findings, it was proposed that MDMs are important for preventing the dissemination of bacteria from the peritoneal cavity into the liver (Sierro, 2017). Pathogens, such as those originating from the gut, can migrate through the wall of the peritoneal cavity and rapidly spread into the systemic circulation (Guirat, 2011). Bacterial infection in the peritoneal cavity occurs infrequently but is often fatal (Dever and Sheikh, 2015). It is possible that the ability of MDMs to produce a potent inflammatory response and capture peritoneal bacteria is responsible for the rare occurrence of peritoneal infections.

By contrast to MDMs, Kupffer cells are frequently exposed to pathogens or other immunoreactive materials entering the liver from the portal circulation. For example, studies have shown that LPS concentrations are higher in the portal circulation when compared to the systemic circulation (Jiang, 1995) (Guerville and Boudry, 2016). Kupffer cells have a high capacity to phagocytose pathogens, however, our studies indicate that this may not stimulate a potent inflammatory response. It is possible that Kupffer cells produce a diminished inflammatory response to prevent development of chronic inflammation elicited by the persistent exposure to gut-derived pathogens.

While the mechanistic basis for the differential sensitivity of MDMs and Kupffer cells to LPS is not known, it is possible that it may result from differential expression of components of the LPS signaling pathway. Surprisingly, though, comparison of the genetic profiles of MDMs and KCs showed that components of the LPS signaling pathway, such as Tlr4, were actually enriched in Kupffer cells (David, 2016) (Sierro, 2017) (Lu, 2008). Another possible explanation for the decreased sensitivity of Kupffer cells to pathogens, is that Kupffer cells are exposed to greater levels of anti-inflammatory mediators. In support of this, Kupffer cells were shown to

express higher levels of the anti-inflammatory cytokine, interleukin-10 (II-10) (David, 2016). IL-10 is a potent anti-inflammatory cytokine, that inhibits secretion of proinflammatory cytokines and other inflammatory mediators (Mosser and Zhang, 2008) (Moore, 2001). Increased expression of IL-10 by Kupffer cells may therefore function to inhibit LPS-induced upregulation of proinflammatory cytokines. Further studies are needed, however, to test this possibility.

In our studies, mice that received whole body irradiation (no shielding of the liver) followed by bone marrow transplantation, resulted in livers populated with macrophages that costained for CD45.1 and F4/80, as well as macrophages that co-stained for CD45.2 and F4/80. This indicated that a population of mature Kupffer cells originated from bone marrow-derived monocytes. At the time of completion of our studies, this contradicted what had been reported in the literature, which stated that Kupffer cells only arise from local proliferation of mature Kupffer cells in the liver. Studies since, however, have reported that when a high percentage of liver resident Kupffer cells are depleted, bone marrow-derived monocytes can fill the empty niche and fully differentiate into self-renewing, fully differentiated Kupffer cells exhibiting the same transcriptional profile as yolk sac-derived Kupffer cells (Scott, 2015) (David, 2016). This indicates that the Kupffer cell phenotype is generated by cues received locally in the liver and that MDMs can become Kupffer cells if a proper niche is available.

In conclusion, our studies demonstrate that Kupffer cells and MDMs are differentially sensitive to pathogens with MDMs demonstrating enhanced induction of proinflammatory cytokines after exposure to LPS. This differential sensitivity may have evolved to prevent peritoneal bacterial infections and chronic hepatic inflammation.

Chapter 5

Crosstalk Among Kupffer Cells and Hepatic Stellate Cells is Critical for Kupffer Cell Activation during Liver Injury

5.1 Abstract

The mechanisms that regulate Kupffer cell activation in the liver after injury are not fully understood. Our recent studies demonstrated that activation of hypoxia-inducible factor-1α (HIF-1α) in hepatic stellate cells (HSCs) is critical for Kupffer cell activation after liver injury. This indicates that crosstalk among HSCs and Kupffer cells during liver injury is critically important for Kupffer cell activation. In our current studies, we tested the hypothesis that necrotic hepatocytes activate HIF-1α in HSCs which stimulates release of a mediator that activates Kupffer cells. Our results demonstrate that treatment of primary, mouse HSCs with necrotic hepatocytes activates HIF-1α. Necrotic hepatocytes failed to activate HIF-1α in HSCs isolated from MyD88 knockout mice or in HSCs pretreated with the IKK2 inhibitor TPCA1. This indicated a key role for toll-like receptor and/or interleukin receptor signaling in activation of HIF-1α in HSCs by necrotic hepatocytes. Treatment of Kupffer cells with necrotic hepatocytes did not increase expression of inflammatory cytokines, however, treatment of Kupffer cells with conditioned medium from HSCs treated with necrotic hepatocytes upregulated CXCL2 and other inflammatory cytokines in Kupffer cells. Pretreatment of HSCs with the phospholipase A2 inhibitor methyl arachidonyl fluorophosphonate (MAFP) prevented HSC-mediated Kupffer cell activation, suggesting that HSCs release an arachidonic acid metabolite after exposure to necrotic hepatocytes that activates Kupffer cells. In conclusion, these in vitro studies support our in vivo findings, and expand upon these studies by demonstrating that necrotic cells activate HIF-1α in HSCs in a Myd88- and NF-kB-dependent manner, leading to the release of an arachidonic acid metabolite that activates Kupffer cells. Further characterization of this pathway could lead to the development of therapies aimed at reducing Kupffer cell-mediated liver injury or increasing Kupffer cell-mediated liver repair.

5.2 Introduction

After acute liver injury, Kupffer cells, the resident macrophage of the liver, are activated by a variety of stimuli, including damage-associated molecular pattern molecules (DAMPs),

released from dead cells, and the fibrinolytic enzyme, plasmin (Huebener, 2015) (Yang, 2019) (Roth, 2019). Once activated, Kupffer cells release proinflammatory cytokines, that increase expression of adhesion molecules on endothelial cells and other cell types, and release chemokines, that stimulate recruitment of immune cells, such as monocyte-derived macrophages and neutrophils, to the liver. This process culminates in the recruitment of immune cells that not only kill pathogens that infiltrate the liver, but also perform key functions in repair of the liver, including the removal of dead cell debris and the production of pro-mitogenic and proangiogenic growth factors and cytokines. Recent studies have indicated that Kupffer cell activation is more complex than originally thought, and that other liver cells types, including hepatic stellate cells, play an active role in regulating Kupffer cell activation.

Hepatic stellate cells (HSC) are resident mesenchymal cells that reside in the perisinusoidal space, also known as the space of Disse, which lies between the sinusoidal endothelial cells and the hepatocytes. HSCs are a dynamic population of cells that exist in either a quiescent or an activated state (Kawada, 1997). Under normal physiological conditions, HSCs are quiescent and function to store and release retinoids and regulate sinusoidal blood flow (Friedman, 2008). When the liver is injured, however, various cytokines, growth factors, and non-protein mediators trigger HSCs to become "activated". Once activated, HSCs differentiate into myofibroblasts that proliferate and synthesize extracellular matrix proteins, including collagen (Tsuchida, 2017). If liver injury persists, HSCs continue to deposit extracellular matrix proteins forming a scar that can expand, producing fibrosis and eventually cirrhosis (Higashi, 2017).

In addition to an important role in matrix formation, it is becoming increasingly clear that HSCs play an active role in liver immunology. HSCs can present antigens, produce proinflammatory cytokines and chemokines, and directly interact with various immune cell types, including macrophages (Weiskirchen, 2014) (Winau, 2007). Remarkably, a recent study demonstrated reduced hepatic inflammation after ischemia/reperfusion and endotoxemia in

mice in which HSCs were selectively deleted (Stewart, 2014). Further, we recently demonstrated that Kupffer cell activation was reduced in carbon tetrachloride-treated mice in which the transcription factor, hypoxia-inducible factor- 1α (HIF- 1α), was selectively deleted in HSCs, suggesting an important regulatory role for HSCs in Kupffer cell activation (Mochizuki, 2014).

The HIF-1 α transcription factor is constitutively produced and degraded in normoxic cells. In hypoxic cells, the mechanisms that target HIF-1 α for degradation become inhibited allowing it to translocate to the nucleus where it heterodimerizes with HIF-1 β . The HIF heterodimer then regulates expression of genes involved in several processes, including glycolysis, angiogenesis, and immunomodulation (Semenza, 2012) (Wang, 1993). In addition to hypoxia, several reports have demonstrated that HIF-1 α can be activated by other stimuli, such as growth factors, cytokines, and oxidative stress (Takeda, 2010) (Movafagh, 2015).

We recently demonstrated that HIF-1 α is rapidly activated in HSCs in mice treated with the hepatotoxicant carbon tetrachloride independent of hepatocellular hypoxia (Mochizuki, 2014). Interestingly, selective deletion of HIF-1 α in HSCs prevented upregulation of several macrophage-derived cytokines and chemokines, including TNF- α , IL-1 β , CXCL1, and CXCL2 independent of any impact on liver injury. Further, this prevented an increase in the percentage of pro-inflammatory F4/80⁺CD11b^{hi} Gr1⁺ macrophages in the liver and prevented macrophage-dependent clearance of dead cells. While these studies indicated an important role for HSCs in regulation of hepatic macrophage activation, what remains unknown, however, is the mechanism by which HIF-1 α is activated in HSCs after liver injury and the mechanism by which HSCs stimulate macrophage activation. The studies presented here tested the hypothesis that damage-associated molecular pattern molecules (DAMPs) activate HIF-1 α in HSCs leading to the production of a factor that activates macrophages.

5.3 Materials and Methods

5.3.1 Animal Treatments. 6-12 week old male C57BL/6 and *Myd88* knockout mice (Jackson Laboratories, Bar Harbor, ME) were used for all studies. Mice were housed in a 12 hr light/dark cycle under controlled temperature (18-21°C) and humidity. Food (Rodent Chow; Harlan-Teklad) and tap water were allowed *ad libitum*.

5.3.2 Isolation of Cells. HSCs were isolated from mice as described by us previously (Mochizuki, 2014). Briefly, livers from C57BL/6 mice (Jackson Laboratories) were perfused and digested with collagenase (Collagenase H, Sigma-Aldrich) as described previously (Kim, 2006). Following removal of hepatocytes by centrifugation, the supernatant was centrifuged at 1000 × *g* for 6 min. The resulting pellet was resuspended in 12.6 ml HBSS. The HSCs were then separated from other nonparenchymal cells by using an 8% Histodenz gradient. 4.9 ml 28.7% Histodenz (Sigma-Aldrich), made in sodium chloride-free HBSS, was added to the cell suspension. This solution was mixed and divided between two 15-ml tubes (Greiner Bio-One, Monroe, NC). These solutions were overlaid with 3 ml HBSS and centrifuged at 1500 × *g* for 15 min at 4°C without break. The HSCs, contained at the interface, were removed and diluted to 50 ml with HBSS. This solution was centrifuged at 1000 × *g* for 8 min at 4°C. The HSCs were cultured in DMEM containing 10% FBS and penicillin–streptomycin solution.

To isolate Kupffer cells, livers from C57BL/6 mice (Jackson Laboratories) were perfused and digested with collagenase (Collagenase H, Sigma-Aldrich) as described previously (Kim, 2006). Following removal of hepatocytes by centrifugation, Kupffer cells were isolated from the non-parenchymal cell fraction by using biotinylated anti-F4/80 antibody (Miltenyi Biotec, Bergisch Gladbach, Germany) and streptavidin-labeled magnetic beads as described by us previously (Roth, 2019).

Hepatocytes were isolated from the livers of C57BL/6 mice as described by us previously (Kim, 2006). To generate necrotic hepatocytes, the cells were diluted to 2.5 X 10⁵

cells/mL in serum-free Williams Medium E (Thermo-Fischer Scientific) and subjected to 3 cycles of freeze thaw at -80°C. Trypan blue staining confirmed that 100% of the cells were necrotic.

Peritoneal macrophages were isolated from mice by lavaging the peritoneal cavity with serum-free Williams Medium E. The cells were plated in Williams Medium E containing 10% FBS.

5.3.3 Culture and Treatment of Cells. HSCs were cultured in serum-free Williams

Medium E (Thermo-Fischer Scientific) at 37°C and 5% CO₂ in a humidified incubator. For

treatment of HSCs with necrotic hepatocytes, HSCs (9 X 10⁴ cells/well) were treated with 1

mL/well of necrotic hepatocytes (2.5 X 10⁶) in a 12 well plate (Grenier Bio-One, Kremsmunster,

Austria). For inhibitor studies, necrotic hepatocytes were pretreated with either SB202190 (LC

Laboratories), PD98059 (LC Laboratories), SP600125 (LC Laboratories), wortmannin (LC

Laboratories), TPCA-1 (Cayman Chemical), methyl arachidonyl fluorophosphonate (MAFP)

(Cayman Chemical) or vehicle for 30 minutes prior to the addition of cells. For hypoxia studies,

cells were cultured in a cell culture chamber containing 0.5% oxygen and 5% CO₂ balanced with

nitrogen as described previously (Copple, 2011). Cell-free supernatants were collected and

used as HSC conditioned medium.

Kupffer cells were cultured in serum-free Williams Medium E (Thermo-Fischer Scientific). For necrotic hepatocyte studies, Kupffer cells (2.5 X 10⁵ cells/well) were treated with 1 mL/well of necrotic hepatocytes (2.5 X 10⁶) in a 12 well plate. For studies using HSC-conditioned medium, Kupffer cells were treated with 1 mL of conditioned medium in a 12 well plate. For LPS studies, cells were treated with 10 ng/ml lipopolysaccharide (LPS) (Sigma Chemical Company) for 2 hours.

5.3.4 Immunohistochemistry. Immunofluorescence was used to detect HIF1 α as described by us previously (Mochizuki, 2014). Cultured HSCs isolated from mice were incubated with rabbit anti-mouse HIF1 α antibody (Novus Biologicals) diluted 1:800. The HSCs

were then incubated with goat anti-rabbit secondary antibody conjugated to Alexa Fluor 594 (diluted 1:500, Thermo-Fisher Scientific).

5.3.5 Western Blot. Cultured cells were lysed with RIPA buffer. Protein was separated on a 4-20% polyacrylamide gel (Bio-Rad), transferred to PVDF membrane, and then incubated with anti-HIF-1α, anti-phospho-p38, anti-total p38, anti-phospho-ERK1/2, anti-total ERK1/2, anti-phospho-IκB, anti- total IκB, anti-phospho-JNK, anti-total JNK, anti-phospho-AKT, or anti-total AKT using the recommended dilutions (all antibodies from Cell Signaling Technology). Membranes were incubated with secondary antibody conjugated to horseradish peroxidase (Sigma-Aldrich) and protein bands were detected using Clarity Western ECL Substrate (Bio-Rad) on a LI-COR Odyssey Fc (LI-COR Biosciences).

5.3.6 Real-Time PCR. RNA was isolated from cell culture samples by using the E.Z.N.A Total RNA Kit I (Omega Bio-Tek) according to manufacturer's instructions. Real-time PCR was performed as described by us previously (Kim, 2006). The following primer sequences were used: *Cxcl1*: Forward- 5'-TGGCTGGGATTCACCTCAAG-3', Reverse- 5'-GTGGCTATGACTTCGGTTTGG-3'; *Cxcl2*: Forward- 5'-CTCAGACAGCGAGGCACATC-3', Reverse- 5'-CCTCAACGGAAGAACCAAAGAG-3'; *Rpl13a*: Forward- 5'-GACCTCCTCTTCCCAGGC-3', Reverse- 5'-AAGTACCTGCTTGGCCACAA-3'. *Alox12*: Forward- 5'-CTACCAGAGTGATGATATTGTG-3', Reverse- 5'-GGTGAGGAAATGGCAGAG-3'; *Cox2*: Forward- 5'-CAAGACAGATCATAAGCGAGGA-3', Reverse- 5'-GGTGAGGAGATGACCCAG-3', Reverse- 5'-ATGAGTACACGAAGCCGAGG-3'; *Vegfa*: Forward- 5'-CAAGACTGACACAGAGCCAG-3', Reverse- 5'-ATGAGTACACGAAGCCGAGG-3', Reverse- 5'-AACACTGGTGTCATCAACGC-3'.

5.3.7 Statistical Analysis. The graphed results are presented as the mean + SEM. Data were analyzed by a one-way or two-way Analysis of Variance (ANOVA) where appropriate, and

comparisons among group means used the Student-Newman-Keuls test. The criterion for significance was p < 0.05 for all studies. *In vitro* studies were repeated a minimum of three times with cells isolated from separate groups of mice.

5.4 Results

5.4.1 Necrotic hepatocytes activate HIF1\alpha in HSCs. We showed previously that HIF-1 α is activated in HSCs in carbon tetrachloride-treated mice in the absence of hepatocellular hypoxia (Mochizuki, 2014). After liver injury, a subset of alarmins, called damage-associated molecular pattern molecules (DAMPs) are released from necrotic cells and activate pattern recognition receptors on cells, including the receptor for advanced glycation end products (RAGE) and toll-like receptors (TLR)- 2, 4, and 9 (Bianchi, 2007) (Mihm, 2018) (Park, 2006) (Paudel, 2019). Because toll-like receptor signaling can activate HIF-1 α , we hypothesized that DAMPs released from necrotic hepatocytes activate HIF-1 α in HSCs. To test this hypothesis, HSCs were isolated from wild-type mice and exposed to media containing necrotic hepatocytes. Exposure of HSCs to either necrotic hepatocytes or hypoxia, used as a positive control, resulted in stabilization of HIF-1 α by 2 hours (Fig. 5.1A). In addition, necrotic hepatocytes increased expression of glucose transporter 1 (GLUT1) and vascular endothelial growth factor-A (VEGF-A), which have been shown to be HIF-1 α -regulated genes (Copple, 2011). Furthermore, treatment of HSCs with necrotic hepatocytes stimulated the accumulation of HIF-1 α in the nucleus (Fig. 5.1C).

5.4.2 MyD88 and IKK2 are critical for activation of HIF-1α in HSCs by necrotic hepatocytes. To examine whether pattern recognition receptors were involved in activation of HIF-1α in HSCs, we first investigated the role of Myd88 in this process. MyD88 is an adaptor protein that facilitates signaling by TLRs and RAGE (Drexler and Foxwell, 2010) (Sakaguchi, 2011). Through this adaptor, TLRs and RAGE activate the mitogen-activated protein kinases (MAPKs), p38, Jnk, and Erk1/2, and activate Akt and NF-κB pathways as diagrammed in Fig.

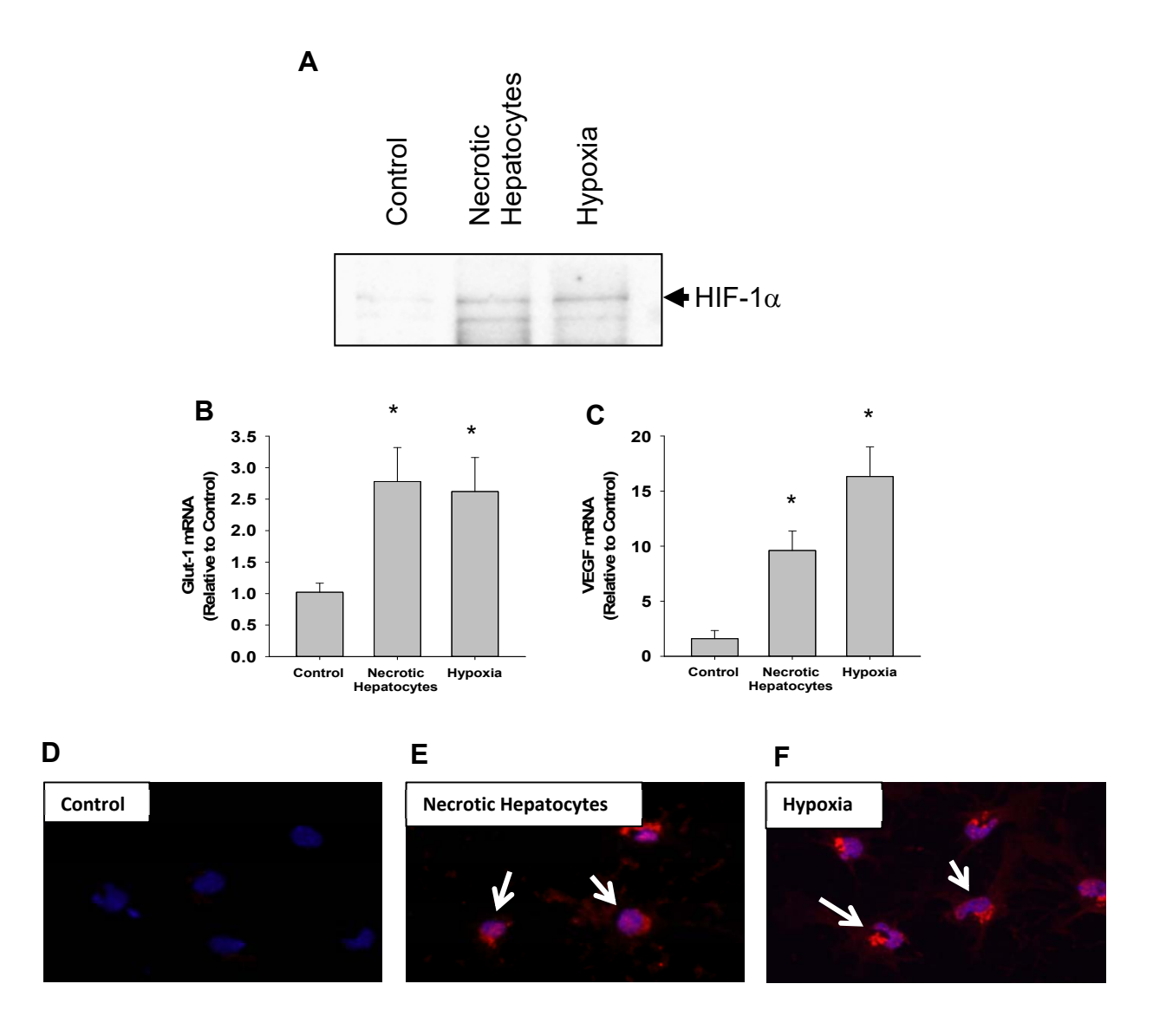


Figure 5.1: Necrotic Hepatocytes Activate HIF-1α in HSCs. HSCs were isolated from wild-type mice and cultured for 24 hours. The cells were then exposed to media alone, necrotic hepatocytes, or hypoxia (0.5% oxygen). (A) HIF-1α was detected 2 hours later. mRNA levels of (B) GLUT-1 and (C) VEGF were measured by real-time PCR after 24 hours. HIF-1α (red) was detected by immunofluorescence in HSCs exposed to (D) control media (E) necrotic hepatocytes, and (F) hypoxia. Nuclei appear blue in the photomicrographs. Data are expressed as mean +/- SEM. *Significantly different from HSCs exposed to control medium at p<0.05.

5.2A (Drexler and Foxwell, 2010) (Park, 2006) (Paik, 2003) (Kuper, 2012) (Li, 2015) (Liu, 2010) (Yeh, 2001). To evaluate the role of MyD88, HSCs were isolated from wild-type and MyD88 knockout mice and then treated with necrotic hepatocytes. The HIF-1α target genes, *Vegf* and *Glut-1*, were measured as a surrogate marker for HIF activation. Treatment of HSCs from wild-type mice with necrotic hepatocytes increased expression of Vegf-A and Glut-1 (Fig. 5.2B). This effect was completely prevented in HSCs isolated from MyD88 knockout mice (Fig. 5.2B). Treatment of HSCs with necrotic hepatocytes activated several pathways downstream of pattern recognition receptors including, Akt, Erk1/2, Jnk, and p38 (Fig. 5.2C). Pharmacological inhibitors of Akt, Erk1/2, Jnk, and p38 signaling, however, did not prevent upregulation of HIF-1α target genes (Fig. 5.3A-D). However, pharmacological inhibition of IκB kinase β (IKK2), a kinase that phosphorylates and inhibits IκB and leads to NfκB activation, did prevent upregulation of HIF-1α target genes (Fig. 5.3E).

5.4.3 Necrotic hepatocytes do not directly induce cytokine expression in Kupffer cells. It has been proposed that DAMPs released from necrotic hepatocytes directly activate Kupffer cells after acute liver injury. To examine this further, we isolated Kupffer cells from mice and exposed them to necrotic hepatocytes. In addition, we isolated peritoneal macrophages to compare the response of these cells to Kupffer cells. Treatment of peritoneal macrophages with either LPS (positive control) or necrotic hepatocytes increased expression of Cxcl2 (Fig. 5.4A). While treatment of Kupffer cells with LPS increased expression of Cxcl2, treatment of Kupffer cells with necrotic hepatocytes had no effect on expression of Cxcl2 (Fig. 5.4B).

5.4.4 Conditioned medium from HSCs treated with necrotic hepatocytes induces cytokine expression in Kupffer cells. Our results suggest that DAMPs released from necrotic hepatocytes do not directly activate Kupffer cells, suggesting a more complex mechanism of activation. We showed previously that activation of HIF-1α in HSCs is critical for activation of Kupffer cells *in vivo* after carbon tetrachloride-induced liver injury (Mochizuki, 2014). This suggests that DAMPs may stimulate HSCs to release a HIF-1α-regulated mediator that directly

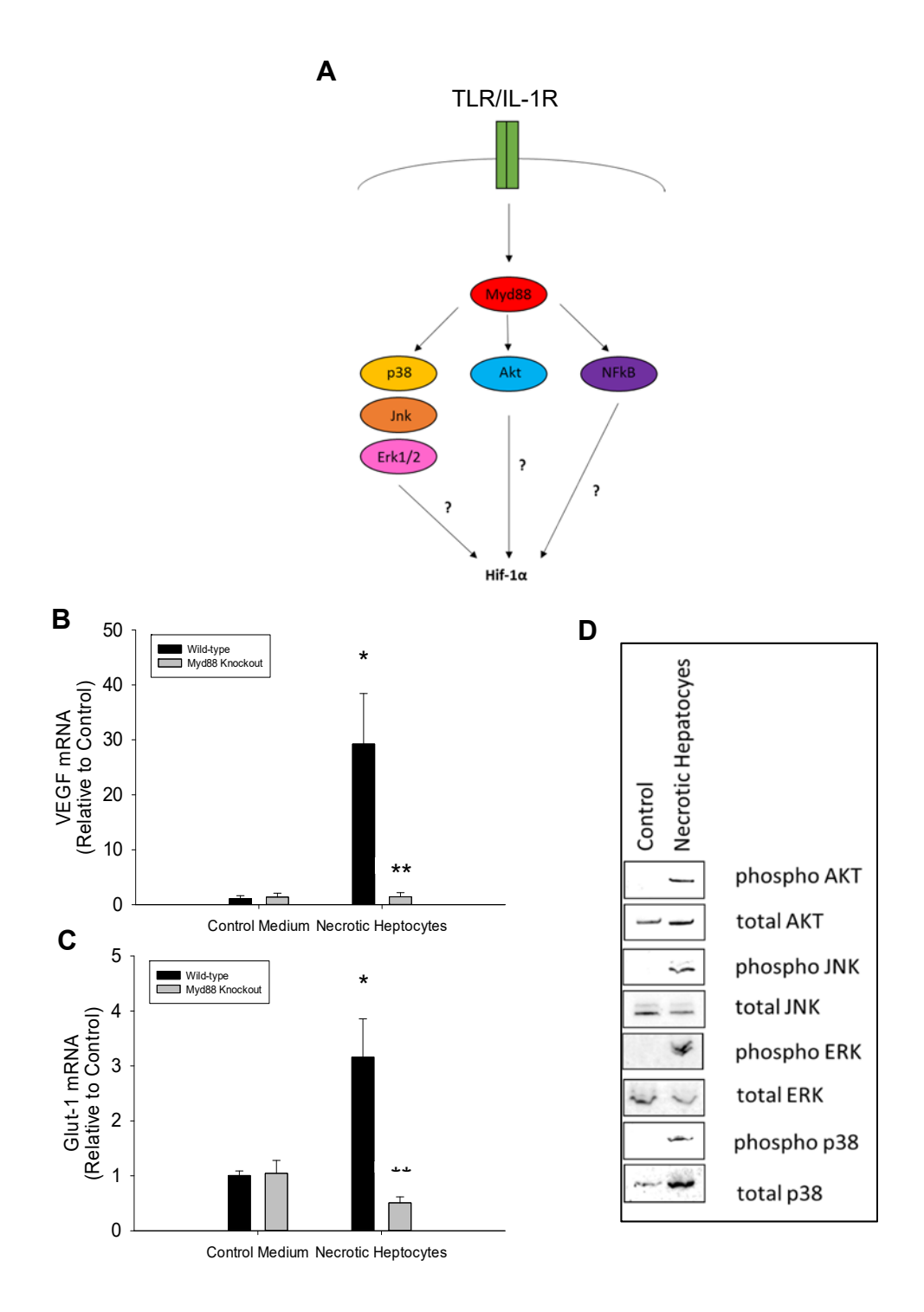


Figure 5.2: Signaling Pathways Involved in Activation of HIF-1 α in HSCs. (A) Diagram of MyD88-dependent signaling downstream of toll-like receptors. HSCs were isolated from wild-type and MyD88 KO mice. The cells were treated with necrotic hepatocytes and (B) VEGF-A and (C) GLUT-1 mRNA levels were measured as a surrogate marker of HIF-1 α activation.

Figure 5.2 (cont'd)

(D) HSCs were isolated from wild-type mice and treated with necrotic hepatocytes for 30 minutes. Phospho- and total Akt, Jnk, Erk1/2, and p38 were detected by western blot. Data are expressed as mean +/- SEM. *Significantly different from wild-type cells treated with control medium. **Significantly different from wild-type cells treated with necrotic hepatocytes.

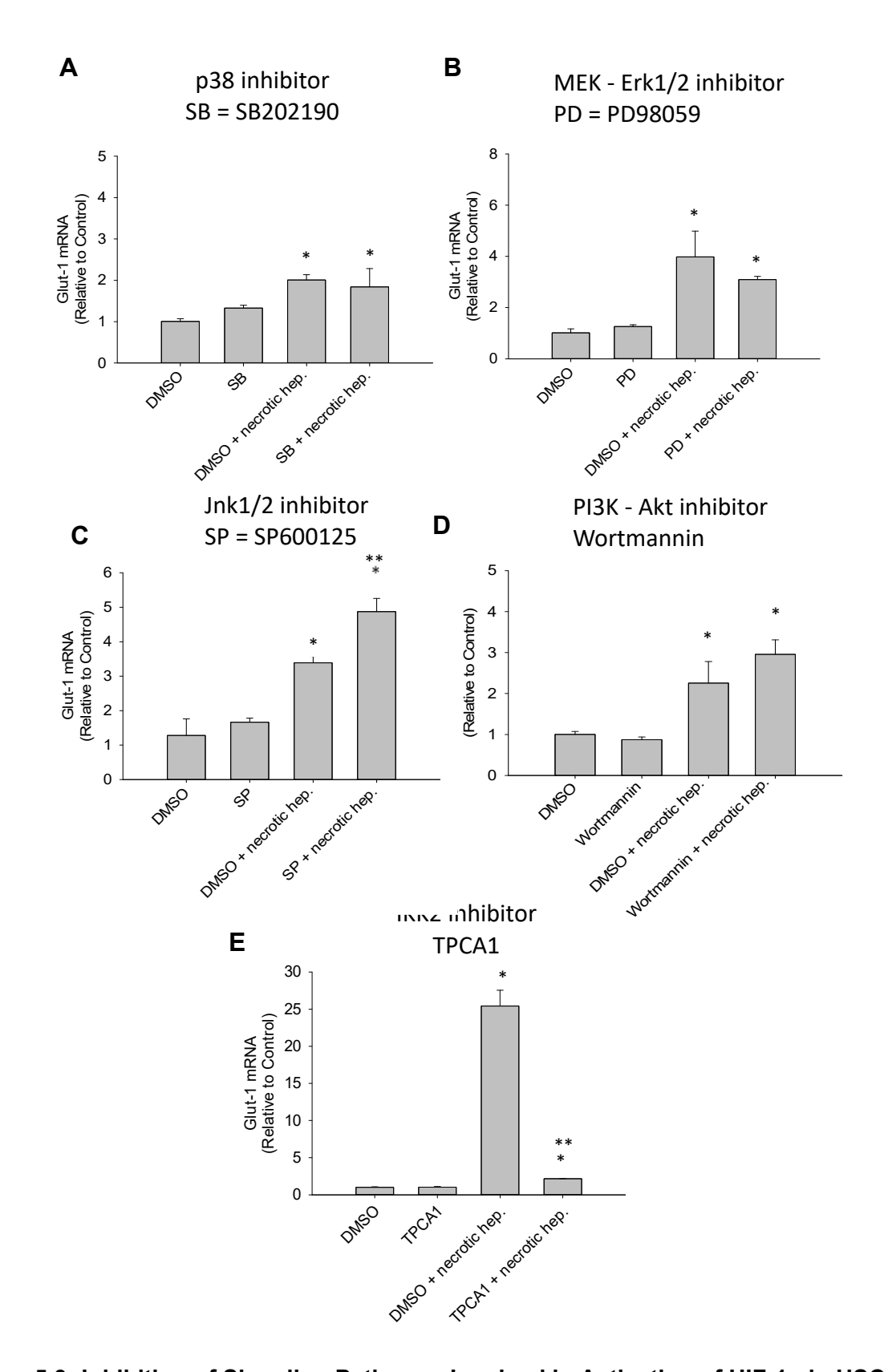


Figure 5.3: Inhibition of Signaling Pathways Involved in Activation of HIF-1α in HSCs.

Figure 5.3 (cont'd)

HSCs were isolated from wild-type mice and pretreated with (A) SB202190, (B) PD98059, (C) SP600125, (D) wortmannin, and (E) TPCA1 for 30 minutes. The cells were then treated with necrotic hepatocytes and GLUT-1 mRNA levels were measured. Data are expressed as mean +/- SEM. *Significantly different from DMSO. **Significantly different from wild-type cells treated with necrotic hepatocytes.

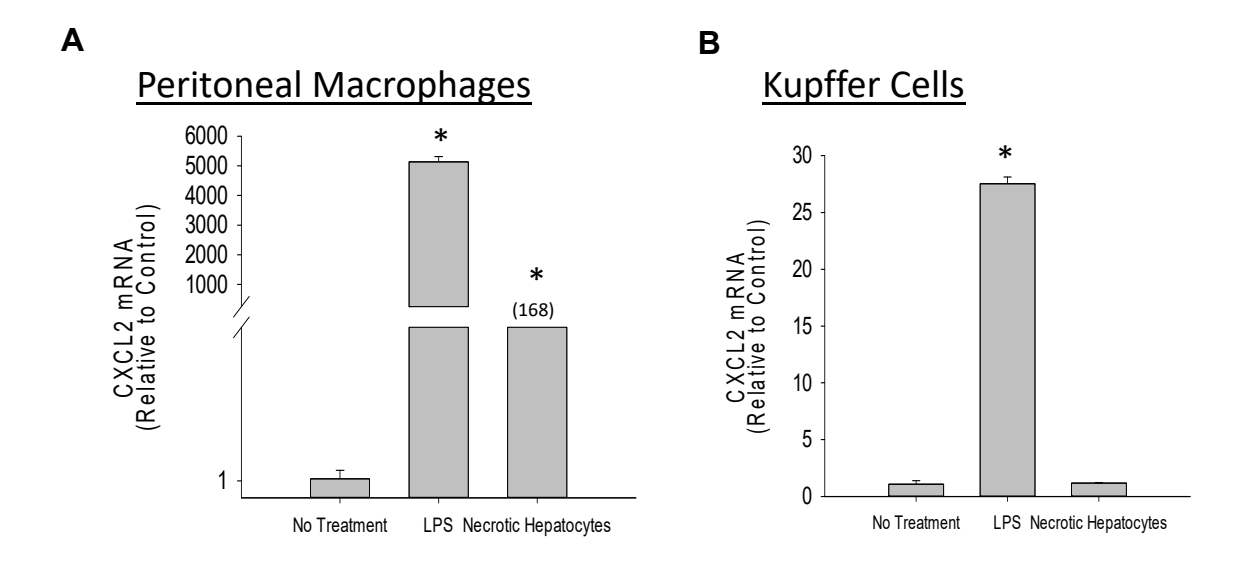


Figure 5.4: Differential Upregulation of Cytokines by Peritoneal Macrophages and Kupffer Cells. (A) Peritoneal macrophages and (B) Kupffer cells were isolated from wild-type mice and treated with either LPS or necrotic hepatocytes. mRNA levels of CXCL2 were measured. Data are expressed as mean +/- SEM. *Significantly different from untreated cells, p<0.05.

activates Kupffer cells. To test this hypothesis, HSCs were isolated from mice and exposed to necrotic hepatocytes. After 24 hours, the conditioned medium was removed and added to Kupffer cells. mRNA levels of the chemokines, Cxcl1 and Cxcl2, were then measured in the Kupffer cells (Fig. 5.5A). As a control, Kupffer cells were also exposed to media alone or media containing necrotic hepatocytes. Exposure of Kupffer cells to media containing necrotic hepatocytes had no effect on the expression of Cxcl1 or Cxcl2 (Fig. 5.5B-C). Similarly, treatment of Kupffer cells with conditioned medium from HSCs treated with media alone failed to increase expression of Cxcl1 and Cxcl2 in Kupffer cells (Fig. 5.5B-C). However, treatment of Kupffer cells with conditioned medium from HSCs treated with necrotic hepatocytes increased expression of Cxcl1 and Cxcl2 in Kupffer cells (Fig. 5.5B-C).

5.4.5 Potential role of arachidonic acid metabolites in activation of Kupffer cells by **HSCs.** Our results above suggested that HSCs release a soluble mediator that directly activates Kupffer cells. In an attempt to identify this mediator, we first tested the hypothesis that an eicosanoid produced by HSCs may be responsible for activation of Kupffer cells. Eicosanoids are bioactive lipids produced from arachidonic acid (Esser-von Bieren, 2017). The first step in the synthesis of eicosanoids is the cleavage of arachidonic acid from the cell membrane by phospholipase A2 (Murakami, 2017). To test the hypothesis that HSCs produce an eicosanoid that activates Kupffer cells, HSCs were pre-treated with the phospholipase A2 inhibitor methyl arachidonyl fluorophosphonate (MAFP) (Fig. 5.6A). When Kupffer cells were exposed to conditioned medium from HSCs exposed to necrotic hepatocytes, levels of Cxcl2 and Cxcl1 were increased as described above (Fig. 5.6B-C). Pretreatment of HSCs with MAFP, however, completely prevented upregulation of Cxcl2 and Cxcl1 in Kupffer cells (Fig. 5.6B-C). To gain some insight into the eicosanoid that may be involved in Kupffer cell activation, HSCs were exposed to necrotic hepatocytes and mRNA levels of several enzymes involved in the synthesis of various eicosanoids were measured. Treatment of HSCs with necrotic hepatocytes increased expression of arachidonate 12-lipoxygenase (ALOX12), cyclooxygenase 2 (COX2),

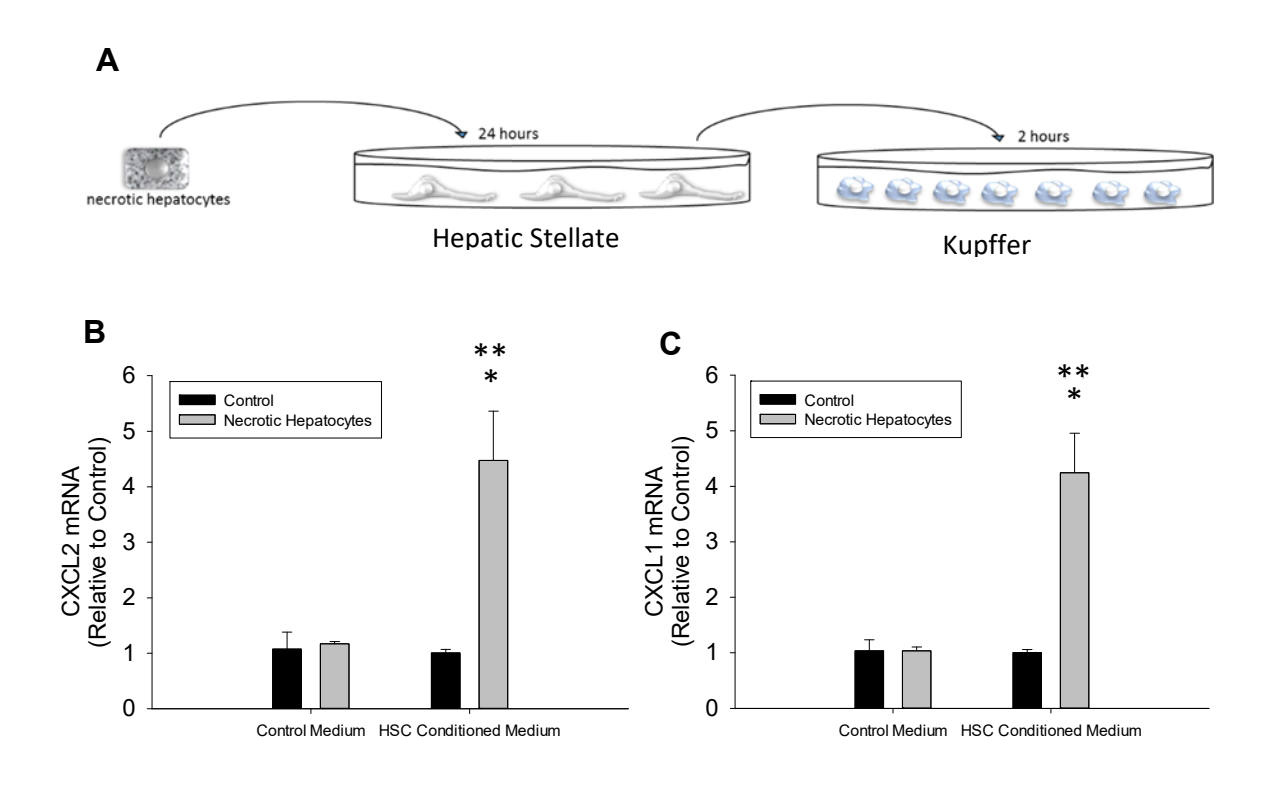


Figure 5.5: Conditioned Medium from HSCs Treated with Necrotic Hepatocytes Induces Cytokine Expression in Kupffer Cells. (A) Diagram of the experimental design. HSCs were isolated from wild-type mice and treated with medium alone or medium containing necrotic hepatocytes. After 24 hours, the conditioned medium was collected and transferred to Kupffer cells for 2 hours. Levels of (B) Cxcl2 and (C) Cxcl1 mRNA were measured in the Kupffer cells. Data are expressed as mean +/- SEM. *Significantly different from Kupffer cells treated with control media. **Significantly different from Kupffer cells treated with conditioned medium from HSCs incubated with media alone, p<0.05.

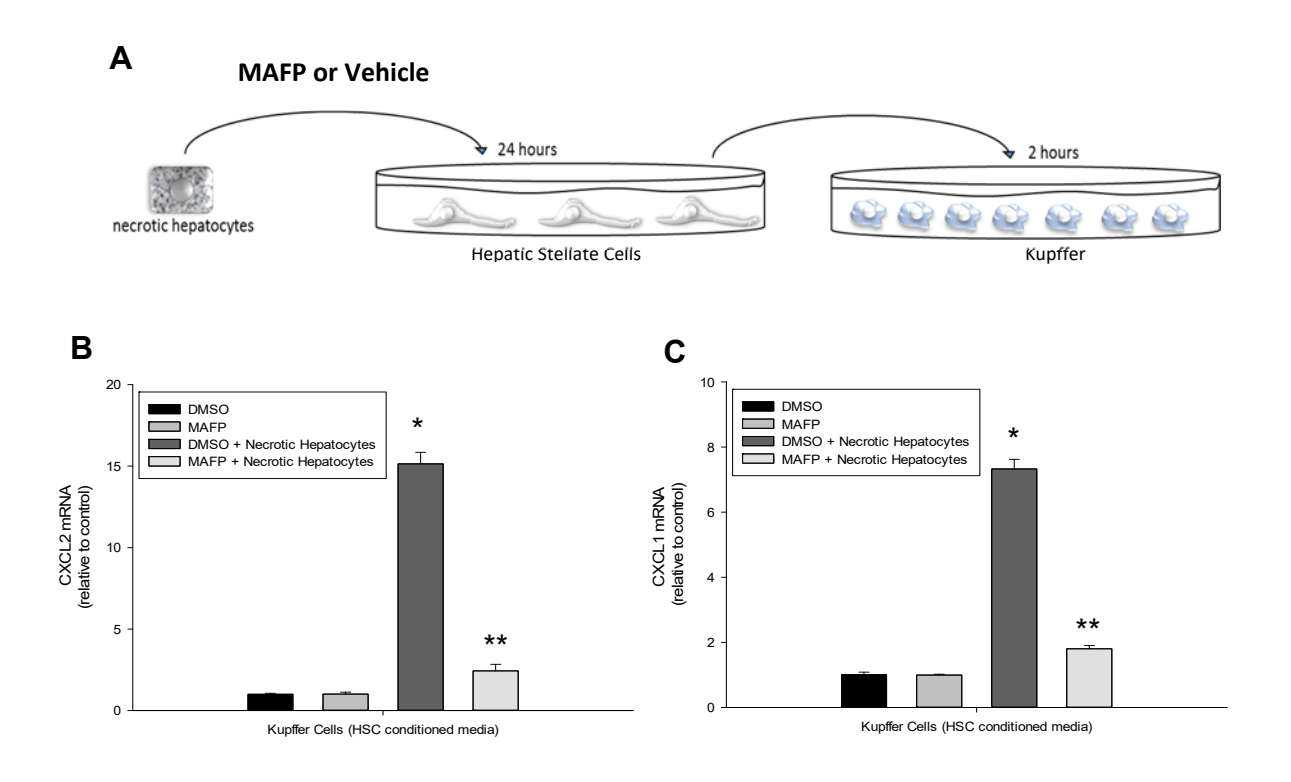


Figure 5.6: Effect of Inhibition of Eicosanoid Production in HSCs on Induction of Cytokine Expression in Kupffer Cells. (A) Diagram of experimental design. HSCs were isolated from wild-type mice and pre-treated with MAFP or vehicle for 30 minutes before being exposed media alone or media containing necrotic hepatocytes for 24 hours. Conditioned medium from HSCs was then transferred to Kupffer cells for 2 hours. Levels of (B) Cxcl2 and (C) Cxcl1 mRNA were measured in the Kupffer cells. Data are expressed as mean +/- SEM. *Significantly different from DMSO. **Significantly different from DMSO and necrotic hepatocytes.

and prostaglandin E synthase (PTGES) (Fig. 5.7A-C). Expression levels of ALOX5, ALOX5ap, and LTA4H, however, were not affected. (Fig. 5.7D-F).

5.5 Discussion

Although HIF-1 α is most well-known for its role in hypoxic conditions, recent reports have demonstrated the ability of several growth factors, cytokines, and oxidative stress to activate HIF-1 α (Du, 2008) (Takeda, 2010) (Zhan, 2015). We showed previously that HIF-1 α is rapidly activated in HSCs after liver injury and that this is critical for activation of macrophages and resolution of liver injury (Mochizuki, 2014). However, the mechanism by which HIF-1 α is activated in HSCs after liver injury and the mechanism by which HSCs activate macrophages in a HIF-1 α -dependent manner remain unclear. In the present studies, we show that HIF-1 α is activated in HSCs by necrotic hepatocytes through MyD88-dependent and NF κ B-dependent signaling pathways, and that HSCs produce an eicosanoid that is required for Kupffer cell activation.

It is well documented that DAMPs released from necrotic cells activate various pattern recognition receptors, including RAGE and TLRs 2, 4, and 9 (Bianchi, 2007) (Mihm, 2018) (Park, 2006) (Paudel, 2019). MyD88 is a downstream adaptor protein that facilitates signaling by TLRs and RAGE (Drexler and Foxwell, 2010) (Sakaguchi, 2011). When we treated HSCs isolated from *Myd88* KO mice with necrotic hepatocytes, upregulation of the HIF-1α target genes, *Vegf* and *Glut-1*, was prevented. This indicates that activation of HIF-1α in HSCs by necrotic hepatocytes requires a Myd88-associated receptor. Myd88 is known to mediate signaling through a variety of pattern recognition receptors, including RAGE and the toll-like/IL-1 receptor superfamily (Drexler and Foxwell, 2010) (Sakaguchi, 2011) (Warner and Nunez, 2013). Signaling may be mediated by TLR4, as it has been shown that activation of TLR4 can stimulate activation of HIF-1α through NfκB (Han, 2016). Further studies into the specific myd88-associated receptor or combination of receptors are needed to completely elucidate this

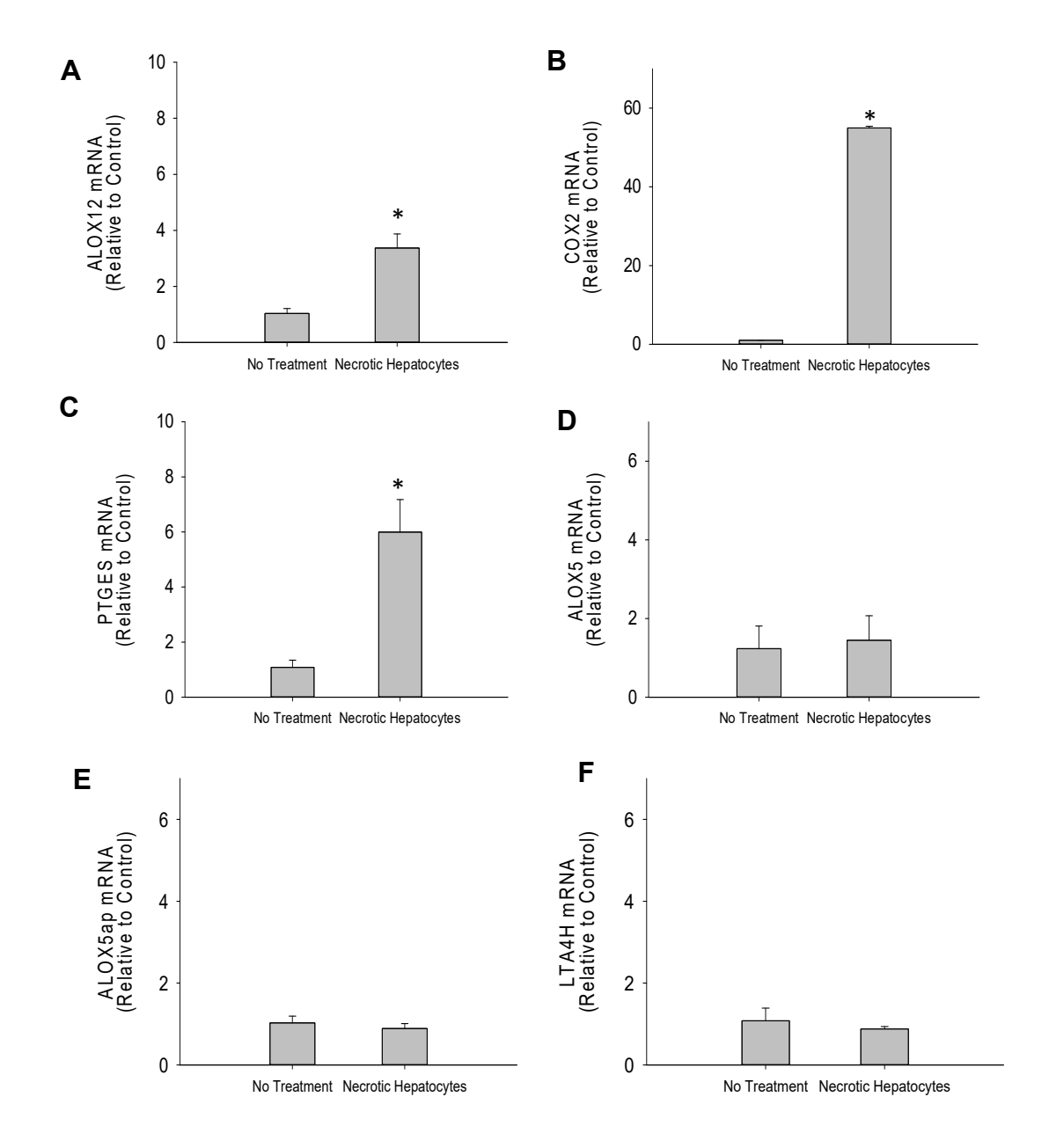


Figure 5.7: Induction of Arachidonic Acid Metabolizing Enzymes in HSCs by Necrotic Hepatocytes. HSCs were isolated from wild-type mice and exposed to medium alone or medium containing necrotic hepatocytes for 24 hours. mRNA expression levels of (A) ALOX12, (B) COX2, (C) PTGES (D) ALOX5 (E) ALOX5ap and (F) LTA4H were measured. Data are expressed as mean +/- SEM. *Significantly different from HSCs treated with medium alone, p<0.05.

mechanism. In addition, when HSCs were treated with necrotic hepatocytes, pharmacological inhibition of IKK2 prevented upregulation of the HIF-1α target genes *Vegf* and *Glut-1*, suggesting that activation of HIF-1α was through an NfκB-dependent mechanism.

It has been shown that eicosanoids are proinflammatory mediators in various disease states (Powell, 2015) (Tilley, 2001). When we pre-treated HSCs with MAFP, then exposed them to necrotic hepatocytes, the HSC conditioned media failed to increase expression of proinflammatory cytokines in Kupffer cells. These results suggest that an arachidonic acid metabolite produced by HSCs is critical for activation of Kupffer cells. In our studies, treatment of HSCs with necrotic hepatocytes increased expression of ALOX12, COX2, and PTGES, suggesting that these enzymes may be involved in this mechanism. COX2 is a major enzyme in the cyclooxygenase pathway of arachidonic acid metabolism that catalyzes the oxidation of arachidonic acid, giving rise to prostanoids (Esser-von Bieren, 2017). It has been shown that HIF-1 α directly regulates COX2 through a hypoxia response element in the promoter of this gene (Kaidi, 2006). Furthermore, it has been shown COX2 can be activated in hepatic stellate cells (Xu, 2016) and its production is induced following APAP-induced acute liver injury (Reilly, 2001). As stated above, COX2 can give rise to prostanoids, which include prostacyclins, thromboxanes, and prostaglandins, such as PGE2 (Narumiya, 1999). Studies have demonstrated that HIF-1 α can also directly regulate PTGES (Lee, 2010) and that activation of HIF1 α can stimulate production of PGE2 via the COX2-PTGES axis (Kaidi, 2006) (Lee, 2010). Although PGE2 has been shown to induce an anti-inflammatory phenotype in macrophages (Rodriguez, 2014) (Takayama, 2002), it has also been shown to increase production of chemokines, such as Ccl2, and promote the migration of monocytes and neutrophils (Van Epps, 1978) (McClatchey, 1976) (Hara, 2010).

Arachidonic acid can also be metabolized by the lipoxygenase pathway, which gives rise to lipid mediators such as leukotrienes and hydroxyeicosatetraenoates (HETEs) (Esser-von

Bieren, 2017). In our studies, necrotic hepatocytes increased exression of ALOX12 in HSCs, which gives rise to 12S-HETE (Mashima and Okiyama, 2015). 12S-HETE has been shown to increase chemokine production in macrophages (Wen, 2008). Since we observed upregulation of the chemokines, Cxcl1 and Cxcl2, in Kupffer cells, it is possible that release of 12S-HETE by HSCs is an important stimulus for Kupffer cell activation. Further studies are needed, however, to gain insight into the importance of this pathway in regulating Kupffer cell activation.

Collectively, our studies indicate that activation of HIF-1 α in HSCs by necrotic hepatocytes occurs via a MyD88-dependent and NF α B-dependent pathway. Activation of HIF-1 α in HSCs lead to the production of an arachidonic acid metabolite that is important for activation of Kupffer cells by necrotic hepatocytes.

Chapter 6

Discussion

6.1 Summary and Significance

In extreme cases of APAP overdose, acute liver injury rapidly progresses to ALF, which is often fatal, having a mortality rate of approximately 40% (Bernal, 2013). The only effective pharmacological therapy for APAP overdose is N-acetyl-cysteine (NAC). NAC is highly efficacious when administered early after APAP overdose (Rumack, 1981) (Smilkstein, 1985). However, early administration is often problematic since patients often do not seek help until injury is extensive and this early, active phase of injury has completed. The study of the mechanisms underlying the inflammatory and reparative response during liver injury could provide therapeutic targets for patients with ALF, in which these mechanisms are often dysregulated. Therefore, we have begun to investigate the mechanisms regulating the innate immune response during liver injury and how these mechanisms are dysregulated during ALF. In the studies presented in this dissertation, we focused on investigating the activation and regulation of macrophages during acute livery injury and ALF.

Recent evidence from patients and from mouse models indicate that cytokine production and phagocytosis are dysregulated in ALF (Antoniades, 2008) (Berry, 2010) (Bhushan, 2014). These studies suggest that monocyte/macrophage dysfunction may contribute to failed recovery in some APAP overdose patients. However, how and whether this dysfunction contributes to the pathogenesis of ALF remained unclear. Studies have shown that plasmin can regulate macrophage cytokine production, phagocytosis, and trafficking, and that plasminogen, the zymogen of plasmin, deficiency occurs in patients with ALF during various inflammatory injuries (Ploplis, 1998) (Lisman, 2012) (Das, 2014) (Bezerra, 2014). In addition, studies have also demonstrated that IL-10 can regulate macrophage cytokine production and migration, and that IL-10 levels are highest in ALF patients with the poorest outcomes (Vicioso, 1998) (Berry, 2010). The data presented in this dissertation demonstrate that monocyte/macrophage trafficking, cytokine secretion, and phagocytosis become dysregulated in APAP-induced ALF and contribute to its pathogenesis. Furthermore, our results suggest plasmin and IL-10 as

critical regulators of these macrophage functions during ALF. A general overview of macrophage functions following APAP-induced liver injury and APAP-induced liver failure are diagrammed in Figure 6.1, as well as the effects of different mediators discussed in this dissertation on macrophage functions.

To investigate the role of plasmin as a regulator of macrophage function after APAP overdose, we treated mice with 300 mg/kg APAP followed by the plasmin inhibitor tranexamic acid. Inhibition of plasmin suppressed upregulation of proinflammatory cytokine/chemokines early at 8 hours (Fig. 2.1B-D). In culture, treatment with plasmin directly, and in synergy with HMGB1, stimulated macrophages to produce cytokines via an NF-κB-dependent mechanism (Fig.2.2, 2.3, 2.4). Inhibition of plasmin in vivo after APAP overdose also prevented the removal of dead cells from necrotic lesions and prevented trafficking of monocyte-derived macrophages into lesions during the reparative phase (Fig. 2.5, Fig. 2.8). In addition, inhibition of plasmin prevented maturation of monocyte-derived macrophages into F4/80-expressing macrophages and prevented the downregulation of proinflammatory cytokine production (Fig. 2.8, 2.11). First, these data suggest that plasmin is an important stimulus of cytokine production early by Kupffer cells. Second, these results demonstrate that plasmin stimulates resolution of inflammation by promoting macrophage trafficking into lesions, their maturation, and phagocytosis of dead cells. It was recently shown that plasminogen levels are substantially reduced in patients with ALF, and that the capacity to produce plasmin activity was completely absent in 75% of the ALF patients (Lisman, 2012). In patients with ALF that have reduced levels of plasminogen, restoration of plasminogen levels at later times may be an important factor in restoring macrophage function and improving their condition.

To investigate the impact of macrophage dysfunction on the pathogenesis of APAP-induced ALF, we utilized a murine model of APAP-induced ALF, in which mice were treated with 600 mg/kg APAP, that recapitulates many of the features of acute liver failure in patients (Bhushan, 2014). In mice treated with 600 mg/kg APAP, the inability of macrophages to traffic

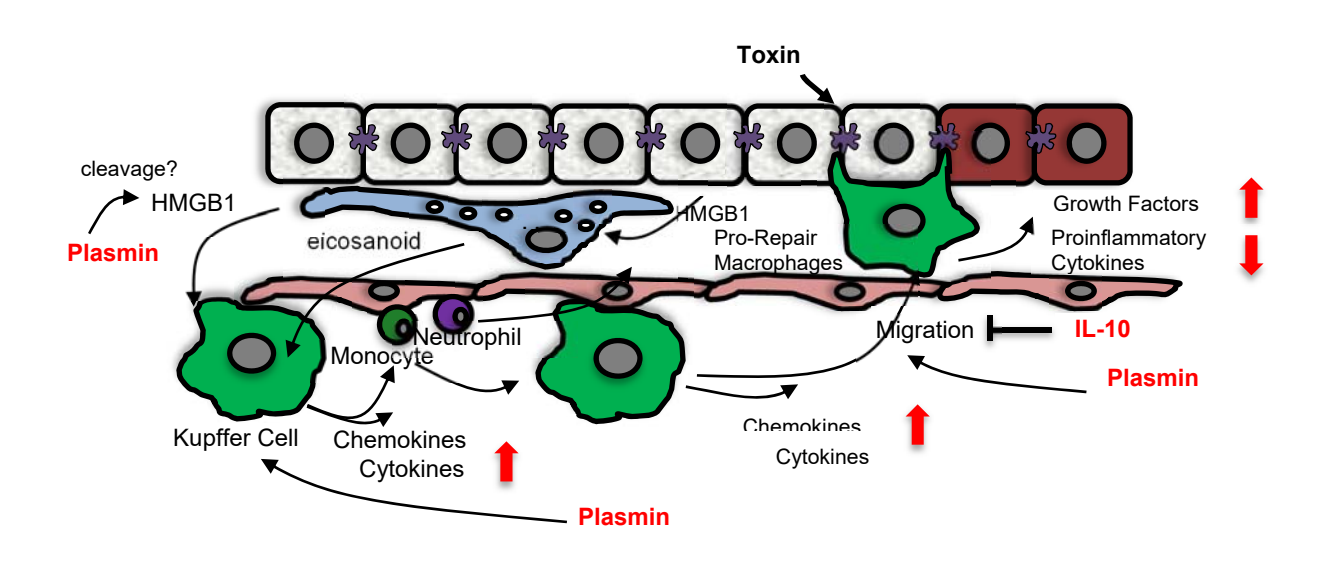


Figure 6.1 Macrophage Functions and Associated Mediators Following APAP-induced Liver Injury. A general overview of macrophage functions following APAP-induced liver injury and APAP-induced acute liver failure. The effects of important mediators investigated in this dissertation, including a HSC-produced eicosanoid, HMGB1, plasmin, and IL-10, are

also diagrammed.

into necrotic lesions was associated with failed clearance of necrotic cells in mice (Fig. 3.1-3.3). Furthermore, these mice displayed a sustained production of both proinflammatory cytokines and anti-inflammatory cytokines, including IL-10 (Fig. 3.4-3.6). Neutralization of IL-10 24 hours after treatment with 600 mg/kg APAP restored macrophage trafficking into necrotic lesions (Fig. 3.7). Furthermore, administration of recombinant IL-10 after treatment with 300 mg/kg APAP prevented macrophage trafficking into necrotic lesions and delayed repair (Fig. 3.7-3.8). These data suggest that elevated levels of IL-10 in the late repair phase of APAP-induced ALF impairs macrophage trafficking, resulting in failed liver repair. Interestingly, although neutralization of IL-10 following 600 mg/kg APAP restored macrophage trafficking into lesions, it did not restore the clearance of necrotic lesions in these mice, indicating that another stimulus is required for this effect.

As we had already demonstrated in Chapter 2, plasmin is important in the migration of macrophages into necrotic lesions following APAP-induced liver injury. Because ALF patients have been shown to have reduced levels of plasminogen (Lisman, 2012), it is possible that the macrophage dysregulation seen in our ALF model was caused by reduced plasmin levels. Our initial studies suggest that restoration of plasminogen levels intravenously at 24 hours following 600 mg/kg APAP does not improve survival, but it did allow macrophages to migrate into the necrotic lesions (data not shown). As demonstrated in ALF patients and in our murine model of ALF, high IL-10 levels correlate with low plasminogen levels. Although the exact mechanism remains unknown, it is possible that high IL-10 levels lead to lower plasmin activity levels in the local environment surrounding macrophages, such as by IL-10-induced inhibition of macrophage production of plasmin activators.

Another area of interest in this dissertation involves the different hepatic macrophage populations present in the steady-state liver. Studies have shown that the liver contains two distinct populations of macrophages under steady-state conditions – Kupffer cells and monocyte-derived macrophages (MDMs) – that have distinct transcriptomic profiles (Yona,

2013) (Sierro, 2017). We investigated whether these macrophages also possess functional differences. Basal expression levels of TNF- α were higher in purified MDMs compared to Kupffer cells (Fig. 4.4). After treatment with LPS, expression levels of proinflammatory cytokines such as TNF- α , Cxcl1, and Cxcl2 were induced to a greater extent in MDMs compared to Kupffer cells (Fig. 4.4, 4.8). These data indicate that resident hepatic MDMs exhibit a greater proinflammatory phenotype in the liver compared to Kupffer cells. Our results also build upon the idea that these different phenotypes are key to the different roles of these two populations, allowing MDMs to prevent bacterial infections from the peritoneum while Kupffer cells regulate chronic inflammatory mediators from the gut.

Our previous studies also demonstrated that activation of HIF-1α in HSCs is critical for macrophage activation after liver injury. We therefore wanted to investigate whether crosstalk between HSCs and Kupffer cells during liver injury is critically important for Kupffer cell activation. Treatment with necrotic hepatocytes activated HIF-1α in HSCs, and this activation was prevented in Myd88-deficient HSCs and when HSCs were treated with the IKK2 inhibitor TPCA-1 (Fig. 5.1-5.3). Necrotic hepatocytes were not able to increase Kupffer cell expression of inflammatory cytokines (Fig. 5.4). However, conditioned medium from HSCs treated with necrotic hepatocytes was able to increase Kupffer cell expression of inflammatory cytokines (Fig. 5.5). Inhibition of phospholipase A2 prevented HSC-mediated Kupffer cell activation (Fig. 5.6). First, these results suggest that necrotic cells activate HIF-1α in HSCs in a Myd88- and NF-kB-dependent manner. Second, these results suggest that necrotic hepatocytes stimulate HSCs to release of an arachidonic acid-derived mediator that modulates Kupffer cell function. Further characterization of this pathway is needed in order to better understand the mechanisms of Kupffer cell activation.

As we demonstrated in Chapter 2, Kupffer cells become activated to produce proinflammatory cytokines and chemokines early after acute liver injury. Therefore, it is possible

that the HSC-derived mediator, induced by necrotic hepatocytes, is important in the activation of Kupffer cells following APAP overdose. As we demonstrated in Chapter 2 and Chapter 5, both plasmin and a HSC-derived eicosanoid can activate Kupffer cells. It is possible that these mechanisms are related. Previous studies have demonstrated that PGE2 can upregulate both uPA and tPA in rat osteoblasts (Allan, 1995). Therefore, it is possible that eicosanoids upregulate plasminogen activators in Kupffer cells, leading to increased local plasmin activity and enhanced Kupffer cell activation early after APAP-induced liver injury.

Furthermore, we have previously shown that deletion of HIF-1α in HSCs leads to reduced accumulation of neutrophils in the liver following acute liver injury induced by carbon tetrachloride (Mochizuki, 2014). This correlates with our findings in Chapter 5 that Kupffer cells are activated by a HSC-mediated eicosanoid to produce proinflammatory cytokines, such as Cxcl2 and Cxcl2, that recruit neutrophils. As demonstrated in out studies of ALF in Chapter 3, neutrophils do not accumulate in the liver and do not traffic into the necrotic lesions following APAP-induced ALF. It is possible that HSCs contribute to macrophage dysregulation through their effects on macrophage-mediated neutrophil recruitment. In support of this, it has been shown previously that neutrophils are able to manipulate macrophage phenotype (Yang, 2019). However, further studies are needed to investigate this relationship.

6.2 Future Directions

We have shown that activation of macrophages by plasmin upregulates proinflammatory cytokines via an NF-κB-dependent mechanism that is synergistically enhanced by HMGB1. We have also shown that this upregulation occurs independent of annexin A2 and PAR-1. However, the receptor through which plasmin activates macrophages remains unknown. Previous studies have demonstrated that plasmin can facilitate signaling in macrophages through other receptors as well, such as enolase-1 and Plg-Rkt (Wygrecka, 2009) (Miles, 2017). The prevention of plasmin-mediated upregulation of cytokines in knockout mice for either of these receptors would indicate its importance for plasmin-mediated signaling in macrophages. Furthermore, treatment

of receptor knockout mice with APAP, followed by staining for macrophages at various timepoints, could show if this receptor and pathway for plasmin-mediated activation of macrophages is also important for macrophage trafficking and function at later stages of APAP overdose.

Our studies also demonstrate that HMGB1 synergistically enhances plasmin-mediated activation of macrophages. However, the mechanism through which this occurs is not known. Previous studies have shown that plasmin can cleave HMGB1 (Parkkinen, 1991). It is possible that plasmin cleaves HMGB1, which increases the affinity of HMGB1 for TLR4. Inhibition of HMGB1-induced activation of TLR4 would provide insight into whether the synergistic effect between plasmin and HMGB1 requires binding of HMGB1 to TLR4.

We have also shown that inhibition of plasmin prevents macrophage trafficking into lesions, macrophage maturation, and phagocytosis of dead cells. Our studies suggest that plasmin stimulates resolution of inflammation after APAP overdose indirectly through the modulation of macrophage trafficking. However, the mechanism by which plasmin promotes these macrophage functions remains unclear. Plasmin is known to activate macrophages to produce MMPs, which degrade collagen and other extracellular matrix proteins (Monea, 2002) (Gong, 2008). The excessive or continual presence of extracellular matrix in the lesions of APAP-treated mice co-treated with a plasmin inhibitor would suggest that plasmin, or plasmin-dependent MMPs, are important for degradation of extracellular matrix. Studies examining extracellular matrix accumulation and macrophage trafficking in APAP overdose mice deficient in MMPs would illustrate whether MMPs are required for macrophage trafficking into necrotic lesions.

Our studies demonstrate that inhibition of plasmin prevents macrophage trafficking into lesions, macrophage maturation, and phagocytosis of dead cells. One intriguing question is whether restoration of plasminogen would restore macrophage function. Preliminary data from our lab demonstrates that administration of plasminogen to mice 24 hours after treatment with

600 mg/kg APAP allowed macrophages to enter the necrotic lesions, but clearance of the necrotic cells was still prevented. This is similar to our studies demonstrating that neutralization of IL-10 in mice treated with 600 mg/kg APAP allowed macrophages to traffic into the lesion, but clearance of the necrotic cells was still prevented. These studies suggest that although plasmin and IL-10 are important regulators in macrophage trafficking, an additional signal is needed to stimulate phagocytic clearance. It has been shown that mediators released by neutrophils can stimulate macrophages to switch from a proinflammatory phenotype to a pro-restorative, antiinflammatory phenotype (Yang, 2019). We have shown that neutrophils are reduced in the liver in the 600 mg/kg APAP-treated mice and that they do not traffic into the necrotic lesions (Fig. 3.1). In mice treated with 300 mg/kg APAP and TA, neutrophils were able to enter the lesions, but macrophages were not. If neutrophil numbers and trafficking are still impaired in 600 mg/kg APAP-treated mice in which IL-10 has been neutralized or plasminogen has been restored, this would suggest neutrophil-dependent mediators might play a role in stimulating phagocytic clearance. Restoration of neutrophils in mice after treatment with 600 mg/kg APAP would help uncover whether neutrophil mediators are the additional signal needed to stimulate phagocytic clearance of necrotic lesions.

BIBLIOGRAPHY

BIBLIOGRAPHY

Abdel-Misih SR, Bloomston M: Liver anatomy. The Surgical clinics of North America 2010, 90:643-53.

Abraham E, Arcaroli J, Carmody A, Wang H, Tracey KJ: HMG-1 as a mediator of acute lung inflammation. Journal of immunology (Baltimore, Md: 1950) 2000, 165:2950-4.

Allan EH, Martin TJ: Prostaglandin E2 regulates production of plasminogen activator isoenzymes, urokinase receptor, and plasminogen activator inhibitor-1 in primary cultures of rat calvarial osteoblasts. Journal of cellular physiology 1995, 165:521-9.

Andersson U, Wang H, Palmblad K, Aveberger AC, Bloom O, Erlandsson-Harris H, Janson A, Kokkola R, Zhang M, Yang H, Tracey KJ: High mobility group 1 protein (HMG-1) stimulates proinflammatory cytokine synthesis in human monocytes. The Journal of experimental medicine 2000, 192:565-70.

Antoine DJ, Williams DP, Kipar A, Jenkins RE, Regan SL, Sathish JG, Kitteringham NR, Park BK: High-mobility group box-1 protein and keratin-18, circulating serum proteins informative of acetaminophen-induced necrosis and apoptosis in vivo. Toxicological sciences: an official journal of the Society of Toxicology 2009, 112:521-31.

Antoniades CG, Berry PA, Davies ET, Hussain M, Bernal W, Vergani D, Wendon J: Reduced monocyte HLA-DR expression: a novel biomarker of disease severity and outcome in acetaminophen-induced acute liver failure. Hepatology (Baltimore, Md) 2006, 44:34-43.

Antoniades CG, Berry PA, Wendon JA, Vergani D: The importance of immune dysfunction in determining outcome in acute liver failure. Journal of hepatology 2008, 49:845-61.

Antoniades CG, Quaglia A, Taams LS, Mitry RR, Hussain M, Abeles R, Possamai LA, Bruce M, McPhail M, Starling C, Wagner B, Barnardo A, Pomplun S, Auzinger G, Bernal W, Heaton N, Vergani D, Thursz MR, Wendon J: Source and characterization of hepatic macrophages in acetaminophen-induced acute liver failure in humans. Hepatology (Baltimore, Md) 2012, 56:735-46.

Arnold L, Henry A, Poron F, Baba-Amer Y, van Rooijen N, Plonquet A, Gherardi RK, Chazaud B: Inflammatory monocytes recruited after skeletal muscle injury switch into antiinflammatory macrophages to support myogenesis. The Journal of experimental medicine 2007, 204:1057-69.

Barth MW, Hendrzak JA, Melnicoff MJ, Morahan PS: Review of the macrophage disappearance reaction. Journal of leukocyte biology 1995, 57:361-7.

Beattie L, Sawtell A, Mann J, Frame TCM, Teal B, de Labastida Rivera F, Brown N, Walwyn-Brown K, Moore JWJ, MacDonald S, Lim EK, Dalton JE, Engwerda CR, MacDonald KP, Kaye PM: Bone marrow-derived and resident liver macrophages display unique transcriptomic signatures but similar biological functions. Journal of hepatology 2016, 65:758-68.

Benoit M, Desnues B, Mege JL: Macrophage polarization in bacterial infections. Journal of immunology (Baltimore, Md: 1950) 2008, 181:3733-9.

Bernal W, Hyyrylainen A, Gera A, Audimoolam VK, McPhail MJ, Auzinger G, Rela M, Heaton N, O'Grady JG, Wendon J, Williams R: Lessons from look-back in acute liver failure? A single centre experience of 3300 patients. Journal of hepatology 2013, 59:74-80.

Bernal W, Wendon J: Acute liver failure. The New England journal of medicine 2013, 369:2525-34

Bernsmeier C, Triantafyllou E, Brenig R, Lebosse FJ, Singanayagam A, Patel VC, Pop OT, Khamri W, Nathwani R, Tidswell R, Weston CJ, Adams DH, Thursz MR, Wendon JA, Antoniades CG: CD14(+) CD15(-) HLA-DR(-) myeloid-derived suppressor cells impair antimicrobial responses in patients with acute-on-chronic liver failure. Gut 2018, 67:1155-67.

Berry PA, Antoniades CG, Hussain MJ, McPhail MJ, Bernal W, Vergani D, Wendon JA: Admission levels and early changes in serum interleukin-10 are predictive of poor outcome in acute liver failure and decompensated cirrhosis. Liver international: official journal of the International Association for the Study of the Liver 2010, 30:733-40.

Bezerra JA, Bugge TH, Melin-Aldana H, Sabla G, Kombrinck KW, Witte DP, Degen JL: Plasminogen deficiency leads to impaired remodeling after a toxic injury to the liver. Proceedings of the National Academy of Sciences of the United States of America 1999, 96:15143-8.

Bhushan B, Walesky C, Manley M, Gallagher T, Borude P, Edwards G, Monga SP, Apte U: Proregenerative signaling after acetaminophen-induced acute liver injury in mice identified using a novel incremental dose model. The American journal of pathology 2014, 184:3013-25.

Bianchi ME: DAMPs, PAMPs and alarmins: all we need to know about danger. Journal of leukocyte biology 2007, 81:1-5.

Blackmore L, Bernal W: Acute liver failure. Clinical medicine (London, England) 2015, 15:468-72.

Bone RC, Balk RA, Cerra FB, Dellinger RP, Fein AM, Knaus WA, Schein RM, Sibbald WJ: Definitions for sepsis and organ failure and guidelines for the use of innovative therapies in sepsis. The ACCP/SCCM Consensus Conference Committee. American College of Chest Physicians/Society of Critical Care Medicine. Chest 1992, 101:1644-55.

Borg RJ, Samson AL, Au AE, Scholzen A, Fuchsberger M, Kong YY, Freeman R, Mifsud NA, Plebanski M, Medcalf RL: Dendritic Cell-Mediated Phagocytosis but Not Immune Activation Is Enhanced by Plasmin. PloS one 2015, 10:e0131216.

Bourdi M, Masubuchi Y, Reilly TP, Amouzadeh HR, Martin JL, George JW, Shah AG, Pohl LR: Protection against acetaminophen-induced liver injury and lethality by interleukin 10: role of inducible nitric oxide synthase. Hepatology (Baltimore, Md) 2002, 35:289-98.

Burysek L, Syrovets T, Simmet T: The serine protease plasmin triggers expression of MCP-1 and CD40 in human primary monocytes via activation of p38 MAPK and janus kinase (JAK)/STAT signaling pathways. The Journal of biological chemistry 2002, 277:33509-17.

Calandra T, Baumgartner JD, Grau GE, Wu MM, Lambert PH, Schellekens J, Verhoef J, Glauser MP: Prognostic values of tumor necrosis factor/cachectin, interleukin-1, interferonalpha, and interferon-gamma in the serum of patients with septic shock. Swiss-Dutch J5 Immunoglobulin Study Group. The Journal of infectious diseases 1990, 161:982-7.

Calandra T, Gerain J, Heumann D, Baumgartner JD, Glauser MP: High circulating levels of interleukin-6 in patients with septic shock: evolution during sepsis, prognostic value, and interplay with other cytokines. The Swiss-Dutch J5 Immunoglobulin Study Group. The American journal of medicine 1991, 91:23-9.

Carmo AA, Costa BR, Vago JP, de Oliveira LC, Tavares LP, Nogueira CR, Ribeiro AL, Garcia CC, Barbosa AS, Brasil BS, Dusse LM, Barcelos LS, Bonjardim CA, Teixeira MM, Sousa LP: Plasmin induces in vivo monocyte recruitment through protease-activated receptor-1-, MEK/ERK-, and CCR2-mediated signaling. Journal of immunology (Baltimore, Md: 1950) 2014, 193:3654-63.

Cassetta L, Baekkevold ES, Brandau S, Bujko A, Cassatella MA, Dorhoi A, Krieg C, Lin A, Lore K, Marini O, Pollard JW, Roussel M, Scapini P, Umansky V, Adema GJ: Deciphering myeloid-derived suppressor cells: isolation and markers in humans, mice and non-human primates. Cancer immunology, immunotherapy: CII 2019, 68:687-97.

Cesarman-Maus G, Hajjar KA: Molecular mechanisms of fibrinolysis. British journal of haematology 2005, 129:307-21.

Copple BL, Bai S, Burgoon LD, Moon JO: Hypoxia-inducible factor-1alpha regulates the expression of genes in hypoxic hepatic stellate cells important for collagen deposition and angiogenesis. Liver international: official journal of the International Association for the Study of the Liver 2011, 31:230-44.

Coughlin SR: How the protease thrombin talks to cells. Proceedings of the National Academy of Sciences of the United States of America 1999, 96:11023-7.

Couper KN, Blount DG, Riley EM: IL-10: the master regulator of immunity to infection. Journal of immunology (Baltimore, Md: 1950) 2008, 180:5771-7.

Cresci GA, Allende D, McMullen MR, Nagy LE: Alternative complement pathway component Factor D contributes to efficient clearance of tissue debris following acute CCI(4)-induced injury. Molecular immunology 2015, 64:9-17.

Dambach DM, Watson LM, Gray KR, Durham SK, Laskin DL: Role of CCR2 in macrophage migration into the liver during acetaminophen-induced hepatotoxicity in the mouse. Hepatology (Baltimore, Md) 2002, 35:1093-103.

Das R, Ganapathy S, Settle M, Plow EF: Plasminogen promotes macrophage phagocytosis in mice. Blood 2014, 124:679-88.

David BA, Rezende RM, Antunes MM, Santos MM, Freitas Lopes MA, Diniz AB, Sousa Pereira RV, Marchesi SC, Alvarenga DM, Nakagaki BN, Araujo AM, Dos Reis DS, Rocha RM, Marques PE, Lee WY, Deniset J, Liew PX, Rubino S, Cox L, Pinho V, Cunha TM, Fernandes GR, Oliveira AG, Teixeira MM, Kubes P, Menezes GB: Combination of Mass Cytometry and Imaging Analysis Reveals Origin, Location, and Functional Repopulation of Liver Myeloid Cells in Mice. Gastroenterology 2016, 151:1176-91.

de Ataide EC, Reges Perales S, Bastos Eloy da Costa L, Valerini FG, Shiyoiti Hirano E, Chueiri Neto F, Silveira Bello Stucchi R, de Fatima Santana Ferreira Boin I: Acute Liver Failure-25 Years at a Single Center: Role of Liver Transplantation in the Survival of Adult Patients. Transplantation proceedings 2018, 50:472-5.

De Sousa LP, Brasil BS, Silva BM, Freitas MH, Nogueira SV, Ferreira PC, Kroon EG, Bonjardim CA: Plasminogen/plasmin regulates c-fos and egr-1 expression via the MEK/ERK pathway. Biochemical and biophysical research communications 2005, 329:237-45.

Deng M, Tang Y, Li W, Wang X, Zhang R, Zhang X, Zhao X, Liu J, Tang C, Liu Z, Huang Y, Peng H, Xiao L, Tang D, Scott MJ, Wang Q, Liu J, Xiao X, Watkins S, Li J, Yang H, Wang H, Chen F, Tracey KJ, Billiar TR, Lu B: The Endotoxin Delivery Protein HMGB1 Mediates Caspase-11-Dependent Lethality in Sepsis. Immunity 2018, 49:740-53 e7.

Dever JB, Sheikh MY: Review article: spontaneous bacterial peritonitis--bacteriology, diagnosis, treatment, risk factors and prevention. Alimentary pharmacology & therapeutics 2015, 41:1116-31.

Donahower BC, McCullough SS, Hennings L, Simpson PM, Stowe CD, Saad AG, Kurten RC, Hinson JA, James LP: Human recombinant vascular endothelial growth factor reduces necrosis and enhances hepatocyte regeneration in a mouse model of acetaminophen toxicity. The Journal of pharmacology and experimental therapeutics 2010, 334:33-43.

Drexler SK, Foxwell BM: The role of toll-like receptors in chronic inflammation. The international journal of biochemistry & cell biology 2010, 42:506-18.

Epelman S, Lavine KJ, Randolph GJ: Origin and functions of tissue macrophages. Immunity 2014, 41:21-35.

Esser-von Bieren J: Immune-regulation and -functions of eicosanoid lipid mediators. Biological chemistry 2017, 398:1177-91.

Fadok VA, Bratton DL, Konowal A, Freed PW, Westcott JY, Henson PM: Macrophages that have ingested apoptotic cells in vitro inhibit proinflammatory cytokine production through autocrine/paracrine mechanisms involving TGF-beta, PGE2, and PAF. The Journal of clinical investigation 1998, 101:890-8.

Fisher JE, McKenzie TJ, Lillegard JB, Yu Y, Juskewitch JE, Nedredal GI, Brunn GJ, Yi ES, Malhi H, Smyrk TC, Nyberg SL: Role of Kupffer cells and toll-like receptor 4 in acetaminophen-induced acute liver failure. The Journal of surgical research 2013, 180:147-55.

Friedman G, Jankowski S, Marchant A, Goldman M, Kahn RJ, Vincent JL: Blood interleukin 10 levels parallel the severity of septic shock. Journal of critical care 1997, 12:183-7.

Friedman SL: Hepatic stellate cells: protean, multifunctional, and enigmatic cells of the liver. Physiological reviews 2008, 88:125-72.

Gao S, Silasi-Mansat R, Behar AR, Lupu F, Griffin CT: Excessive Plasmin Compromises Hepatic Sinusoidal Vascular Integrity After Acetaminophen Overdose. Hepatology (Baltimore, Md) 2018, 68:1991-2003.

Ge X, Antoine DJ, Lu Y, Arriazu E, Leung TM, Klepper AL, Branch AD, Fiel MI, Nieto N: High mobility group box-1 (HMGB1) participates in the pathogenesis of alcoholic liver disease (ALD). The Journal of biological chemistry 2014, 289:22672-91.

Germani G, Theocharidou E, Adam R, Karam V, Wendon J, O'Grady J, Burra P, Senzolo M, Mirza D, Castaing D, Klempnauer J, Pollard S, Paul A, Belghiti J, Tsochatzis E, Burroughs AK: Liver transplantation for acute liver failure in Europe: outcomes over 20 years from the ELTR database. Journal of hepatology 2012, 57:288-96.

Godier A, Hunt BJ: Plasminogen receptors and their role in the pathogenesis of inflammatory, autoimmune and malignant disease. Journal of thrombosis and haemostasis: JTH 2013, 11:26-34.

Goerdt S, Politz O, Schledzewski K, Birk R, Gratchev A, Guillot P, Hakiy N, Klemke CD, Dippel E, Kodelja V, Orfanos CE: Alternative versus classical activation of macrophages. Pathobiology: journal of immunopathology, molecular and cellular biology 1999, 67:222-6.

Gong Y, Hart E, Shchurin A, Hoover-Plow J: Inflammatory macrophage migration requires MMP-9 activation by plasminogen in mice. The Journal of clinical investigation 2008, 118:3012-24

Gong Y, Kim SO, Felez J, Grella DK, Castellino FJ, Miles LA: Conversion of Glu-plasminogen to Lys-plasminogen is necessary for optimal stimulation of plasminogen activation on the endothelial cell surface. The Journal of biological chemistry 2001, 276:19078-83.

Gordon S: Alternative activation of macrophages. Nature reviews Immunology 2003, 3:23-35.

Griffin CT, Srinivasan Y, Zheng YW, Huang W, Coughlin SR: A role for thrombin receptor signaling in endothelial cells during embryonic development. Science (New York, NY) 2001, 293:1666-70.

Guerville M, Boudry G: Gastrointestinal and hepatic mechanisms limiting entry and dissemination of lipopolysaccharide into the systemic circulation. American journal of physiology Gastrointestinal and liver physiology 2016, 311:G1-G15.

Guillot A, Tacke F: Liver Macrophages: Old Dogmas and New Insights. Hepatology communications 2019, 3:730-43.

Guirat A, Koubaa M, Mzali R, Abid B, Ellouz S, Affes N, Ben Jemaa M, Frikha F, Ben Amar M, Beyrouti MI: Peritoneal tuberculosis. Clinics and research in hepatology and gastroenterology 2011, 35:60-9.

Han S, Xu W, Wang Z, Qi X, Wang Y, Ni Y, Shen H, Hu Q, Han W: Crosstalk between the HIF-1 and Toll-like receptor/nuclear factor-kappaB pathways in the oral squamous cell carcinoma microenvironment. Oncotarget 2016, 7:37773-89.

Hara S, Kamei D, Sasaki Y, Tanemoto A, Nakatani Y, Murakami M: Prostaglandin E synthases: Understanding their pathophysiological roles through mouse genetic models. Biochimie 2010, 92:651-9.

Henrion J: Hypoxic hepatitis. Liver international: official journal of the International Association for the Study of the Liver 2012, 32:1039-52.

Higashi T, Friedman SL, Hoshida Y: Hepatic stellate cells as key target in liver fibrosis. Advanced drug delivery reviews 2017, 121:27-42.

Hinson JA, Roberts DW, James LP: Mechanisms of acetaminophen-induced liver necrosis. Handbook of experimental pharmacology 2010:369-405.

Holt MP, Cheng L, Ju C: Identification and characterization of infiltrating macrophages in acetaminophen-induced liver injury. Journal of leukocyte biology 2008, 84:1410-21.

Huang B, Pan PY, Li Q, Sato AI, Levy DE, Bromberg J, Divino CM, Chen SH: Gr-1+CD115+ immature myeloid suppressor cells mediate the development of tumor-induced T regulatory cells and T-cell anergy in tumor-bearing host. Cancer research 2006, 66:1123-31.

Huang L, Zhao A, Wong F, Ayala JM, Struthers M, Ujjainwalla F, Wright SD, Springer MS, Evans J, Cui J: Leukotriene B4 strongly increases monocyte chemoattractant protein-1 in human monocytes. Arteriosclerosis, thrombosis, and vascular biology 2004, 24:1783-8.

Huebener P, Pradere JP, Hernandez C, Gwak GY, Caviglia JM, Mu X, Loike JD, Jenkins RE, Antoine DJ, Schwabe RF: The HMGB1/RAGE axis triggers neutrophil-mediated injury amplification following necrosis. The Journal of clinical investigation 2015, 125:539-50.

Huebener P, Pradere JP, Hernandez C, Gwak GY, Caviglia JM, Mu X, Loike JD, Jenkins RE, Antoine DJ, Schwabe RF: The HMGB1/RAGE axis triggers neutrophil-mediated injury amplification following necrosis. The Journal of clinical investigation 2015, 125:539-50.

Hultman K, Cortes-Canteli M, Bounoutas A, Richards AT, Strickland S, Norris EH: Plasmin deficiency leads to fibrin accumulation and a compromised inflammatory response in the mouse brain. Journal of thrombosis and haemostasis: JTH 2014, 12:701-12.

Ichai P, Samuel D: Etiology and prognosis of fulminant hepatitis in adults. Liver transplantation: official publication of the American Association for the Study of Liver Diseases and the International Liver Transplantation Society 2008, 14 Suppl 2:S67-79.

Ito T, Kawahara K, Okamoto K, Yamada S, Yasuda M, Imaizumi H, Nawa Y, Meng X, Shrestha B, Hashiguchi T, Maruyama I: Proteolytic cleavage of high mobility group box 1 protein by thrombin-thrombomodulin complexes. Arteriosclerosis, thrombosis, and vascular biology 2008, 28:1825-30.

Ito Y, Abril ER, Bethea NW, McCuskey RS: Inhibition of matrix metalloproteinases minimizes hepatic microvascular injury in response to acetaminophen in mice. Toxicological sciences: an official journal of the Society of Toxicology 2005, 83:190-6.

Jiang J, Bahrami S, Leichtfried G, Redl H, Ohlinger W, Schlag G: Kinetics of endotoxin and tumor necrosis factor appearance in portal and systemic circulation after hemorrhagic shock in rats. Annals of surgery 1995, 221:100-6.

Ju C, Reilly TP, Bourdi M, Radonovich MF, Brady JN, George JW, Pohl LR: Protective role of Kupffer cells in acetaminophen-induced hepatic injury in mice. Chemical research in toxicology 2002, 15:1504-13.

Ju C, Tacke F: Hepatic macrophages in homeostasis and liver diseases: from pathogenesis to novel therapeutic strategies. Cellular & molecular immunology 2016, 13:316-27.

Kaidi A, Qualtrough D, Williams AC, Paraskeva C: Direct transcriptional up-regulation of cyclooxygenase-2 by hypoxia-inducible factor (HIF)-1 promotes colorectal tumor cell survival and enhances HIF-1 transcriptional activity during hypoxia. Cancer research 2006, 66:6683-91.

Kawada N: The hepatic perisinusoidal stellate cell. Histology and histopathology 1997, 12:1069-80.

Kawao N, Nagai N, Okada K, Okumoto K, Ueshima S, Matsuo O: Role of plasminogen in macrophage accumulation during liver repair. Thrombosis research 2010, 125:e214-21.

Kim ND, Moon JO, Slitt AL, Copple BL: Early growth response factor-1 is critical for cholestatic liver injury. Toxicological sciences: an official journal of the Society of Toxicology 2006, 90:586-95.

Kopec AK, Joshi N, Cline-Fedewa H, Wojcicki AV, Ray JL, Sullivan BP, Froehlich JE, Johnson BF, Flick MJ, Luyendyk JP: Fibrin(ogen) drives repair after acetaminophen-induced liver injury via leukocyte alphaMbeta2 integrin-dependent upregulation of Mmp12. Journal of hepatology 2017, 66:787-97.

Kuper C, Beck FX, Neuhofer W: Toll-like receptor 4 activates NF-kappaB and MAP kinase pathways to regulate expression of proinflammatory COX-2 in renal medullary collecting duct cells. American journal of physiology Renal physiology 2012, 302:F38-46.

Kurihara T, Warr G, Loy J, Bravo R: Defects in macrophage recruitment and host defense in mice lacking the CCR2 chemokine receptor. The Journal of experimental medicine 1997, 186:1757-62.

Laskin DL, Gardner CR, Price VF, Jollow DJ: Modulation of macrophage functioning abrogates the acute hepatotoxicity of acetaminophen. Hepatology (Baltimore, Md) 1995, 21:1045-50.

Lau AH, Thomson AW: Dendritic cells and immune regulation in the liver. Gut 2003, 52:307-14.

Laumonnier Y, Syrovets T, Burysek L, Simmet T: Identification of the annexin A2 heterotetramer as a receptor for the plasmin-induced signaling in human peripheral monocytes. Blood 2006, 107:3342-9.

Lauterburg BH, Corcoran GB, Mitchell JR: Mechanism of action of N-acetylcysteine in the protection against the hepatotoxicity of acetaminophen in rats in vivo. The Journal of clinical investigation 1983, 71:980-91.

Law RH, Abu-Ssaydeh D, Whisstock JC: New insights into the structure and function of the plasminogen/plasmin system. Current opinion in structural biology 2013, 23:836-41.

Lee JJ, Natsuizaka M, Ohashi S, Wong GS, Takaoka M, Michaylira CZ, Budo D, Tobias JW, Kanai M, Shirakawa Y, Naomoto Y, Klein-Szanto AJ, Haase VH, Nakagawa H: Hypoxia activates the cyclooxygenase-2-prostaglandin E synthase axis. Carcinogenesis 2010, 31:427-34.

Lee M, Lee Y, Song J, Lee J, Chang SY: Tissue-specific Role of CX3CR1 Expressing Immune Cells and Their Relationships with Human Disease. Immune network 2018, 18:e5.

Lee WM: Acetaminophen and the U.S. Acute Liver Failure Study Group: lowering the risks of hepatic failure. Hepatology (Baltimore, Md) 2004, 40:6-9.

Lee WM: Acute liver failure. Seminars in respiratory and critical care medicine 2012, 33:36-45.

Lee WM: Acetaminophen (APAP) hepatotoxicity-Isn't it time for APAP to go away? Journal of hepatology 2017, 67:1324-31.

Lee WM, Squires RH, Jr., Nyberg SL, Doo E, Hoofnagle JH: Acute liver failure: Summary of a workshop. Hepatology (Baltimore, Md) 2008, 47:1401-15.

Leenen PJ, de Bruijn MF, Voerman JS, Campbell PA, van Ewijk W: Markers of mouse macrophage development detected by monoclonal antibodies. Journal of immunological methods 1994, 174:5-19.

Li Y, Wu R, Tian Y, Yu M, Tang Y, Cheng H, Tian Z: RAGE/NF-kappaB signaling mediates lipopolysaccharide induced acute lung injury in neonate rat model. International journal of clinical and experimental medicine 2015, 8:13371-6.

Lighvani S, Baik N, Diggs JE, Khaldoyanidi S, Parmer RJ, Miles LA: Regulation of macrophage migration by a novel plasminogen receptor Plg-R KT. Blood 2011, 118:5622-30.

Ling Q, Jacovina AT, Deora A, Febbraio M, Simantov R, Silverstein RL, Hempstead B, Mark WH, Hajjar KA: Annexin II regulates fibrin homeostasis and neoangiogenesis in vivo. The Journal of clinical investigation 2004, 113:38-48.

Lisman T, Bakhtiari K, Adelmeijer J, Meijers JC, Porte RJ, Stravitz RT: Intact thrombin generation and decreased fibrinolytic capacity in patients with acute liver injury or acute liver failure. Journal of thrombosis and haemostasis: JTH 2012, 10:1312-9.

Liu Y, Liang C, Liu X, Liao B, Pan X, Ren Y, Fan M, Li M, He Z, Wu J, Wu Z: AGEs increased migration and inflammatory responses of adventitial fibroblasts via RAGE, MAPK and NF-kappaB pathways. Atherosclerosis 2010, 208:34-42.

Lu YC, Yeh WC, Ohashi PS: LPS/TLR4 signal transduction pathway. Cytokine 2008, 42:145-51.

Macdougall BR, Bailey RJ, Williams R: H2-receptor antagonists and antacids in the prevention of acute gastrointestinal haemorrhage in fulminant hepatic failure. Two controlled trials. Lancet (London, England) 1977, 1:617-9.

Maloney JP, Gao L: Proinflammatory Cytokines Increase Vascular Endothelial Growth Factor Expression in Alveolar Epithelial Cells. Mediators of inflammation 2015, 2015:387842.

Marchant A, Alegre ML, Hakim A, Pierard G, Marecaux G, Friedman G, De Groote D, Kahn RJ, Vincent JL, Goldman M: Clinical and biological significance of interleukin-10 plasma levels in patients with septic shock. Journal of clinical immunology 1995, 15:266-73.

Marchetti C, Di Carlo A, Facchiano F, Senatore C, De Cristofaro R, Luzi A, Federici M, Romani M, Napolitano M, Capogrossi MC, Germani A: High mobility group box 1 is a novel substrate of dipeptidyl peptidase-IV. Diabetologia 2012, 55:236-44.

Martin C, Saux P, Mege JL, Perrin G, Papazian L, Gouin F: Prognostic values of serum cytokines in septic shock. Intensive care medicine 1994, 20:272-7.

Martinez FO, Gordon S: The M1 and M2 paradigm of macrophage activation: time for reassessment. F1000prime reports 2014, 6:13.

Mashima R, Okuyama T: The role of lipoxygenases in pathophysiology; new insights and future perspectives. Redox biology 2015, 6:297-310.

McClatchey W, Snyderman R: Prostaglandins and inflammation: enhancement of monocyte chemotactic responsiveness by prostaglandin E2. Prostaglandins 1976, 12:415-26.

Mehendale HM: Tissue repair: an important determinant of final outcome of toxicant-induced injury. Toxicologic pathology 2005, 33:41-51.

Michael SL, Pumford NR, Mayeux PR, Niesman MR, Hinson JA: Pretreatment of mice with macrophage inactivators decreases acetaminophen hepatotoxicity and the formation of reactive oxygen and nitrogen species. Hepatology (Baltimore, Md) 1999, 30:186-95.

Michalopoulos GK: Liver regeneration. Journal of cellular physiology 2007, 213:286-300.

Mihm S: Danger-Associated Molecular Patterns (DAMPs): Molecular Triggers for Sterile Inflammation in the Liver. International journal of molecular sciences 2018, 19.

Miles LA, Baik N, Lighvani S, Khaldoyanidi S, Varki NM, Bai H, Mueller BM, Parmer RJ: Deficiency of plasminogen receptor, Plg-RKT, causes defects in plasminogen binding and inflammatory macrophage recruitment in vivo. Journal of thrombosis and haemostasis: JTH 2017, 15:155-62.

Miles LA, Castellino FJ, Gong Y: Critical role for conversion of glu-plasminogen to Lys-plasminogen for optimal stimulation of plasminogen activation on cell surfaces. Trends in cardiovascular medicine 2003, 13:21-30.

Miles LA, Dahlberg CM, Plescia J, Felez J, Kato K, Plow EF: Role of cell-surface lysines in plasminogen binding to cells: identification of alpha-enolase as a candidate plasminogen receptor. Biochemistry 1991, 30:1682-91.

Mills CD, Kincaid K, Alt JM, Heilman MJ, Hill AM: M-1/M-2 macrophages and the Th1/Th2 paradigm. Journal of immunology (Baltimore, Md: 1950) 2000, 164:6166-73.

Mochizuki A, Pace A, Rockwell CE, Roth KJ, Chow A, O'Brien KM, Albee R, Kelly K, Towery K, Luyendyk JP, Copple BL: Hepatic stellate cells orchestrate clearance of necrotic cells in a hypoxia-inducible factor-1alpha-dependent manner by modulating macrophage phenotype in mice. Journal of immunology (Baltimore, Md: 1950) 2014, 192:3847-57.

Monea S, Lehti K, Keski-Oja J, Mignatti P: Plasmin activates pro-matrix metalloproteinase-2 with a membrane-type 1 matrix metalloproteinase-dependent mechanism. Journal of cellular physiology 2002, 192:160-70.

Moore JK, MacKinnon AC, Man TY, Manning JR, Forbes SJ, Simpson KJ: Patients with the worst outcomes after paracetamol (acetaminophen)-induced liver failure have an early monocytopenia. Alimentary pharmacology & therapeutics 2017, 45:443-54.

Moore KW, de Waal Malefyt R, Coffman RL, O'Garra A: Interleukin-10 and the interleukin-10 receptor. Annual review of immunology 2001, 19:683-765.

Mossanen JC, Krenkel O, Ergen C, Govaere O, Liepelt A, Puengel T, Heymann F, Kalthoff S, Lefebvre E, Eulberg D, Luedde T, Marx G, Strassburg CP, Roskams T, Trautwein C, Tacke F: Chemokine (C-C motif) receptor 2-positive monocytes aggravate the early phase of acetaminophen-induced acute liver injury. Hepatology (Baltimore, Md) 2016, 64:1667-82.

Mosser DM, Zhang X: Interleukin-10: new perspectives on an old cytokine. Immunological reviews 2008, 226:205-18.

Movafagh S, Crook S, Vo K: Regulation of hypoxia-inducible factor-1a by reactive oxygen species: new developments in an old debate. Journal of cellular biochemistry 2015, 116:696-703.

Munoz SJ: Prothrombin time in fulminant hepatic failure. Gastroenterology 1991, 100:1480-1.

Munoz SJ: Complications of Acute Liver Failure. Gastroenterology & hepatology 2014, 10:665-8.

Munoz SJ, Stravitz RT, Gabriel DA: Coagulopathy of acute liver failure. Clinics in liver disease 2009, 13:95-107.

Murakami M, Nakatani Y, Atsumi GI, Inoue K, Kudo I: Regulatory Functions of Phospholipase A2. Critical reviews in immunology 2017, 37:121-79.

Narumiya S, Sugimoto Y, Ushikubi F: Prostanoid receptors: structures, properties, and functions. Physiological reviews 1999, 79:1193-226.

Nourjah P, Ahmad SR, Karwoski C, Willy M: Estimates of acetaminophen (Paracetomal)-associated overdoses in the United States. Pharmacoepidemiology and drug safety 2006, 15:398-405.

O'Connell PA, Surette AP, Liwski RS, Svenningsson P, Waisman DM: S100A10 regulates plasminogen-dependent macrophage invasion. Blood 2010, 116:1136-46.

Odaka C, Mizuochi T, Yang J, Ding A: Murine macrophages produce secretory leukocyte protease inhibitor during clearance of apoptotic cells: implications for resolution of the inflammatory response. Journal of immunology (Baltimore, Md: 1950) 2003, 171:1507-14.

O'Grady JG, Schalm SW, Williams R: Acute liver failure: redefining the syndromes. Lancet (London, England) 1993, 342:273-5.

Ortega-Gomez A, Perretti M, Soehnlein O: Resolution of inflammation: an integrated view. EMBO molecular medicine 2013, 5:661-74.

Paik YH, Schwabe RF, Bataller R, Russo MP, Jobin C, Brenner DA: Toll-like receptor 4 mediates inflammatory signaling by bacterial lipopolysaccharide in human hepatic stellate cells. Hepatology (Baltimore, Md) 2003, 37:1043-55.

Park JS, Gamboni-Robertson F, He Q, Svetkauskaite D, Kim JY, Strassheim D, Sohn JW, Yamada S, Maruyama I, Banerjee A, Ishizaka A, Abraham E: High mobility group box 1 protein interacts with multiple Toll-like receptors. American journal of physiology Cell physiology 2006, 290:C917-24.

Parkkinen J, Rauvala H: Interactions of plasminogen and tissue plasminogen activator (t-PA) with amphoterin. Enhancement of t-PA-catalyzed plasminogen activation by amphoterin. The Journal of biological chemistry 1991, 266:16730-5.

Paudel YN, Angelopoulou E, Piperi C, Balasubramaniam V, Othman I, Shaikh MF: Enlightening the role of high mobility group box 1 (HMGB1) in inflammation: Updates on receptor signalling. European journal of pharmacology 2019, 858:172487.

Ploplis VA, French EL, Carmeliet P, Collen D, Plow EF: Plasminogen deficiency differentially affects recruitment of inflammatory cell populations in mice. Blood 1998, 91:2005-9.

Pluskota E, Soloviev DA, Bdeir K, Cines DB, Plow EF: Integrin alphaMbeta2 orchestrates and accelerates plasminogen activation and fibrinolysis by neutrophils. The Journal of biological chemistry 2004, 279:18063-72.

Porcheray F, Viaud S, Rimaniol AC, Leone C, Samah B, Dereuddre-Bosquet N, Dormont D, Gras G: Macrophage activation switching: an asset for the resolution of inflammation. Clinical and experimental immunology 2005, 142:481-9.

Powell WS, Rokach J: Biosynthesis, biological effects, and receptors of hydroxyeicosatetraenoic acids (HETEs) and oxoeicosatetraenoic acids (oxo-ETEs) derived from arachidonic acid. Biochimica et biophysica acta 2015, 1851:340-55.

Qin YH, Dai SM, Tang GS, Zhang J, Ren D, Wang ZW, Shen Q: HMGB1 enhances the proinflammatory activity of lipopolysaccharide by promoting the phosphorylation of MAPK p38 through receptor for advanced glycation end products. Journal of immunology (Baltimore, Md: 1950) 2009, 183:6244-50.

Raum D, Marcus D, Alper CA, Levey R, Taylor PD, Starzl TE: Synthesis of human plasminogen by the liver. Science (New York, NY) 1980, 208:1036-7.

Reilly TP, Brady JN, Marchick MR, Bourdi M, George JW, Radonovich MF, Pise-Masison CA, Pohl LR: A protective role for cyclooxygenase-2 in drug-induced liver injury in mice. Chemical research in toxicology 2001, 14:1620-8.

Robbins KC, Summaria L, Hsieh B, Shah RJ: The peptide chains of human plasmin. Mechanism of activation of human plasminogen to plasmin. The Journal of biological chemistry 1967, 242:2333-42.

Rodriguez M, Domingo E, Municio C, Alvarez Y, Hugo E, Fernandez N, Sanchez Crespo M: Polarization of the innate immune response by prostaglandin E2: a puzzle of receptors and signals. Molecular pharmacology 2014, 85:187-97.

Rolando N, Wade J, Davalos M, Wendon J, Philpott-Howard J, Williams R: The systemic inflammatory response syndrome in acute liver failure. Hepatology (Baltimore, Md) 2000, 32:734-9.

Rosenwald M, Koppe U, Keppeler H, Sauer G, Hennel R, Ernst A, Blume KE, Peter C, Herrmann M, Belka C, Schulze-Osthoff K, Wesselborg S, Lauber K: Serum-derived plasminogen is activated by apoptotic cells and promotes their phagocytic clearance. Journal of immunology (Baltimore, Md: 1950) 2012, 189:5722-8.

Rossi D, Zlotnik A: The biology of chemokines and their receptors. Annual review of immunology 2000, 18:217-42.

Roth GA, Faybik P, Hetz H, Ankersmit HJ, Hoetzenecker K, Bacher A, Thalhammer T, Krenn CG: MCP-1 and MIP3-alpha serum levels in acute liver failure and molecular adsorbent recirculating system (MARS) treatment: a pilot study. Scandinavian journal of gastroenterology 2009, 44:745-51.

Roth K, Strickland J, Joshi N, Deng M, Kennedy R, Rockwell C, Luyendyk JP, Billiar TR, Copple BL: Dichotomous role of plasmin in regulation of macrophage function after acetaminophen overdose. American journal of pathology 2019, In Press.

Roy A, Ganesh G, Sippola H, Bolin S, Sawesi O, Dagalv A, Schlenner SM, Feyerabend T, Rodewald HR, Kjellen L, Hellman L, Abrink M: Mast cell chymase degrades the alarmins heat shock protein 70, biglycan, HMGB1, and interleukin-33 (IL-33) and limits danger-induced inflammation. The Journal of biological chemistry 2014, 289:237-50.

Rumack BH, Peterson RC, Koch GG, Amara IA: Acetaminophen overdose. 662 cases with evaluation of oral acetylcysteine treatment. Archives of internal medicine 1981, 141:380-5.

Saito C, Zwingmann C, Jaeschke H: Novel mechanisms of protection against acetaminophen hepatotoxicity in mice by glutathione and N-acetylcysteine. Hepatology (Baltimore, Md) 2010, 51:246-54.

Sakaguchi M, Murata H, Yamamoto K, Ono T, Sakaguchi Y, Motoyama A, Hibino T, Kataoka K, Huh NH: TIRAP, an adaptor protein for TLR2/4, transduces a signal from RAGE phosphorylated upon ligand binding. PloS one 2011, 6:e23132.

Schiraldi M, Raucci A, Munoz LM, Livoti E, Celona B, Venereau E, Apuzzo T, De Marchis F, Pedotti M, Bachi A, Thelen M, Varani L, Mellado M, Proudfoot A, Bianchi ME, Uguccioni M: HMGB1 promotes recruitment of inflammatory cells to damaged tissues by forming a complex with CXCL12 and signaling via CXCR4. The Journal of experimental medicine 2012, 209:551-63.

Schmidt LE, Dalhoff K: Alpha-fetoprotein is a predictor of outcome in acetaminophen-induced liver injury. Hepatology (Baltimore, Md) 2005, 41:26-31.

Schulz C, Gomez Perdiguero E, Chorro L, Szabo-Rogers H, Cagnard N, Kierdorf K, Prinz M, Wu B, Jacobsen SE, Pollard JW, Frampton J, Liu KJ, Geissmann F: A lineage of myeloid cells independent of Myb and hematopoietic stem cells. Science (New York, NY) 2012, 336:86-90.

Schutters K, Kusters DH, Chatrou ML, Montero-Melendez T, Donners M, Deckers NM, Krysko DV, Vandenabeele P, Perretti M, Schurgers LJ, Reutelingsperger CP: Cell surface-expressed phosphatidylserine as therapeutic target to enhance phagocytosis of apoptotic cells. Cell death and differentiation 2013, 20:49-56.

Schwarz H, Schmittner M, Duschl A, Horejs-Hoeck J: Residual endotoxin contaminations in recombinant proteins are sufficient to activate human CD1c+ dendritic cells. PloS one 2014, 9:e113840.

Scott CL, Zheng F, De Baetselier P, Martens L, Saeys Y, De Prijck S, Lippens S, Abels C, Schoonooghe S, Raes G, Devoogdt N, Lambrecht BN, Beschin A, Guilliams M: Bone marrow-derived monocytes give rise to self-renewing and fully differentiated Kupffer cells. Nature communications 2016, 7:10321.

Semenza GL: Hypoxia-inducible factors in physiology and medicine. Cell 2012, 148:399-408.

Sierro F, Evrard M, Rizzetto S, Melino M, Mitchell AJ, Florido M, Beattie L, Walters SB, Tay SS, Lu B, Holz LE, Roediger B, Wong YC, Warren A, Ritchie W, McGuffog C, Weninger W, Le Couteur DG, Ginhoux F, Britton WJ, Heath WR, Saunders BM, McCaughan GW, Luciani F, MacDonald KPA, Ng LG, Bowen DG, Bertolino P: A Liver Capsular Network of Monocyte-Derived Macrophages Restricts Hepatic Dissemination of Intraperitoneal Bacteria by Neutrophil Recruitment. Immunity 2017, 47:374-88 e6.

Simpson KJ, Bates CM, Henderson NC, Wigmore SJ, Garden OJ, Lee A, Pollok A, Masterton G, Hayes PC: The utilization of liver transplantation in the management of acute liver failure: comparison between acetaminophen and non-acetaminophen etiologies. Liver transplantation: official publication of the American Association for the Study of Liver Diseases and the International Liver Transplantation Society 2009, 15:600-9.

Smilkstein MJ, Knapp GL, Kulig KW, Rumack BH: Efficacy of oral N-acetylcysteine in the treatment of acetaminophen overdose. Analysis of the national multicenter study (1976 to 1985). The New England journal of medicine 1988, 319:1557-62.

Stewart RK, Dangi A, Huang C, Murase N, Kimura S, Stolz DB, Wilson GC, Lentsch AB, Gandhi CR: A novel mouse model of depletion of stellate cells clarifies their role in ischemia/reperfusion- and endotoxin-induced acute liver injury. Journal of hepatology 2014, 60:298-305.

Su GL, Klein RD, Aminlari A, Zhang HY, Steinstraesser L, Alarcon WH, Remick DG, Wang SC: Kupffer cell activation by lipopolysaccharide in rats: role for lipopolysaccharide binding protein and toll-like receptor 4. Hepatology (Baltimore, Md) 2000, 31:932-6.

Sugimoto MA, Ribeiro ALC, Costa BRC, Vago JP, Lima KM, Carneiro FS, Ortiz MMO, Lima GLN, Carmo AAF, Rocha RM, Perez DA, Reis AC, Pinho V, Miles LA, Garcia CC, Teixeira MM, Sousa LP: Plasmin and plasminogen induce macrophage reprogramming and regulate key steps of inflammation resolution via annexin A1. Blood 2017, 129:2896-907.

Swaisgood CM, Aronica MA, Swaidani S, Plow EF: Plasminogen is an important regulator in the pathogenesis of a murine model of asthma. American journal of respiratory and critical care medicine 2007, 176:333-42.

Swisher JF, Khatri U, Feldman GM: Annexin A2 is a soluble mediator of macrophage activation. Journal of leukocyte biology 2007, 82:1174-84.

Syrovets T, Jendrach M, Rohwedder A, Schule A, Simmet T: Plasmin-induced expression of cytokines and tissue factor in human monocytes involves AP-1 and IKKbeta-mediated NF-kappaB activation. Blood 2001, 97:3941-50.

Takayama K, Garcia-Cardena G, Sukhova GK, Comander J, Gimbrone MA, Jr., Libby P: Prostaglandin E2 suppresses chemokine production in human macrophages through the EP4 receptor. The Journal of biological chemistry 2002, 277:44147-54.

Takeda N, O'Dea EL, Doedens A, Kim JW, Weidemann A, Stockmann C, Asagiri M, Simon MC, Hoffmann A, Johnson RS: Differential activation and antagonistic function of HIF-{alpha} isoforms in macrophages are essential for NO homeostasis. Genes & development 2010, 24:491-501.

Taylor NJ, Nishtala A, Manakkat Vijay GK, Abeles RD, Auzinger G, Bernal W, Ma Y, Wendon JA, Shawcross DL: Circulating neutrophil dysfunction in acute liver failure. Hepatology (Baltimore, Md) 2013, 57:1142-52.

Tian J, Avalos AM, Mao SY, Chen B, Senthil K, Wu H, Parroche P, Drabic S, Golenbock D, Sirois C, Hua J, An LL, Audoly L, La Rosa G, Bierhaus A, Naworth P, Marshak-Rothstein A, Crow MK, Fitzgerald KA, Latz E, Kiener PA, Coyle AJ: Toll-like receptor 9-dependent activation by DNA-containing immune complexes is mediated by HMGB1 and RAGE. Nature immunology 2007, 8:487-96.

Tilley SL, Coffman TM, Koller BH: Mixed messages: modulation of inflammation and immune responses by prostaglandins and thromboxanes. The Journal of clinical investigation 2001, 108:15-23.

Trefts E, Gannon M, Wasserman DH: The liver. Current biology: CB 2017, 27:R1147-R51.

Trey C, Davidson CS: The management of fulminant hepatic failure. Progress in liver diseases 1970, 3:282-98.

Tsuchida T, Friedman SL: Mechanisms of hepatic stellate cell activation. Nature reviews Gastroenterology & hepatology 2017, 14:397-411.

Van Epps DE, Wiik A, Garcia ML, Williams RC, Jr.: Enhancement of human neutrophil migration by prostaglandin E2. Cellular immunology 1978, 37:142-50.

Vaquero J, Polson J, Chung C, Helenowski I, Schiodt FV, Reisch J, Lee WM, Blei AT: Infection and the progression of hepatic encephalopathy in acute liver failure. Gastroenterology 2003, 125:755-64.

Varol C, Mildner A, Jung S: Macrophages: development and tissue specialization. Annual review of immunology 2015, 33:643-75.

Vicioso MA, Garaud JJ, Reglier-Poupet H, Lebeaut A, Gougerot-Pocidalo MA, Chollet-Martin S: Moderate inhibitory effect of interleukin-10 on human neutrophil and monocyte chemotaxis in vitro. European cytokine network 1998, 9:247-53.

Wang GL, Semenza GL: Characterization of hypoxia-inducible factor 1 and regulation of DNA binding activity by hypoxia. The Journal of biological chemistry 1993, 268:21513-8.

Warner N, Nunez G: MyD88: a critical adaptor protein in innate immunity signal transduction. Journal of immunology (Baltimore, Md: 1950) 2013, 190:3-4.

Weide I, Tippler B, Syrovets T, Simmet T: Plasmin is a specific stimulus of the 5-lipoxygenase pathway of human peripheral monocytes. Thrombosis and haemostasis 1996, 76:561-8.

Weiskirchen R, Tacke F: Cellular and molecular functions of hepatic stellate cells in inflammatory responses and liver immunology. Hepatobiliary surgery and nutrition 2014, 3:344-63.

Wen Y, Gu J, Vandenhoff GE, Liu X, Nadler JL: Role of 12/15-lipoxygenase in the expression of MCP-1 in mouse macrophages. American journal of physiology Heart and circulatory physiology 2008, 294:H1933-8.

Winau F, Hegasy G, Weiskirchen R, Weber S, Cassan C, Sieling PA, Modlin RL, Liblau RS, Gressner AM, Kaufmann SH: Ito cells are liver-resident antigen-presenting cells for activating T cell responses. Immunity 2007, 26:117-29.

Wu Z, Han M, Chen T, Yan W, Ning Q: Acute liver failure: mechanisms of immune-mediated liver injury. Liver international: official journal of the International Association for the Study of the Liver 2010, 30:782-94.

Wygrecka M, Marsh LM, Morty RE, Henneke I, Guenther A, Lohmeyer J, Markart P, Preissner KT: Enolase-1 promotes plasminogen-mediated recruitment of monocytes to the acutely inflamed lung. Blood 2009, 113:5588-98.

Wynn TA, Vannella KM: Macrophages in Tissue Repair, Regeneration, and Fibrosis. Immunity 2016, 44:450-62.

Xu Y, Zhao W, Xu J, Li J, Hong Z, Yin Z, Wang X: Activated hepatic stellate cells promote liver cancer by induction of myeloid-derived suppressor cells through cyclooxygenase-2. Oncotarget 2016, 7:8866-78.

Yang H, Antoine DJ, Andersson U, Tracey KJ: The many faces of HMGB1: molecular structure-functional activity in inflammation, apoptosis, and chemotaxis. Journal of leukocyte biology 2013, 93:865-73.

Yang J, Zhang L, Yu C, Yang XF, Wang H: Monocyte and macrophage differentiation: circulation inflammatory monocyte as biomarker for inflammatory diseases. Biomarker research 2014, 2:1.

Yang R, Tonnesseen TI: DAMPs and sterile inflammation in drug hepatotoxicity. Hepatology international 2019, 13:42-50.

Yang W, Tao Y, Wu Y, Zhao X, Ye W, Zhao D, Fu L, Tian C, Yang J, He F, Tang L: Neutrophils promote the development of reparative macrophages mediated by ROS to orchestrate liver repair. Nature communications 2019, 10:1076.

Yeh CH, Sturgis L, Haidacher J, Zhang XN, Sherwood SJ, Bjercke RJ, Juhasz O, Crow MT, Tilton RG, Denner L: Requirement for p38 and p44/p42 mitogen-activated protein kinases in RAGE-mediated nuclear factor-kappaB transcriptional activation and cytokine secretion. Diabetes 2001, 50:1495-504.

Yona S, Kim KW, Wolf Y, Mildner A, Varol D, Breker M, Strauss-Ayali D, Viukov S, Guilliams M, Misharin A, Hume DA, Perlman H, Malissen B, Zelzer E, Jung S: Fate mapping reveals origins and dynamics of monocytes and tissue macrophages under homeostasis. Immunity 2013, 38:79-91.

Youn JH, Oh YJ, Kim ES, Choi JE, Shin JS: High mobility group box 1 protein binding to lipopolysaccharide facilitates transfer of lipopolysaccharide to CD14 and enhances lipopolysaccharide-mediated TNF-alpha production in human monocytes. Journal of immunology (Baltimore, Md: 1950) 2008, 180:5067-74.

Zigmond E, Samia-Grinberg S, Pasmanik-Chor M, Brazowski E, Shibolet O, Halpern Z, Varol C: Infiltrating monocyte-derived macrophages and resident kupffer cells display different ontogeny and functions in acute liver injury. Journal of immunology (Baltimore, Md: 1950) 2014, 193:344-53.